Hartree-Fock approximation for deformed nuclei with a general two-nucleon potential and pairing correlations with a consistent residual interaction.

Duy Duc Dao

université de BORDEAUX

Centre d'Études Nucléaires de Bordeaux – Gradignan

THÈSE

PRÉSENTÉE À

L'UNIVERSITÉ DE BORDEAUX

ÉCOLE DOCTORALE DE

SCIENCES PHYSIQUES ET DE L'INGÉNIEUR

par M. DUY DUC DAO

POUR OBTENIR LE GRADE DE

DOCTEUR DE L'UNIVERSITÉ DE BORDEAUX

SPÉCIALITÉ : ASTROPHYSIQUE, PLASMAS, NUCLÉAIRE

APPROXIMATION DE HARTREE-FOCK POUR LES NOYAUX DÉFORMÉS AVEC UN POTENTIEL GÉNÉRAL À 2-CORPS ET CORRÉLATIONS D'APPARIEMENT AVEC UNE INTERACTION RÉSIDUELLE COHÉRENTE

Soutenue le 26 novembre 2019

Après avis de MM. M. Bender, T. Duguet — Rapporteurs

Devant la commission d'examen formée de :

M.	M. Bender,	Directeur de recherche, CNRS, IPN Lyon	Président
M.	J. Dobaczewski,	Professeur, Université de York, UK	Examinateurs
M.	T. Duguet,	Chercheur, CEA/DSM/IRFU/SPhN	
Mme.	M. Grasso,	Directrice de recherche, CNRS	
Mme.	N. Smirnova,	Maître de conférence, CENBG	
M.	L. Bonneau,	Maître de conférence, CENBG (Directeur de thèse)	

Je voudrais premièrement addresser mes profondes gratitudes à Ludovic Bonneau pour m'avoir donné l'opportunité de travailler sur ce sujet de thèse intéressant. J'ai beaucoup appris et apprécié nos discussions quasi quotidiennes qui m'ont fait sortir des difficultés rencontrées pendant ces trois années, qu'elles soient formelles ou techniques. Je le remercie pour sa présence, sa patience et sa rigueur scientifique qui m'ont guidé tout au long de ce travail, sans quoi je n'y aurais pas abouti.

Je tiens à remercier Philippe Quentin pour son amitié et son support qui m'avait permis de continuer dans ce domaine d'études et grâce à qui j'avais connu Ludovic. Je garde toujours un vif souvenir de nos rencontres et discussions à Hanoï et à Ho Chi Minh ville. C'est aussi par son aide constante que j'ai pu venir de nouveau à Bordeaux pour la thèse.

Je souhaite remercier Michael Bender et Thomas Duguet pour avoir accepté d'être rapporteurs de ce travail. Leurs commentaires, questions et corrections minutieuses ont été très illuminantes et m'ont beaucoup aidé dans la rédaction du manuscrit. Mes remerciements vont également à Nadezda Smirnova, Marcella Grasso et Jacek Dobaczewski pour avoir accepté d'être examinateurs de ma soutenance.

Merci aussi à l'ensemble des membres de l'administration et du service informatique pour leur aide et sympathie.

Table of contents

List of figures

List of tables

Introduction

Since the pionneering works of Vautherin and Brink [1], [2], the Hartree-Fock theory [3], [4] has become a powerful tool in the study of nuclear structure. The success of this theory is however intimately connected to the use of effective phenomenological density-dependent forces of Skyrme and Gogny (see e.g. [5]–[7] for recent reviews) such that the distinction between the Hartree-Fock method itself and its (historical) incarnation in a density functional form is often omitted. The reason behind is partly due to the unknown nuclear interaction which should be used in such approach to be competitive with its phenomenological counterparts when one tries to explain how protons and neutrons interact and lead to a self-bound system.

With the discovery of Quantum Chromo-Dynamics (QCD) in the early seventies [8], the nuclear interaction is considered as a residual force of the strong interaction between quarks and gluons as elementary degrees of freedom. A proper understanding of the nuclear interaction must then be rooted in QCD. So nuclear physicists aim at deriving the nuclear force from this theory. These attempts have reached some success through the chiral perturbation theory [9]. First proposed by S. Weinberg [10], this theory makes use of the fact that the relevant degrees of freedom at low energy are hadrons. In this framework, nuclear forces emerge from an effective Lagrangian which has the same symmetries of QCD at the considered scale $\Lambda_\chi \sim 1$ GeV. The pion is identified with the Goldstone boson resulting from the breaking of chiral symmetry. One can then expand the Lagrangian in powers of Q/Λ_χ where Q is a soft scale of the same order as the pion mass. Accordingly, nuclear forces can be derived in a systematic way order by order. In this theory one has also to consistently take into account many-body forces arising at higher orders of the expansion. The neglected degrees of freedom beyond Λ_χ are accounted for by the low-energy constants (LECs) that can be extracted for example from experimental data. In the two-body sector, let us cite for example

- the semilocal momentum-regularized potential developed by the Bochum group [11] ;
- the chiral potential up to fourth order by Entem and collaborators [12], [13].

Alternatively, one has also purely phenomenological or semi-phenomenological high-precision potentials [14]–[16] and effective low momentum interactions [17], [18]. The construction of effective low momentum interactions can be realized by the similarity renormalization group (SRG) approach that consists of evolving the bare two-body potential to the low momentum sector by a series of unitary transformations. For the two-body system, low-energy observables therefore remains

unaffected by the transformation. In fact, this is only a special case where one evolves the bare interaction in free space. It is worth noting that although chiral potentials have been designed to be applied directly in nuclear structure calculations, much effort have been devoted to first transform them through the SRG method to weaken the role of correlations and improve the convergence in many-body calculations. Among ab-initio approaches, let us mention for instance the No-Core Shell Model [19]–[21] which has recently had a touch on open-shell nuclei of mass $A \sim 30$. The In-Medium Similarity Renormalization Group (IM-SRG) directly diagonalizes the A-body hamiltonian by a series of continuous unitary transformation [22], [23]. One even witnesses a marriage of these two methods [24] in their path to heavier systems. Finally, there is the Coupled Cluster [25], [26] which is based on the transformation of an uncorrelated state through an exponential operator and the Self-Consistent Green's Function [27], [28] whose description relies on one-particle propagator. At the moment, those ab-initio approaches are mostly restricted to magic or semi-magic nuclei in the medium mass region.

Mean-field and beyond mean-field approaches share a similar path as most of the above mentioned ab-initio methods. That is, at the first step, one tries to obtain the best description of bulk nuclear ground states properties (especially binding energy, radii, deformation) with the mean-field derived from the nuclear interaction. In the second step, the neglected correlations among nucleons are taken into account via the residual interaction. The difference is that instead of a realistic Hamiltonian based on a two- and three-body non-empirical interactions as in ab-initio methods, mean-field and beyond mean-field approaches are often formulated and applied in practice using the concept of an energy density functional that is postulated in terms of a set of transition density matrices (see e.g. [29] for a recent review). More precisely, the energy functional contains energy kernels that are often inspired from the exact structure of the Hamiltonian expectation value calculated in the Hartree-Fock(-Bogoliubov) or beyond Hartree-Fock(-Bogoliubov) theories. Such a parametrization implies for example an inconsistency between the interactions used in the particle-hole and particle-particle channels [30]–[32] which can eventually lead to divergences and finite steps in the calculated energy. Furthermore, the use of density-dependent forces that do not correspond to a genuine operator means that matrix elements might not be anti-symmetrized. As pointed out in [30], one obtains spurious self-interaction contributions in the functional. It is important to stress that one does not encounter such problems in the strict mean-field and beyond mean-field approaches that use a genuine Hamitonian.

In this context, our present work focuses on the development of the Hartree-Fock approximation with the aim to treat a general two-body interaction. This gives the possibility to perform a comparison between different existing non-empirical interactions or to test the newly developed ones when they are made available. Secondly, to describe deformed nuclei, it is necessary to break the rotational symmetry in Hartree-Fock [33] and restore it later when one goes beyond the mean-field approximation. To this end, the choice of a mimimal symmetry to be imposed in Hartree-Fock is important. Specifically, it must

i) allow to describe spherical and deformed nuclei in the same single-particle basis ;

ii) render a Hartree-Fock calculation tractable in practice.

This requires a study of representation bases that must be efficient to calculate matrix elements of the interaction when implementing such a symmetry. We have preferred momentum space rather than the usual harmonic oscillator basis because of its asymtotic behavior (see for example [34], [35]). Moreover, as non-empirical potentials are often expressed in momentum space, one can treat the center-of-mass motion without performing further transformations.

The thesis is organized as follows:

- The first chapter studies the structure of the bare nucleon-nucleon interaction in momentum space as constrained by symmetries;
- The second chapter presents the SRG approach in free space that will serves to transform the two-body potential;
- In chapters III and IV a detailed study of the Hartree-Fock approximation in various momentum bases is presented. Differences and advantages between them are compared and analyzed;
- In chapter V, the study of the confined plane-wave truncation is performed in several deformed nuclei employing different interactions. The role of the basis parameters is analyzed;
- In chapter VI, we perform a beyond-mean-field calculation to investigate pairing properties of the non-empirical consistent residual interaction. This is done in the framework of the Highly Truncated Diagonalization Approach developed in Ref. [36].
- Appendix A provides materials to study the two-nucleon system (scattering and bound state properties) that serves to validate the transformation of the nucleon-nucleon interaction by the SRG approach.

Before closing this introdution, let us mention that in practice, when implementing the two-nucleon potential developed in Ref. [11] in the three-dimensional plane-wave representation, we find that this potential does not provide enough binding at the Hartree-Fock approximation and requires a strong renormalization by SRG. Therefore, we will not present its implementation and in chapter V, we will present only the results obtained with the potential developed by the authors of Ref. [13].

Chapter I

Two-nucleon interactions

I.1 General structure of the nucleon-nucleon interaction

I.1.1 Decomposition in spin space

For a particle of spin s, the vector space $\mathcal{L}(\mathcal{E}_s)$ of operators acting on $\mathcal{E}_s$ is isomorphic to the vector space of complex matrices of order $(2s+1)$. Its dimension is $(2s+1)^2$. An operator living in $\mathcal{E}_s \otimes \mathcal{E}_s$ can be decomposed into a linear combination of $(2s+1)^4$ basis operators. Such a basis could be contructed, either by direct tensor products of the basis vectors of $\mathcal{L}(\mathcal{E}_s)$, or by seeking for all irreducible tensors acting on $\mathcal{E}_s \otimes \mathcal{E}_s$. In the case $s = 1/2$, hence $\dim \mathcal{L}(\mathcal{E}_s \otimes \mathcal{E}_s) = 16$, the irreducible tensors constructed from the set of three Pauli matrices $\hat{\boldsymbol{\sigma}}$

$$\{\hat{\boldsymbol{\sigma}} \otimes \hat{\boldsymbol{\sigma}}\}_{\lambda\mu} = \sum_{\alpha=-1}^{1} \sum_{\beta=-1}^{1} C^{\lambda\mu}_{1\alpha1\beta}\, \hat{\sigma}_\alpha \otimes \hat{\sigma}_\beta, \quad (0 \leq \lambda \leq 2,\ -\lambda \leq \mu \leq \lambda), \tag{I.1}$$

and the combinations $\hat{\boldsymbol{\sigma}}_1 \pm \hat{\boldsymbol{\sigma}}_2 = \hat{\boldsymbol{\sigma}} \otimes \mathbb{1}_s \pm \mathbb{1}_s \otimes \hat{\boldsymbol{\sigma}}$ together with the identity $\mathbb{1}_s \otimes \mathbb{1}_s$ constitute one possible choice as basis. A two-body operator $\hat{V}$ cans thus be decomposed as

$$\boxed{\hat{V} = c_0(\mathbb{1}_s \otimes \mathbb{1}_s) + \sum_\alpha \left[a_{1\alpha} \left(\hat{\boldsymbol{\sigma}}_1 + \hat{\boldsymbol{\sigma}}_2\right)_\alpha + b_{1\alpha} \left(\hat{\boldsymbol{\sigma}}_1 - \hat{\boldsymbol{\sigma}}_2\right)_\alpha \right] + \sum_{\lambda=0}^{2} \sum_{\mu=-\lambda}^{\lambda} c_{\lambda\mu} \{\hat{\boldsymbol{\sigma}} \otimes \hat{\boldsymbol{\sigma}}\}_{\lambda\mu},} \tag{I.2}$$

where $c_0, a_1, b_1, c_{\lambda\mu}$ are constants in $\mathcal{L}(\mathcal{E}_s \otimes \mathcal{E}_s)$.

Let us consider now the Hilbert space of the two-particle system $\mathcal{E}^{\otimes 2} = \mathcal{E}_k \otimes (\mathcal{E}_s \otimes \mathcal{E}_s) \otimes (\mathcal{E}_t \otimes \mathcal{E}_t)$ $(t = 1/2)$ in which we add the spatial and isospin degrees of freedom. The latter yields a similar expansion of $\hat{V}$ in terms of $\hat{\boldsymbol{\tau}}$ (acting on $\mathcal{E}_t$ and by definition having the same algebra as $\hat{\boldsymbol{\sigma}}$) as in (I.2) whereas the former generally provides the spatial dependence upon our choice of representation.

Note that for the terms $\{\hat{\boldsymbol{\sigma}} \otimes \hat{\boldsymbol{\sigma}}\}_{\lambda\mu}$:

- when $\lambda = 0$,

$$\{\hat{\boldsymbol{\sigma}} \otimes \hat{\boldsymbol{\sigma}}\}_{00} = \sum_{\alpha=-1}^{1} \sum_{\beta=-1}^{1} C^{00}_{1\alpha1\beta}\, \hat{\sigma}_\alpha \otimes \hat{\sigma}_\beta = -\frac{1}{\sqrt{3}} \left(\hat{\boldsymbol{\sigma}}_1 \cdot \hat{\boldsymbol{\sigma}}_2\right); \tag{I.3}$$

- when $\lambda = 1$,

$$\{\hat{\boldsymbol{\sigma}} \otimes \hat{\boldsymbol{\sigma}}\}_{1\mu} = \frac{i}{\sqrt{2}} \left(\hat{\boldsymbol{\sigma}}_1 \times \hat{\boldsymbol{\sigma}}_2\right)_\mu. \tag{I.4}$$

I.1.2 Henley-Miller classification

In $\mathcal{L}(\mathcal{E}_t \otimes \mathcal{E}_t)$, as for spin $s = 1/2$, the decomposition of the two-body interaction $\hat{V}$ reads as

$$\hat{V} = \hat{c}_0 \otimes (\mathbb{1}_t \otimes \mathbb{1}_t) + \sum_\alpha \left[\hat{a}_{1\alpha} \otimes (\hat{\boldsymbol{\tau}}_1 + \hat{\boldsymbol{\tau}}_2)_\alpha + \hat{b}_{1\alpha} \otimes (\hat{\boldsymbol{\tau}}_1 - \hat{\boldsymbol{\tau}}_2)_\alpha\right] + \sum_{\lambda=0}^{2} \sum_{\mu=-\lambda}^{\lambda} \hat{c}_{\lambda\mu} \otimes \{\hat{\boldsymbol{\tau}} \otimes \hat{\boldsymbol{\tau}}\}_{\lambda\mu}. \tag{I.5}$$

The decomposition (I.5) of $\hat{V}$ in isospin space can be further constrained by

i) the charge conservation of the nuclear force characterized by the third component $\hat{T}_z$ of the two-nucleons total isospin operator $\hat{\mathbf{T}}$, i.e.

$$\left[\hat{V}, \hat{T}_z\right] = 0, \tag{I.6}$$

ii) and the rotational invariances of $\hat{V}$ in isospin space, also known as the *charge independence* (CI) and *charge symmetry* (CS) of the nuclear force. The latter is described by the charge symmetry operator

$$\hat{P}_{cs} = e^{i\pi \hat{T}_y}. \tag{I.7}$$

Owing to the classification of Henley *et al.* [37], the nucleon-nucleon interaction falls into four categories:

- class I: $\left[\hat{V}, \hat{\mathbf{T}}\right] = 0$ (CI)
- class II: $\left[\hat{V}, \hat{\mathbf{T}}\right] \neq 0$, $\left[\hat{V}, \hat{P}_{cs}\right] = 0$, $\left[\hat{V}, \hat{\mathbf{T}}^2\right] = 0$ (CS but no CI)
- class III: $\left[\hat{V}, \hat{\mathbf{T}}\right] \neq 0$, $\left[\hat{V}, \hat{P}_{cs}\right] \neq 0$, $\left[\hat{V}, \hat{\mathbf{T}}^2\right] = 0$ (no CI and no CS without isospin mixing)
- class IV: $\left[\hat{V}, \hat{\mathbf{T}}\right] \neq 0$, $\left[\hat{V}, \hat{P}_{cs}\right] \neq 0$, $\left[\hat{V}, \hat{\mathbf{T}}^2\right] \neq 0$ (no CI and no CS with isospin mixing)

Omitting the identity operator, the general structure of a two-body interaction in isospin space is given by

$$\boxed{\hat{V} = \underbrace{\hat{a} + \hat{b} \otimes (\hat{\boldsymbol{\tau}}_1 \cdot \hat{\boldsymbol{\tau}}_2)}_{\text{class I}} + \underbrace{\hat{c} \otimes \{\hat{\boldsymbol{\tau}} \otimes \hat{\boldsymbol{\tau}}\}_{20}}_{\text{class II}} + \underbrace{\hat{d} \otimes (\hat{\boldsymbol{\tau}}_1 + \hat{\boldsymbol{\tau}}_2)_0}_{\text{class III}} + \underbrace{\hat{e} \otimes (\hat{\boldsymbol{\tau}}_1 - \hat{\boldsymbol{\tau}}_2)_0 + \hat{f} \otimes (\hat{\boldsymbol{\tau}}_1 \times \hat{\boldsymbol{\tau}}_2)_0}_{\text{class IV}}} \tag{I.8}$$

where $\hat{a}, \hat{b}, \hat{c}, \hat{d}, \hat{e}$ and $\hat{f}$ are spin operators (I.2) acting on $\mathcal{E}_s \otimes \mathcal{E}_s$.

I.2 Symmetries of the nucleon-nucleon interaction

For a two-body system, using the center of mass transformation

$$\mathbf{k} = \frac{1}{2}(\mathbf{k}_1 - \mathbf{k}_2),\ \mathbf{K} = \mathbf{k}_1 + \mathbf{k}_2,\ \mathbf{r} = \mathbf{r}_1 - \mathbf{r}_2,\ \mathbf{R} = \frac{1}{2}(\mathbf{r}_1 + \mathbf{r}_2) \tag{I.9}$$

where $\mathbf{k}_i, \mathbf{r}_i$ $(i = 1, 2)$ denote the momentum and position of the particle i, one can express the matrix element of a two-body interaction $\hat{V}$ as a function of the Jacobi momenta $(\mathbf{k}, \mathbf{K})$ and the relative coordinates $(\mathbf{r}, \mathbf{R})$

$$\langle \mathbf{k}_1' \mathbf{k}_2' | \hat{V} | \mathbf{k}_1 \mathbf{k}_2 \rangle = \langle \mathbf{K}', \mathbf{k}' | \hat{V} | \mathbf{K}, \mathbf{k} \rangle,\ \ \langle \mathbf{r}_1' \mathbf{r}_2' | \hat{V} | \mathbf{r}_1 \mathbf{r}_2 \rangle = \langle \mathbf{R}', \mathbf{r}' | \hat{V} | \mathbf{R}, \mathbf{r} \rangle. \tag{I.10}$$

I.2.1 Space transformations and hermiticity

(i) *Translation in space:* $\hat{V}$ commutes with the total momentum operator of the two-nucleon system. The total momentum before and after the interaction process is conserved, i.e. $\mathbf{K}' = \mathbf{K}$. Hence, the matrix element $\langle \mathbf{k}_1' \mathbf{k}_2' | \hat{V} | \mathbf{k}_1 \mathbf{k}_2 \rangle$ is proportional to the delta function $\delta(\mathbf{K}' - \mathbf{K})$. In coordinate space, this leads to a dependence on relative distance $\mathbf{R}' - \mathbf{R}$ in the matrix element $\langle \mathbf{R}', \mathbf{r}' | \hat{V} | \mathbf{R}, \mathbf{r} \rangle$.

(ii) *Change of Galilean reference:* In considering the nucleus as an isolated system, the interaction $\hat{V}$, being the internal property between nucleons, should solely depend on the relative total momentum $(\mathbf{K}' - \mathbf{K})$ (see for example Ref. [38]). Combining with the translational invariance, this allows one to write

$$\langle \mathbf{k}_1' \mathbf{k}_2' | \hat{V} | \mathbf{k}_1 \mathbf{k}_2 \rangle = \langle \mathbf{K}' \,|\, \mathbf{K} \rangle \langle \mathbf{k}' | \hat{V} | \mathbf{k} \rangle,\ \ \langle \mathbf{r}_1' \mathbf{r}_2' | \hat{|} \mathbf{r}_1 \mathbf{r}_2 \rangle = \langle \mathbf{R}' \,|\, \mathbf{R} \rangle \langle \mathbf{r}' | \hat{V} | \mathbf{r} \rangle. \tag{I.11}$$

(iii) *Inversion of space:* The interaction $\hat{V}$ is invariant under parity transformation $\hat{\Pi}$ that reverses the sign of the particle momentum and position, that is

$$\hat{\Pi} | \mathbf{k} \rangle = | -\mathbf{k} \rangle,\ \ \hat{\Pi} | \mathbf{r} \rangle = | -\mathbf{r} \rangle. \tag{I.12}$$

(iv) *Hermiticity:* one has the following constraint on the spatial part of the interaction

$$\langle \mathbf{k} | \hat{V} | \mathbf{k}' \rangle = \langle \mathbf{k}' | \hat{V} | \mathbf{k} \rangle^*,\ \ \langle \mathbf{r} | \hat{V} | \mathbf{r}' \rangle = \langle \mathbf{r}' | \hat{V} | \mathbf{r} \rangle^*. \tag{I.13}$$

(v) *Rotational invariance*: The two-body operator $\hat{V}$ commutes with the total angular momentum of the two-nucleon system $\hat{\mathbf{J}} = \hat{\mathbf{L}} + \hat{\mathbf{S}}$. It is scalar under rotations in the momentum (position) spin space $\mathcal{E}_k \otimes (\mathcal{E}_s \otimes \mathcal{E}_s)$.

I.2.2 Time-reversal and permutation

Unlike the above-mentioned spatial symmetries, time-reversal and permutation transformations affect dynamical variables (momentum and/or position) as well as spin and isospin degrees of freedom. While the permutation $\hat{P}_{12}$ interchanges the indices $1, 2$ of the same physical quantities, that is

$$\begin{cases} \mathbf{r}_1 \to \mathbf{r}_2, & \mathbf{r}_2 \to \mathbf{r}_1 \\ \mathbf{k}_1 \to \mathbf{k}_2, & \mathbf{k}_2 \to \mathbf{k}_1 \\ \hat{\boldsymbol{\sigma}}_1 \to \hat{\boldsymbol{\sigma}}_2, & \hat{\boldsymbol{\sigma}}_2 \to \hat{\boldsymbol{\sigma}}_1 \\ \hat{\boldsymbol{\tau}}_1 \to \hat{\boldsymbol{\tau}}_2, & \hat{\boldsymbol{\tau}}_2 \to \hat{\boldsymbol{\tau}}_1, \end{cases} \tag{I.14}$$

the time-reversal transformation $\hat{\mathcal{T}}$ (within the standard definition in the position representation, see e.g. Ref. [39]) changes sign of both momentum and spin operators, leaving unaltered the position operator. This can be expressed as

$$|\mathbf{k}\rangle \xrightarrow{\hat{\mathcal{T}}} |-\mathbf{k}\rangle, \;\; \hat{\mathcal{T}}^\dagger \, \hat{\boldsymbol{\sigma}} \, \hat{\mathcal{T}} = -\hat{\boldsymbol{\sigma}}, \;\; |\mathbf{r}\rangle \xrightarrow{\hat{\mathcal{T}}} |\mathbf{r}\rangle. \tag{I.15}$$

Taking into account the anti-linear character of $\hat{\mathcal{T}}$, one obtains

$$\langle \mathbf{k}'|\hat{V}|\mathbf{k}\rangle = \langle -\mathbf{k}'|\hat{V}|-\mathbf{k}\rangle^*, \;\; \langle \mathbf{r}'|\hat{V}|\mathbf{r}\rangle = \langle \mathbf{r}'|\hat{V}|\mathbf{r}\rangle^*. \tag{I.16}$$

Also, $\hat{\boldsymbol{\tau}}$ is transformed according to

$$(\hat{\tau}_x, \hat{\tau}_y, \hat{\tau}_z) \xrightarrow{\hat{\mathcal{T}}} (\hat{\tau}_x, -\hat{\tau}_y, \hat{\tau}_z). \tag{I.17}$$

I.3 Fourier transforms of two-body matrix elements

We establish here the Fourier transformation between position and momentum representations of a translational and Galilean invariant two-body interaction $\hat{V}$. By the closure relation in momentum space, one obtains

$$\langle \mathbf{r}_1'\mathbf{r}_2'|\hat{V}|\mathbf{r}_1\mathbf{r}_2\rangle = \frac{N_k^2}{(2\pi)^6}\frac{1}{N_k^4}\int d^3\mathbf{k}_1' \int d^3\mathbf{k}_2' \int d^3\mathbf{k}_1 \int d^3\mathbf{k}_2 \, e^{i(\mathbf{k}_1'\mathbf{r}_1' + \mathbf{k}_2'\mathbf{r}_2')} \langle \mathbf{k}_1'\mathbf{k}_2'|\hat{V}|\mathbf{k}_1\mathbf{k}_2\rangle \times e^{-i(\mathbf{k}_1\mathbf{r}_1 + \mathbf{k}_2\mathbf{r}_2)}. \tag{I.18}$$

In switching to the center of mass coordinates (I.9) and because $\hat{V}$ is translational and Galilean invariant, one has

$$\langle \mathbf{r}_1'\mathbf{r}_2'|\hat{V}|\mathbf{r}_1\mathbf{r}_2\rangle = \frac{1}{(2\pi)^6}\frac{1}{N_k^2} \times N_k \int d^3\mathbf{k}' \, e^{i\mathbf{k}'\cdot\mathbf{r}'} \int d^3\mathbf{k} \, e^{-i\mathbf{k}\cdot\mathbf{r}} \, \langle \mathbf{k}'|\hat{V}|\mathbf{k}\rangle \times \underbrace{\int d^3\mathbf{K} \int d^3\mathbf{K}' \, \delta(\mathbf{K}' - \mathbf{K}) e^{i(\mathbf{K}'\cdot\mathbf{R}' - \mathbf{K}\cdot\mathbf{R})}}_{(2\pi)^3\delta(\mathbf{R}'-\mathbf{R})}, \tag{I.19}$$

which yields

$$\langle \mathbf{r}_1' \mathbf{r}_2' | \hat{V} | \mathbf{r}_1 \mathbf{r}_2 \rangle = \delta(\mathbf{R}' - \mathbf{R}) \, \langle \mathbf{r}' | \hat{V} | \mathbf{r} \rangle, \tag{I.20}$$

with the definition

$$\boxed{\langle \mathbf{r}' | \hat{V} | \mathbf{r} \rangle = \frac{1}{N_k} \frac{1}{(2\pi)^3} \int d^3\mathbf{k}' \, e^{i\mathbf{k}'\cdot\mathbf{r}'} \int d^3\mathbf{k} \, e^{-i\mathbf{k}\cdot\mathbf{r}} \, \langle \mathbf{k}' | \hat{V} | \mathbf{k} \rangle.} \tag{I.21}$$

The inverse transform of (I.21) reads as

$$\boxed{\langle \mathbf{k}' | \hat{V} | \mathbf{k} \rangle = \frac{N_k}{(2\pi)^3} \int d^3\mathbf{r}' \, e^{-i\mathbf{k}'\mathbf{r}'} \int d^3\mathbf{r} \, e^{i\mathbf{k}\mathbf{r}} \, \langle \mathbf{r}' | \hat{V} | \mathbf{r} \rangle.} \tag{I.22}$$

I.4 Locality and velocity dependence

By definition, a translationally invariant interaction is local in space if its matrix element satisfies

$$\langle \mathbf{r}_1' \mathbf{r}_2' | \hat{V} | \mathbf{r}_1 \mathbf{r}_2 \rangle = \langle \mathbf{R}' \, | \, \mathbf{R} \rangle \, \langle \mathbf{r}' | \hat{V} | \mathbf{r} \rangle = \delta(\mathbf{R}' - \mathbf{R}) \, \delta(\mathbf{r}' - \mathbf{r}) \, V(\mathbf{r}). \tag{I.23}$$

where $V(\mathbf{r})$ is a scalar function of the relative distance. In momentum space, this is translated into a dependence of the interaction on the momentum transfer $\mathbf{q} = \mathbf{k}' - \mathbf{k}$ where one finds that from (I.22)

$$\langle \mathbf{k}' | \hat{V} | \mathbf{k} \rangle = \frac{N_k}{(2\pi)^3} \int d^3\mathbf{r} \, e^{-i(\mathbf{k}'-\mathbf{k})\cdot\mathbf{r}} \, V(\mathbf{r}) \equiv \sqrt{\frac{N_k}{(2\pi)^3}} \, \widetilde{V}(\mathbf{q}). \tag{I.24}$$

Also, applying (I.21) for a local interaction, one obtains

$$V(\mathbf{r}) = \frac{1}{\sqrt{N_k}} \frac{1}{(2\pi)^{3/2}} \int d^3\mathbf{q} \, e^{i\mathbf{q}\cdot\mathbf{r}} \, \widetilde{V}(\mathbf{q}). \tag{I.25}$$

Let us consider an interaction defined in coordinate space as

$$\langle \mathbf{r}_1' \mathbf{r}_2' | \hat{V} | \mathbf{r}_1 \mathbf{r}_2 \rangle = \delta(\mathbf{r}_1' - \mathbf{r}_1) \, \delta(\mathbf{r}_2' - \mathbf{r}_2) \, V(\mathbf{r}_1, \mathbf{r}_2). \tag{I.26}$$

In momentum space, the two-body matrix element is given by

$$\begin{aligned} \langle \mathbf{k}_1' \mathbf{k}_2' | \hat{V} | \mathbf{k}_1 \mathbf{k}_2 \rangle &= \frac{N_k^2}{(2\pi)^6} \int d^3\mathbf{r}_1' \int d^3\mathbf{r}_2' \int d^3\mathbf{r}_1 \int d^3\mathbf{r}_2 e^{-i(\mathbf{k}_1'\cdot\mathbf{r}_1' + \mathbf{k}_2'\cdot\mathbf{r}_2')} \times \\ &\qquad \langle \mathbf{r}_1' \mathbf{r}_2' | \hat{V} | \mathbf{r}_1 \mathbf{r}_2 \rangle e^{i(\mathbf{k}_1\cdot\mathbf{r}_1 + \mathbf{k}_2\cdot\mathbf{r}_2)} \\ &= \frac{N_k^2}{(2\pi)^6} \int d^3\mathbf{r}_1 \int d^3\mathbf{r}_2 \, V(\mathbf{r}_1, \mathbf{r}_2) \, e^{i(\mathbf{k}_1 - \mathbf{k}_1')\cdot\mathbf{r}_1} \, e^{i(\mathbf{k}_2 - \mathbf{k}_2')\cdot\mathbf{r}_2}. \end{aligned} \tag{I.27}$$

Using the center of mass transformation (I.9), the momentum representation of (I.26) reads as

$$\boxed{\langle \mathbf{k}_1' \mathbf{k}_2' | \hat{V} | \mathbf{k}_1 \mathbf{k}_2 \rangle = \frac{N_k^2}{(2\pi)^6} \int d^3\mathbf{r}\; e^{-i(\mathbf{k}'-\mathbf{k})\cdot\mathbf{r}} \int d^3\mathbf{R}\; e^{-i(\mathbf{K}'-\mathbf{K})\cdot\mathbf{R}}\; V(\mathbf{R}+\frac{\mathbf{r}}{2}, \mathbf{R}-\frac{\mathbf{r}}{2}).} \tag{I.28}$$

Remarks:

(i) An interaction satisfying (I.26) is Galilean-invariant but not necessarily translationally invariant. Moreover, it exhibits a dependence on the momentum transfer $\mathbf{q} = \mathbf{k}' - \mathbf{k}$;

(ii) If $v(\mathbf{r}_1, \mathbf{r}_2)$ is merely a function of the relative position $\mathbf{r} = \mathbf{r}_1 - \mathbf{r}_2$, we recover (I.24).

I.5 Momentum representation of rotationally invariant spin dependent forces

We consider three types of spin-dependent interactions, defined in Ref. [39] in coordinate space, and find their momentum representations.

• **Central force:** This force contains the scalar part in spin

$$\langle \mathbf{r}' | \hat{V} | \mathbf{r} \rangle = \delta(\mathbf{r}' - \mathbf{r}) \Big(V_C(r)\, \mathbb{1}_s + V_S(r)\, \hat{\boldsymbol{\sigma}}_1 \cdot \hat{\boldsymbol{\sigma}}_2 \Big), \tag{I.29}$$

where $V_C(r), V_S(r)$ are scalar function of the radial variable $r = |\mathbf{r}|$. For this local force, using (I.24), one can write

$$\begin{aligned} \int d^3\mathbf{r}\, e^{-i\mathbf{q}\cdot\mathbf{r}}\, V_C(r) &= \int_0^{+\infty} dr\, r^2\, V_C(r) \int_0^{\pi} d\theta\; \sin\theta\, e^{-iqr\cos\theta} \int_0^{2\pi} d\varphi \\ &= 2\pi \int_0^{+\infty} dr\, r^2\, V_C(r) \int_0^{\pi} d(-\cos\theta)\, e^{iqr(-\cos\theta)} \\ &= 2\pi \int_0^{+\infty} dr\, r^2\, V_C(r)\, \frac{1}{iqr}\, e^{-iqr\cos\theta}\Big|_0^{\pi} \\ &= 4\pi \int_0^{+\infty} dr\, r^2\, V_C(r)\, \frac{\sin(qr)}{qr}. \end{aligned} \tag{I.30}$$

The momentum representation of the central force thus reads

$$\langle \mathbf{k}' | \hat{V} | \mathbf{k} \rangle = \widetilde{V}_C(q) + \widetilde{V}_S(q)\, \hat{\boldsymbol{\sigma}}_1 \cdot \hat{\boldsymbol{\sigma}}_2, \tag{I.31}$$

with the form factors

$$\begin{aligned} \widetilde{V}_C(q) &= \frac{N_k}{(2\pi)^3} \times 4\pi \int_0^{+\infty} dr\, r^2\, j_0(qr)\, V_C(r), \\ \widetilde{V}_S(q) &= \frac{N_k}{(2\pi)^3} \times 4\pi \int_0^{+\infty} dr\, r^2\, j_0(qr)\, V_S(r), \end{aligned} \tag{I.32}$$

which are given in terms of the zero order spherical Bessel function $j_0(x) = \dfrac{\sin(x)}{x}$.

• **Spin-orbit force:** This force is velocity-dependent and couples space and spin variables. It takes the following form

$$\langle \mathbf{r}'|\hat{V}|\mathbf{r}\rangle = \delta(\mathbf{r}' - \mathbf{r})\; V_{LS}(r)\, \hat{\mathbf{L}} \cdot \hat{\mathbf{S}}. \tag{I.33}$$

To obtain the momentum representation of this interaction, let us consider its action onto an arbitrary state vector $|\psi\rangle$

$$\begin{aligned}
\langle \mathbf{k}'|\hat{V}|\psi\rangle &= \int d^3\mathbf{r}'\, \langle \mathbf{k}'\,|\,\mathbf{r}'\rangle \int d^3\mathbf{r}\, \langle \mathbf{r}'|\hat{V}|\mathbf{r}\rangle\, \langle \mathbf{r}\,|\,\psi\rangle \\
&= \sqrt{\frac{N_k}{(2\pi)^3}} \int d^3\mathbf{r}'\, e^{-i\mathbf{k}'\cdot\mathbf{r}'} \int d^3\mathbf{r}\, \delta(\mathbf{r}' - \mathbf{r})\; V_{LS}(r)\, (\hat{\mathbf{L}} \cdot \hat{\mathbf{S}})\, \langle \mathbf{r}\,|\,\psi\rangle \\
&= \sqrt{\frac{N_k}{(2\pi)^3}} \int d^3\mathbf{r}\, e^{-i\mathbf{k}'\cdot\mathbf{r}}\, V_{LS}(r)\, (\hat{\mathbf{L}} \cdot \hat{\mathbf{S}})\, \langle \mathbf{r}\,|\,\psi\rangle.
\end{aligned} \tag{I.34}$$

Using the definition of the Fourier transform and taking the derivative over the components of the position vector $\mathbf{r}$, e.g. in the x–direction, one can write

$$\frac{1}{i}\frac{\partial}{\partial x}\, \langle \mathbf{r}\,|\,\psi\rangle = \frac{1}{\sqrt{N_k}}\, \frac{1}{(2\pi)^{3/2}} \int d^3\mathbf{k}''\; e^{i\mathbf{k}''\cdot\mathbf{r}}\, k_x'' \langle \mathbf{k}''\,|\,\psi\rangle. \tag{I.35}$$

Moreover, in coordinate space $\hat{\mathbf{L}} = \dfrac{1}{i}(\mathbf{r} \times \boldsymbol{\nabla})$ (the Planck constant in the operators $\hat{\mathbf{L}}, \hat{\mathbf{S}}$ is absorbed in the scalar function $V_{LS}(r)$) such that

$$(\hat{\mathbf{L}} \cdot \hat{\mathbf{S}})\, \langle \mathbf{r}\,|\,\psi\rangle = \frac{1}{\sqrt{N_k}}\, \frac{1}{(2\pi)^{3/2}} \int d^3\mathbf{k}''\; e^{i\mathbf{k}''\cdot\mathbf{r}} \left(\mathbf{r}\, \times\, \mathbf{k}''\right) \cdot \hat{\mathbf{S}}\, \langle \mathbf{k}''\,|\,\psi\rangle, \tag{I.36}$$

one can interchange the order of the two integrals and obtains

$$\langle \mathbf{k}'|\hat{V}|\psi\rangle = \int d^3\mathbf{k}''\, \left[\left(\frac{1}{(2\pi)^3} \int d^3\mathbf{r}\; e^{-i(\mathbf{k}'-\mathbf{k}'')\cdot\mathbf{r}}\, V_{LS}(r)\, \mathbf{r} \right) \times\, \mathbf{k}'' \right] \cdot \hat{\mathbf{S}}\, \langle \mathbf{k}''\,|\,\psi\rangle. \tag{I.37}$$

Choosing $|\psi\rangle = |\mathbf{k}\rangle$ (with the Dirac orthogonality $\langle \mathbf{k}''\,|\,\mathbf{k}\rangle = N_k \delta(\mathbf{k}'' - \mathbf{k})$) allows one to perform the integral over $\mathbf{k}''$

$$\langle \mathbf{k}'|\hat{V}|\mathbf{k}\rangle = \left[\left(\frac{N_k}{(2\pi)^3} \int d^3\mathbf{r}\; e^{-i(\mathbf{k}'-\mathbf{k})\cdot\mathbf{r}}\, V_{LS}(r)\, \mathbf{r} \right) \times\, \mathbf{k} \right] \cdot \hat{\mathbf{S}}. \tag{I.38}$$

Let denote now the integral in the bracket by

$$\widetilde{\alpha}_{LS}(\mathbf{q}) = \frac{N_k}{(2\pi)^3} \int d^3\mathbf{r}\; e^{-i(\mathbf{k}'-\mathbf{k})\cdot\mathbf{r}}\, V_{LS}(r), \tag{I.39}$$

again, by taking the derivative over the components of the vector $\mathbf{q} = \mathbf{k}' - \mathbf{k}$, one obtains

$$\langle \mathbf{k}'|\hat{V}|\mathbf{k}\rangle = i \left(\boldsymbol{\nabla} \widetilde{\alpha}_{LS}(\mathbf{q}) \times \mathbf{k} \right) \cdot \hat{\mathbf{S}}. \tag{I.40}$$

Furthermore, writing the nabla operator in spherical coordinates of $\mathbf{q}$ and because $\widetilde{\alpha}_{LS}(\mathbf{q})$ depends on $q = |\mathbf{q}|$, one can express

$$\boldsymbol{\nabla}\widetilde{\alpha}_{LS}(q) = \frac{1}{q}\,\frac{\partial}{\partial q}\widetilde{\alpha}_{LS}(q)\;\mathbf{q}, \tag{I.41}$$

where one has

$$\begin{aligned}\frac{\partial}{\partial q}\widetilde{\alpha}_{LS}(q) &= \frac{N_k}{(2\pi)^3}\;\times 4\pi\int_0^{+\infty} dr\, r^2\, V_{LS}(r)\,\frac{\partial}{\partial q}\Big(\frac{\sin(qr)}{qr}\Big),\\ \frac{\partial}{\partial q}\Big(\frac{\sin(qr)}{qr}\Big) &= \frac{\cos(qr)}{q} - \frac{1}{q^2 r}\sin(qr) = -r\left[\frac{\sin(qr)}{(qr)^2} - \frac{\cos(qr)}{qr}\right].\end{aligned} \tag{I.42}$$

Finally, because of the identity $\mathbf{q}\times\mathbf{k} = (\mathbf{k}'-\mathbf{k})\times\mathbf{k} = \mathbf{k}'\times\mathbf{k}$, the momentum representation of the spin-orbit interaction reads

$$\boxed{\langle\mathbf{k}'|\hat{V}|\mathbf{k}\rangle = \widetilde{V}_{LS}(q)\, i(\mathbf{k}'\times\mathbf{k})\cdot\hat{\mathbf{S}},\;\; \widetilde{V}_{LS}(q) = \frac{N_k}{(2\pi)^3}\;\times\Big(-\frac{4\pi}{q}\int_0^{+\infty} dr\, r^3\, j_1(qr)\, V_{LS}(r)\Big).} \tag{I.43}$$

in which $j_1(x) = \dfrac{\sin x}{x^2} - \dfrac{\cos x}{x}$ is the first order spherical Bessel function.

• **Tensor force:** In coordinate space, the tensor interaction is defined by

$$\langle\mathbf{r}'|\hat{V}|\mathbf{r}\rangle = \delta(\mathbf{r}'-\mathbf{r})\; V_T(r)\,\hat{S}_{12}(\mathbf{r}), \tag{I.44}$$

where the tensor operator (defined in Ref. [39]) is given in the coupled form

$$\hat{S}_{12}(\mathbf{r}) = 3\frac{(\hat{\boldsymbol{\sigma}}_1\cdot\mathbf{r})(\hat{\boldsymbol{\sigma}}_2\cdot\mathbf{r})}{r^2} - \hat{\boldsymbol{\sigma}}_1\cdot\hat{\boldsymbol{\sigma}}_2. \tag{I.45}$$

Using the identity (as a special case of the recoupling relation of commuting irreducible tensors, cf. Ref. [40])

$$\{\hat{\boldsymbol{\sigma}}\otimes\hat{\boldsymbol{\sigma}}\}_2\cdot\{\mathbf{A}\otimes\mathbf{B}\}_2 = (\hat{\boldsymbol{\sigma}}_1\cdot\mathbf{A})(\hat{\boldsymbol{\sigma}}_2\cdot\mathbf{B}) - \frac{1}{3}(\mathbf{A}\cdot\mathbf{B})(\hat{\boldsymbol{\sigma}}_1\cdot\hat{\boldsymbol{\sigma}}_2) + (\mathbf{A}\times\mathbf{B})\cdot(\hat{\boldsymbol{\sigma}}_1\times\hat{\boldsymbol{\sigma}}_2), \tag{I.46}$$

$(\mathbf{A},\mathbf{B}\in\mathbb{R}^3)$ to rewrite $\hat{S}_{12}(\mathbf{r})$ as the scalar product of two second rank irreducible tensors, one can write

$$\hat{S}_{12}(\mathbf{r}) = \frac{3}{r^2}\,\{\mathbf{r}\otimes\mathbf{r}\}_2\cdot\{\hat{\boldsymbol{\sigma}}\otimes\hat{\boldsymbol{\sigma}}\}_2,\;\text{with}\;\{\mathbf{r}\otimes\mathbf{r}\}_2 = \sqrt{\frac{8\pi}{15}}\,r^2\,Y_2(\hat{r}). \tag{I.47}$$

In this separable form, the tensor force is a local interaction in the sense specified in (I.23). From EQ. (I.24), one needs to compute the integral

$$\langle\mathbf{k}'|\hat{V}|\mathbf{k}\rangle = \frac{N_k}{(2\pi)^3}\;\times\;3\sqrt{\frac{8\pi}{15}}\int d^3\mathbf{r}\, e^{-i\mathbf{q}\cdot\mathbf{r}}\, V_T(r)\,\Big(Y_2(\hat{r})\cdot\{\hat{\boldsymbol{\sigma}}\otimes\hat{\boldsymbol{\sigma}}\}_2\Big). \tag{I.48}$$

One can separate the angular parts of $\mathbf{q}$ and $\mathbf{r}$ via the partial wave expansion

$$e^{-i\mathbf{q}\cdot\mathbf{r}} = 4\pi \sum_{l=0}^{\infty} \sum_{m=-l}^{l} i^{-l}\, j_l(qr)\, Y_{lm}(\hat{q}) \Big(Y_{lm}(\hat{r})\Big)^* \tag{I.49}$$

leading to

$$\begin{aligned}
&\int d^3\mathbf{r}\, e^{-i\mathbf{q}\cdot\mathbf{r}}\, V_T(r) \Big(Y_2(\hat{r})\cdot\{\hat{\boldsymbol{\sigma}}\otimes\hat{\boldsymbol{\sigma}}\}_2\Big) \\
&= 4\pi \sum_{l,m} i^{-l} \int_0^{+\infty} dr\, r^2 j_l(qr) V_T(r) \sum_{m_1,m_2} C^{00}_{2m_1 2m_2} Y_{lm}(\hat{q}) \{\hat{\boldsymbol{\sigma}}\otimes\hat{\boldsymbol{\sigma}}\}_{2m_2} \underbrace{\int d\hat{r} \Big(Y_{lm}(\hat{r})\Big)^* Y_{2m_1}(\hat{r})}_{\delta_{l2}\delta m m_1} \\
&= -4\pi \int_0^{+\infty} dr\, r^2\, j_2(qr)\, V_T(r) \;\times\; \Big(Y_2(\hat{q})\cdot\{\hat{\boldsymbol{\sigma}}\otimes\hat{\boldsymbol{\sigma}}\}_2\Big) \\
&= \sqrt{\frac{15}{8\pi}}\frac{1}{3} \times \Big[-\frac{3}{q^2} \times 4\pi \int_0^{+\infty} dr\, r^2\, j_2(qr)\, V_T(r)\Big] \times \Big(\underbrace{\sqrt{\frac{8\pi}{15}} q^2 Y_2(\hat{q})}_{\{\mathbf{q}\otimes\mathbf{q}\}_2} \cdot \{\hat{\boldsymbol{\sigma}}\otimes\hat{\boldsymbol{\sigma}}\}_2\Big).
\end{aligned} \tag{I.50}$$

The momentum representation of the tensor interaction thus reads as

$$\boxed{\begin{aligned}
\langle \mathbf{k}'|\hat{V}|\mathbf{k}\rangle &= \widetilde{V}_T(q) \Big(\{\mathbf{q}\otimes\mathbf{q}\}_2 \cdot \{\hat{\boldsymbol{\sigma}}\otimes\hat{\boldsymbol{\sigma}}\}_2\Big), \\
\widetilde{V}_T(q) &= \frac{N_k}{(2\pi)^3} \;\times\; \Big(-\frac{3}{q^2} \times 4\pi \int_0^{+\infty} dr\, r^2\, j_2(qr)\, V_T(r)\Big),
\end{aligned}} \tag{I.51}$$

where $j_2(x) = \Big(\dfrac{3}{x^3} - \dfrac{1}{x}\Big)\sin x - \dfrac{3}{x^2}\cos x$ denotes the second order spherical Bessel function.

• **Coulomb force:** The Coulomb interaction is local and takes the form

$$\langle \mathbf{r}'|\hat{V}_{\rm Coul}|\mathbf{r}\rangle = \delta(\mathbf{r}'-\mathbf{r})\; \frac{e^2}{r}. \tag{I.52}$$

In momentum space, using (I.24), one can write

$$\langle \mathbf{k}'|\hat{V}_{\rm Coul}|\mathbf{k}\rangle = \frac{N_k}{(2\pi)^3} \int d^3\mathbf{r}\, e^{-i\mathbf{q}\cdot\mathbf{r}}\; \frac{e^2}{r}. \tag{I.53}$$

Let us consider the Fourier transform of the Yukawa potential $\dfrac{e^{-\kappa r}}{r}$ and take the limit when the screening parameter κ tends to zero

$$\int d^3\mathbf{r}\, e^{-i\mathbf{q}\cdot\mathbf{r}}\; \frac{e^{-\kappa r}}{r} = \frac{4\pi}{\mathbf{q}^2+\kappa^2}, \tag{I.54}$$

thus

$$\langle \mathbf{k}'|\hat{V}_{\rm Coul}|\mathbf{k}\rangle = \frac{N_k}{(2\pi)^3}\; \frac{4\pi\, e^2}{|\mathbf{k}'-\mathbf{k}|^2}. \tag{I.55}$$

In the two-nucleon space $\mathcal{E}^{\otimes 2}$, the full representation of the Coulomb interaction reads

$$\boxed{\langle \mathbf{k}'|\hat{V}_{\rm Coul}|\mathbf{k}\rangle = \frac{N_k}{(2\pi)^3}\,\frac{4\pi\,e_0^2}{|\mathbf{k}'-\mathbf{k}|^2}\left(\frac{1}{4}+\frac{1}{12}\,(\hat{\boldsymbol{\tau}}_1\cdot\hat{\boldsymbol{\tau}}_2)+\sqrt{\frac{1}{24}}\,\{\hat{\boldsymbol{\tau}}\otimes\hat{\boldsymbol{\tau}}\}_{20}-\frac{1}{4}\,(\hat{\boldsymbol{\tau}}_1+\hat{\boldsymbol{\tau}}_2)_0\right)} \tag{I.56}$$

where it is supposed to act between proton states only.

I.6 Construction of two-body interaction in momentum space

I.6.1 Structure in momentum

Let us denote by $\mathbf{A}_i$ $(i=1,2,3)$ the combinations of relative momentum vectors $\mathbf{k}'+\mathbf{k}$, $\mathbf{k}'-\mathbf{k}$ and $\mathbf{k}'\times\mathbf{k}$. The following table shows how $\mathbf{A}_i$ behaves under time reversal, parity and permutation operations. Starting with the vectors $\mathbf{A}_i$, one can build

$\mathbf{A}_i$	$\mathbf{k}'+\mathbf{k}$	$\mathbf{k}'-\mathbf{k}$	$\mathbf{k}'\times\mathbf{k}$
$\hat{\mathcal{T}}$	$-$	$+$	$-$
$\hat{\Pi}$	$-$	$-$	$+$
$\hat{P}_{12}$	$-$	$-$	$+$

- scalar quantities of the form $\mathbf{A}_i\cdot\mathbf{A}_j$,
- tensors of first and second rank $\mathbf{A}_i$ and $\{\mathbf{A}_i\otimes\mathbf{A}_j\}_a$ $(a=1,2)$.

In principle, nothing prevents us to repeat infinitely the tensor product to form a tensor $\mathbf{T}_a$ of rank $a=0,1,2$

$$\mathbf{T}_a=\Big\{\{\mathbf{A}_i\otimes\mathbf{A}_j\}_{a_1}\otimes\mathbf{A}_k\}_{a_2}\otimes\ldots\Big\}_a\,. \tag{I.57}$$

In the case of a two-body interaction, we note that the vectors $\{\mathbf{A}_i\}$ can be used to serve as a basis in $\mathbb{R}^3$. Therefore, any tensor $\mathbf{T}_a$ could be expressed in terms of the simplest scalar and tensors of the form $\{\mathbf{A}_i\otimes\mathbf{A}_j\}_a$ as described above. The situation is different in multi-body systems when the number of independent relative momentum vectors is larger than three. For the two-nucleon system, let us summarize in two following tables the behavior of isospin and spin irreducible tensors under time reversal, space inversion and permutation transformations.

From these tables, we deduce that

- Classes I, II and III interactions, because their isospin part are even under all three considered transformations, possess a central force of the form

$$\widetilde{V}_C\,\mathbb{1}_s+\widetilde{V}_S\,(\hat{\boldsymbol{\sigma}}_1\cdot\hat{\boldsymbol{\sigma}}_2), \tag{I.58}$$

	$\mathbb{1}_t$	$\hat{\boldsymbol{\tau}}_1 \cdot \hat{\boldsymbol{\tau}}_2$	$\{\hat{\boldsymbol{\tau}} \otimes \hat{\boldsymbol{\tau}}\}_{20}$	$(\hat{\boldsymbol{\tau}}_1 + \hat{\boldsymbol{\tau}}_2)_0$	$(\hat{\boldsymbol{\tau}}_1 - \hat{\boldsymbol{\tau}}_2)_0$	$(\hat{\boldsymbol{\tau}}_1 \times \hat{\boldsymbol{\tau}}_2)_0$
$\hat{\mathcal{T}}$	+	+	+	+	+	−
$\hat{\Pi}$	+	+	+	+	+	+
$\hat{P}_{12}$	+	+	+	+	−	−

	$\mathbb{1}_s$	$\hat{\boldsymbol{\sigma}}_1 \cdot \hat{\boldsymbol{\sigma}}_2$	$\hat{\boldsymbol{\sigma}}_1 + \hat{\boldsymbol{\sigma}}_2$	$\hat{\boldsymbol{\sigma}}_1 - \hat{\boldsymbol{\sigma}}_2$	$\hat{\boldsymbol{\sigma}}_1 \times \hat{\boldsymbol{\sigma}}_2$	$\{\hat{\boldsymbol{\sigma}} \otimes \hat{\boldsymbol{\sigma}}\}_2$
$\hat{\mathcal{T}}$	+	+	−	−	+	+
$\hat{\Pi}$	+	+	+	+	+	+
$\hat{P}_{12}$	+	+	+	−	−	+

where $\widetilde{V}_C, \widetilde{V}_S$ are functions of the scalar quantities $\mathbf{A}_i \cdot \mathbf{A}_j$. Class IV interactions do not include this contribution because all scalar quantities are even as well as the spin operators.

- Similarly, time reversal and permutation invariances exclude from class IV the tensor contribution of the form

$$\widetilde{V}_T \ \{\mathbf{A}_i \otimes \mathbf{A}_j\}_2 \cdot \{\hat{\boldsymbol{\sigma}} \otimes \hat{\boldsymbol{\sigma}}\}_2 \tag{I.59}$$

  whereas the other classes include it. $\widetilde{V}_T$ should also be a general function of $\mathbf{A}_i \cdot \mathbf{A}_j$.

- Finally, the remaining terms are vectors in spin that can contribute to all four classes under the generic form

$$\sum_{i,j,k} \Big(\mathbf{A}_i \cdot (\hat{\boldsymbol{\sigma}}_1 + \hat{\boldsymbol{\sigma}}_2) + \mathbf{A}_j \cdot (\hat{\boldsymbol{\sigma}}_1 - \hat{\boldsymbol{\sigma}}_2) + \mathbf{A}_k \cdot (\hat{\boldsymbol{\sigma}}_1 \times \hat{\boldsymbol{\sigma}}_2) \Big). \tag{I.60}$$

  Thus for the first three classes, one only retains the term $\mathbf{A}_i = \mathbf{k}' \times \mathbf{k}$ associated to total spin operator while excluding the latter from the class IV and taking $\mathbf{A}_j = \mathbf{A}_k = \mathbf{k}' \times \mathbf{k}$.

I.6.2 Final form of the nucleon-nucleon interaction

Let us denote $\mathbf{k}' - \mathbf{k} = \mathbf{q}$, $\frac{1}{2}(\mathbf{k}' + \mathbf{k}) = \mathbf{p}$ and the total spin operator $\hat{\mathbf{S}} = \frac{1}{2}(\hat{\boldsymbol{\sigma}}_1 + \hat{\boldsymbol{\sigma}}_2)$. In momentum space the four classes of the nucleon-nucleon interaction thus read

(i) Class I:

$$\begin{aligned}\langle \mathbf{k}'|\hat{V}|\mathbf{k}\rangle = (\widetilde{V}_C^{(I)} + \widetilde{W}_C^{(I)}\,\hat{\boldsymbol{\tau}}_1\cdot\hat{\boldsymbol{\tau}}_2) + \Big(\widetilde{V}_S^{(I)} + \widetilde{W}_S^{(I)}\,\hat{\boldsymbol{\tau}}_1\cdot\hat{\boldsymbol{\tau}}_2\Big)\hat{\boldsymbol{\sigma}}_1\cdot\hat{\boldsymbol{\sigma}}_2 + \Big(\widetilde{V}_{LS}^{(I)} + \widetilde{W}_{LS}^{(I)}\,\hat{\boldsymbol{\tau}}_1\cdot\hat{\boldsymbol{\tau}}_2\Big) i(\mathbf{k}'\times\mathbf{k})\cdot\hat{\mathbf{S}} \\ + \Bigg(\Big(\widetilde{V}_T^{(I)} + \widetilde{W}_T^{(I)}\,\hat{\boldsymbol{\tau}}_1\cdot\hat{\boldsymbol{\tau}}_2\Big)\{\mathbf{q}\otimes\mathbf{q}\}_2 + \Big(\widetilde{V}_T^{\prime(I)} + \widetilde{W}_T^{\prime(I)}\,\hat{\boldsymbol{\tau}}_1\cdot\hat{\boldsymbol{\tau}}_2\Big)\{\mathbf{p}\otimes\mathbf{p}\}_2 + \\ \Big(\widetilde{V}_{\sigma L}^{(I)} + \widetilde{W}_{\sigma L}^{(I)}\,\hat{\boldsymbol{\tau}}_1\cdot\hat{\boldsymbol{\tau}}_2\Big)\{(\mathbf{k}'\times\mathbf{k})\otimes(\mathbf{k}'\times\mathbf{k})\}_2\Bigg)\cdot\{\hat{\boldsymbol{\sigma}}\otimes\hat{\boldsymbol{\sigma}}\}_2\end{aligned} \tag{I.61}$$

(ii) Class II:

$$\begin{aligned}\langle \mathbf{k}'|\hat{V}|\mathbf{k}\rangle = \Bigg[\widetilde{V}_C^{(II)}\mathbb{1}_s + \widetilde{V}_S^{(II)}\,\hat{\boldsymbol{\sigma}}_1\cdot\hat{\boldsymbol{\sigma}}_2 + \widetilde{V}_{LS}^{(II)}\,i(\mathbf{k}'\times\mathbf{k})\cdot\hat{\mathbf{S}} + \Big(\widetilde{V}_T^{(II)}\{\mathbf{q}\otimes\mathbf{q}\}_2 + \widetilde{V}_T^{\prime(II)}\{\mathbf{p}\otimes\mathbf{p}\}_2 \\ + \widetilde{V}_{\sigma L}^{(II)}\{(\mathbf{k}'\times\mathbf{k})\otimes(\mathbf{k}'\times\mathbf{k})\}_2\Big)\cdot\{\hat{\boldsymbol{\sigma}}\otimes\hat{\boldsymbol{\sigma}}\}_2\Bigg]\otimes\{\hat{\boldsymbol{\tau}}\otimes\hat{\boldsymbol{\tau}}\}_{20}\end{aligned} \tag{I.62}$$

(iii) Class III:

$$\begin{aligned}\langle \mathbf{k}'|\hat{V}|\mathbf{k}\rangle = \Bigg[\widetilde{V}_C^{(III)}\mathbb{1}_s + \widetilde{V}_S^{(III)}\,\hat{\boldsymbol{\sigma}}_1\cdot\hat{\boldsymbol{\sigma}}_2 + \widetilde{V}_{LS}^{(III)}\,i(\mathbf{k}'\times\mathbf{k})\cdot\hat{\mathbf{S}} + \Big(\widetilde{V}_T^{(III)}\{\mathbf{q}\otimes\mathbf{q}\}_2 + \widetilde{V}_T^{\prime(III)}\{\mathbf{p}\otimes\mathbf{p}\}_2 \\ + \widetilde{V}_{\sigma L}^{(III)}\{(\mathbf{k}'\times\mathbf{k})\otimes(\mathbf{k}'\times\mathbf{k})\}_2\Big)\cdot\{\hat{\boldsymbol{\sigma}}\otimes\hat{\boldsymbol{\sigma}}\}_2\Bigg]\otimes\{\hat{\boldsymbol{\tau}}_1+\hat{\boldsymbol{\tau}}_2\}_0\end{aligned} \tag{I.63}$$

(iv) Class IV:

$$\langle \mathbf{k}'|\hat{V}|\mathbf{k}\rangle = \widetilde{V}_1^{(IV)}\Big[i(\mathbf{k}'\times\mathbf{k})\cdot(\hat{\boldsymbol{\sigma}}_1-\hat{\boldsymbol{\sigma}}_2)\Big]\otimes(\hat{\boldsymbol{\tau}}_1-\hat{\boldsymbol{\tau}}_2)_0 + \widetilde{V}_2^{(IV)}\Big[i(\mathbf{k}'\times\mathbf{k})\cdot(\hat{\boldsymbol{\sigma}}_1\times\hat{\boldsymbol{\sigma}}_2)\Big]\otimes(\hat{\boldsymbol{\tau}}_1\times\hat{\boldsymbol{\tau}}_2)_0 \tag{I.64}$$

where $\widetilde{V}_\alpha, \widetilde{W}_\alpha$ are scalar functions of relative momentums $\mathbf{k}', \mathbf{k}$ and have to respect the hermiticity as well as the time reversal and space inversion invariances.

Chapter II

Low-momentum nuclear interactions

II.1 Brief overview of effective nuclear interactions

The construction of nuclear forces represents the first difficulty one has to deal with while studying properties of nuclei. Although there exists a variety of nuclear potentials that have been constructed: phenomenological, bare or chiral [9], [14], [16], they have a common property of being repulsive at short distance. Consequently, they involve high momentum states, and for that reason, make it difficult to converge many-body calculations due to the necessary basis truncations. Thus they need to be renormalized and be replaced with equivalent interactions where high momentum modes are resummed or absorbed.

Several approaches exist to construct such interactions. In general they differs from each other and each nuclear many-body method has its proper one. For example, the Brueckner G-matrix formalism [41]–[43] has been introduced in the fifties to derive an effective interaction from the nucleon-nucleon interaction in free space. The assumption is that nucleons in the nuclear medium do not feel the bare interaction and that the latter is substantially modified by the presence of other nucleons. By analogy with the scattering equation in free space, the high momentum modes are resummed into an energy-dependent reaction matrix that is determined by the Bethe-Goldstone equation [33]. The Brueckner theory is often employed in a relativistic Hartree-Fock framework [44], [45] with the semi-phenomenological high-precision two-nucleon CD-Bonn potential [16] as the bare interaction.

In contrast, in non-relativistic approaches such as the No-Core Shell Model, one usually uses methods based on the Lee-Suzuki-Okubo similarity transformation [46]–[48]. This method consists in the decoupling of the full Hilbert space into subspaces such that a part of the exact spectrum is conserved in the effective Hamiltonian defined in the chosen subspace. Because the Hamiltonian is rendered effective, as a consequence, to be consistent, it is also necessary to consider effective operators that are transformed in the same way when calculating observables.

More recently, the Similarity Renormalization Group (SRG) approach has been applied to treat the short-distance correlations present in realistic nuclear interactions [18]. In this approach, the

crucial point is to use an appropriate unitary transformation of the Hamiltonian that decouples low- and high-momentum modes while leaving observables unchanged. The desired decoupling is done via a series of infinitesimal unitary transformations under the form of a flow equation of the Hamiltonian. In practice, one often starts with a two- and three-body initial "bare" interactions and applies the SRG method in the two- and three-body spaces (see, e.g. [49]). The unitarity implies however that induced many-body interactions (in general up to A-body interactions, if one considers a nucleus of A nucleons) need to be properly taken into account. While such approach allows to soften the interaction, an other option is to perform the so-called In-Medium SRG (IM-SRG) [22], [50] that consists in evolving the A-body Hamiltonian in the A-body space (i.e. in the nuclear medium), which turns out to directly solve the many-body Schrödinger equation.

Alternatively, there are attempts to perform adjustment of non-empirical interactions to experimental data in finite nuclei. In this regard, the resulting interactions becomes phenomenological and are a priori restricted to the mass region where they are fitted. Typical examples are the cases of the N2LOsat [51] and Daejeon16 [52] forces. While the former is obtained by considering a direct fit of low-energy constants (LECs) of the (two-body) chiral potential [12] and three-body part [53], the Daejeon16 force is conceived quite differently. Starting from the N^{3}LO two-body force [12] evolved by SRG, the resulting interaction is subject to further phase-equivalent transformations (PETs) such that a good description of selected sample of nuclei is achieved. Light nuclei of mass $A \leq 16$ are selected in the case of Daejeon16 while N2LOsat is optimized including ^{3,4}He, ^{14}C and some heavier Oxygen isotopes of $A \leq 25$. In the last chapter of this thesis, we explore the ability of Daejeon16 to describe deformation and pairing correlations in ^{98}Sr which is beyond the mass region of this interaction. We found that it actually provides results at the mean-field level comparable with those obtained using the SRG-softened N^{3}LO chiral potential of Ref. [13].

II.2 Similarity-renormalization group approach to effective interactions

In the present work, we essentially start with the N^{3}LO chiral potential in Ref. [13] to construct a low-momentum interaction through the SRG approach and truncate the SRG flow equation at the two-body level. Let us summarize the SRG formalism and its basic working equations following Ref. [54].

Let us consider a unitary operator $\hat{U}_s$ depending on a real variable s and the corresponding similarity transformation of the hamiltonian $\hat{H}$

$$\hat{H}_s = \hat{U}_s \hat{H} \hat{U}_s^\dagger \, . \tag{II.1}$$

Because of the unitary character of $\hat{U}_s$

$$\forall s \, , \; \hat{U}_s^\dagger \hat{U}_s = \hat{U}_s \hat{U}_s^\dagger = \mathbb{1} \, , \tag{II.2}$$

one can deduce the following relation for the derivative of $\hat{U}_s^\dagger$ with respect to s

$$\hat{U}_s \frac{d\hat{U}_s^\dagger}{ds} = -\frac{d\hat{U}_s}{ds}\hat{U}_s^\dagger \,, \tag{II.3}$$

and rewrite the similarity transformation (II.1) of $\hat{H}$ in the differential form as

$$\begin{aligned}\frac{d\hat{H}_s}{ds} &= \frac{d\hat{U}_s}{ds}\hat{H}\hat{U}_s^\dagger + \hat{U}_s\hat{H}\frac{d\hat{U}_s^\dagger}{ds} \\ &= -\hat{U}_s\frac{d\hat{U}_s^\dagger}{ds}\underbrace{\hat{U}_s\hat{H}\hat{U}_s^\dagger}_{\hat{H}_s} + \underbrace{\hat{U}_s\hat{H}}_{\hat{H}_s\hat{U}_s}\frac{d\hat{U}_s^\dagger}{ds}\end{aligned}$$

Introducing the anti-hermitian operator

$$\hat{\eta}_s = -\hat{U}_s\frac{d\hat{U}_s^\dagger}{ds} = \frac{d\hat{U}_s}{ds}\hat{U}_s^\dagger \,, \tag{II.4}$$

one can write the similarity transformation (II.1) of $\hat{H}$ as a flow equation

$$\frac{d\hat{H}_s}{ds} = \left[\hat{\eta}_s, \hat{H}_s\right] \,. \tag{II.5}$$

With an appropriate choice of the generator defined by $\hat{\eta}_s \equiv \left[\hat{G}_s, \hat{H}_s\right]$, one can tailor the final form of the Hamiltonian $\hat{H}_\infty = \lim_{s\to\infty}\hat{H}_s = \hat{K} + \lim_{s\to\infty}\hat{V}_s$ and obtain

$$\boxed{\frac{d\hat{V}_s}{ds} = \left[\left[\hat{G}_s, \hat{K}+\hat{V}_s\right], \hat{K}+\hat{V}_s\right] \iff \frac{d\hat{V}_s}{ds} = \hat{G}_s(\hat{K}+\hat{V}_s)^2 + (\hat{K}+\hat{V}_s)^2\hat{G}_s - 2(\hat{K}+\hat{V}_s)\hat{G}_s(\hat{K}+\hat{V}_s).} \tag{II.6}$$

Since this is an operator equation, it must be solved in a (truncated) basis. There is a simple rule to write down the projected equation in the two-body space. Let suppose that in some predefined basis, the identity operator $\mathbb{1}$ is represented by a diagonal matrix $\mathcal{W}$ and an operator $\hat{A}$ is represented by the matrix A. Then

- by defining the matrix

$$V_s' = \sqrt{\mathcal{W}}\, V_s \sqrt{\mathcal{W}} \tag{II.7}$$

  the corresponding projected SRG equation takes the same commutator form as the left hand-side of (II.6)

$$\frac{dV_s'}{ds} = \left[\left[G_s, K+V_s'\right], K+V_s'\right] . \tag{II.8}$$

- otherwise, it is sufficient to insert the matrix $\mathcal{W}$ in the same way one inserts the closure relation $\mathbb{1}$ in the operator equation (right hand-side) (II.6).

In practice, the second option is more convenient since it allows to avoid the division by zero which could be present in the matrix $\mathcal{W}$. There are two usual choices of generators

- $\hat{G}_s = \hat{K}$ (relative kinetic energy) and $\hat{H}_s = \hat{K} + \hat{V}_s$: the Hamiltonian is driven to a diagonal form in the momentum basis ;
- $\hat{G}_s = \begin{pmatrix} \hat{P}\hat{H}_s\hat{P} & 0 \\ 0 & \hat{Q}\hat{H}_s\hat{Q} \end{pmatrix}$: the Hamiltonian is driven to a block-diagonal form with sharp cut-off by a decoupling momentum Λ_{NN}.

We find that the block-diagonal generator is more suitable for our purpose of studying the single-particle basis truncation. As we shall see in chapter IV, the decoupling momentum Λ_{NN} can be used to constrain the momentum truncation of the single-particle basis. Finally, although the Coulomb interaction should be consistently renormalized together with the nuclear interaction, we do not include it in the SRG evolution. Apart from the technical problem of treating the singularity at the origin in the partial-wave basis (as the nuclear interaction is transformed in that basis), the effect of renormalization is assumed here to be weak due to the long range and local characters of the Coulomb interaction. Indeed, its momentum dependence (I.55) implies that non-diagonal matrix elements decrease quickly away from the diagonal ones. This property is in line with the renormalization process using the above-defined SRG generators. Moreover, for bulk properties of nuclei (except superheavy nuclei) one could expect the dominance of the nuclear interaction over the Coulomb repulsion.

Chapter III

Hartree-Fock method in momentum space

With the assumption that nucleons (protons and neutrons considered as point-like particles) inside the nucleus move independently in a mean one-body potential commonly generated, the Hartree-Fock (HF) method allows to derive this average potential from a given underlying internucleon interaction. In this approach, one must first choose the imposed symmetries that define the lowest symmetry possessed by the one-body density. Secondly, as the determination of the nuclear self-consistent mean-field can be realized either via a discretized mesh representation or by choosing a predefined single-particle basis, one needs to make a careful study of the representation bases. In the present chapter, we consider two momentum representations, namely the three-dimensional (3D) plane-wave and the partial-wave bases. The HF method is developed with the triaxial symmetry in the former and with the axial symmetry in the latter.

III.1 Nuclear Hamiltonian

Assuming that neutrons and protons are of the same mass m, the nuclear Hamiltonian in the intrinsic frame associated to the nucleus composed of A nucleons is given by

$$\hat{H} = \hat{K} + \hat{V}_{\rm NN} + \hat{V}_{\rm Coul} - \frac{\hat{\mathbf{P}}^2_{\rm cm}}{2Am} \tag{III.1}$$

where $\hat{K}$ denotes the kinetic energy and $\hat{V}_{\rm NN}, \hat{V}_{\rm Coul}$ represent the two-body nuclear and Coulomb interactions respectively. In (III.1), the center-of-mass kinetic energy is subtracted to account for the translational invariance of $\hat{H}$. As $\hat{\mathbf{P}}_{\rm cm} = \sum_{i=1}^{A} \hat{\mathbf{p}}_i$, the Hamiltonian (III.1) can be rewritten as

$$\hat{H} = \Big(1 - \frac{1}{A}\Big)\hat{K} + \hat{V}_{\rm NN} + \hat{V}_{\rm Coul} - \hat{K}_2 \tag{III.2}$$

with the two-body kinetic energy correction

$$\hat{K}_2 = \frac{1}{2Am} \sum_{i \neq j} \hat{\mathbf{p}}_i \cdot \hat{\mathbf{p}}_j. \tag{III.3}$$

In the Hartree-Fock approach, the nuclear state is approximated by a Slater determinant $|\Phi\rangle$ where the Pauli principle is taken into account by anti-symmetrization. In second quantization, it takes the form

$$|\Phi\rangle = \prod_{i=1}^{A} \hat{a}_i^\dagger |0\rangle, \tag{III.4}$$

where $|0\rangle$ denotes the particle vacuum. For each such Slater determinant, there exists a one-to-one correspondence with the idempotent one-body density matrix (see Ref. [33])

$$\hat{\rho} = \sum_{i \in \Phi} |i\rangle\langle i|. \tag{III.5}$$

The desired Slater determinant is obtained by minimization of the Hartree-Fock energy $E_{\mathrm{HF}} = \langle\Phi|\hat{H}|\Phi\rangle$ under the constraint $\langle\Phi \,|\, \Phi\rangle = 1$. This leads to the condition that expresses the commutation of the one-body density matrix and a one-body hamiltonian $\hat{h}$

$$[\hat{h}, \hat{\rho}] = 0. \tag{III.6}$$

In other words, in the basis where the density $\hat{\rho}$ is diagonal, one can find the occupied single-particle states (in the Slater determinant $|\Phi\rangle$) by solving the corresponding one-body eigenvalue equation

$$\hat{h}|i\rangle = e_i|i\rangle. \tag{III.7}$$

This is the Hartree-Fock equation and the one-body Hartree-Fock Hamiltonian takes the form

$$\hat{h} = \Big(1 - \frac{1}{A}\Big)\frac{\hat{\mathbf{p}}^2}{2m} + \overline{v}_{\mathrm{NN}} + \overline{v}_{\mathrm{Coul}} - \overline{K}_2, \tag{III.8}$$

where for a two-body operator $\hat{V}$, its one-body reduction (denoted by $\overline{v}$) is defined by the matrix element

$$\langle a|\overline{v}|b\rangle = \sum_{i \in \Phi} \langle a, i|\hat{V}\,(\mathbb{1} - \hat{P}_{12})|b, i\rangle. \tag{III.9}$$

$\overline{K}_2$ denotes the corresponding one-body reduction of the two-body kinetic energy correction $\hat{K}_2$ while $\hat{P}_{12}$ acting on the two-body product state $|b, i\rangle$ represents the permutation operator. The Hartree-Fock potential is the sum of three contributions that are the one-body reductions of the interaction terms present in the Hamiltonian (III.2)

$$\hat{v}_{\mathrm{HF}} = \overline{v}_{\mathrm{NN}} + \overline{v}_{\mathrm{Coul}} - \overline{K}_2. \tag{III.10}$$

III.2 Three-dimensional plane-wave representation

In the 3D momentum-spin-isospin representation $\{|\mathbf{k}\sigma\tau\rangle, \mathbf{k} \in \mathbb{R}^3, \sigma = \pm\frac{1}{2}, \tau = \pm\frac{1}{2}\}$, the eigenvalue equation (III.7) becomes

$$\left(1 - \frac{1}{A}\right)\frac{(\hbar\mathbf{k})^2}{2m}\,\widetilde{\psi}_i^{(\sigma)}(\mathbf{k}) + \frac{1}{N_k}\sum_{\sigma'}\int_{\mathbb{R}^3} d^3\mathbf{k}'\,\langle\sigma|\widetilde{v}_{\mathrm{HF}}^{(\tau_i)}(\mathbf{k},\mathbf{k}')|\sigma'\rangle\,\widetilde{\psi}_i^{(\sigma')}(\mathbf{k}') = e_i\,\widetilde{\psi}_i^{(\sigma)}(\mathbf{k})\,. \tag{III.11}$$

with the wavefunction $\widetilde{\psi}_i^{(\sigma)}(\mathbf{k}) = \langle\mathbf{k}\sigma\,|\,i\rangle$. The superscript τ_i denotes the corresponding isospin quantum number of the single-particle $|i\rangle$. We have now to determine the matrix elements of the Hartree-Fock potential in the momentum-spin-isospin basis $\langle\sigma|\widetilde{v}_{\mathrm{HF}}^{(\tau_i)}(\mathbf{k},\mathbf{k}')|\sigma'\rangle$.

III.2.1 One-body reduction of a two-body interaction

For a two-body interaction $\hat{V}$, from the definition (III.9), the corresponding one-body reduction $\overline{v}$ reads

$$\langle\sigma|\overline{v}^{(\tau_i)}(\mathbf{k},\mathbf{k}')|\sigma'\rangle = \frac{1}{N_k^2}\sum_{\sigma_1,\sigma_2,\tau}\int d^3\mathbf{k}_1\int d^3\mathbf{k}_2\,\langle\mathbf{k}_2\sigma_2|\hat{\rho}^{(\tau)}|\mathbf{k}_1\sigma_1\rangle\,\langle\mathbf{k}\sigma\tau_i,\mathbf{k}_1\sigma_1\tau|\hat{V}|\widetilde{\mathbf{k}'\sigma'\tau_i,\mathbf{k}_2\sigma_2\tau}\rangle. \tag{III.12}$$

The two-body interaction $\hat{V}$ is Galilean- and translation-invariant. Consequently, the anti-symmetrized matrix element is proportional to a delta function

$$\begin{aligned}\langle\mathbf{k}\sigma\tau_i,\mathbf{k}_1\sigma_1\tau|\hat{V}|\widetilde{\mathbf{k}'\sigma'\tau_i,\mathbf{k}_2\sigma_2\tau}\rangle = N_k\,\delta(\mathbf{k}+\mathbf{k}_1-\mathbf{k}'-\mathbf{k}_2)\times\\ \Big(\langle\sigma\sigma_1,\tau_i\tau|\widetilde{V}(\mathbf{p},\mathbf{p}')|\sigma'\sigma_2,\tau_i\tau\rangle - \langle\sigma\sigma_1,\tau_i\tau|\widetilde{V}(\mathbf{p},-\mathbf{p}')|\sigma_2\sigma',\tau\tau_i\rangle\Big)\end{aligned} \tag{III.13}$$

where we have introduced the relative outgoing and ingoing momenta $\mathbf{p} = (\mathbf{k}-\mathbf{k}_1)/2$, $\mathbf{p}' = (\mathbf{k}'-\mathbf{k}_2)/2$. The delta function allows to suppress one of the integrals present in (III.12). After performing a change of variable, the one-body reduction matrix element becomes

$$\boxed{\begin{aligned}\langle\sigma|\overline{v}^{(\tau_i)}(\mathbf{k},\mathbf{k}')|\sigma'\rangle = 8\sum_{\sigma_1,\sigma_2,\tau}\frac{1}{N_k}\int d^3\mathbf{p}\,\widetilde{\rho}^{(\tau)}(\mathbf{k}'-2\mathbf{p},\sigma_2;\mathbf{k}'-2\mathbf{p}-\mathbf{q},\sigma_1)\times\\ (\langle\sigma\sigma_1,\tau_i\tau|\widetilde{V}(\mathbf{q}+\mathbf{p},\mathbf{p})|\sigma'\sigma_2,\tau_i\tau\rangle - \langle\sigma\sigma_1,\tau_i\tau|\widetilde{V}(\mathbf{q}+\mathbf{p},-\mathbf{p})|\sigma_2\sigma',\tau\tau_i\rangle)\end{aligned}} \tag{III.14}$$

with the momentum transfer $\mathbf{q} = \mathbf{k} - \mathbf{k}'$.

III.2.2 One-body reduction of the Coulomb interaction

In the case of the local Coulomb interaction which is spin-independent and acts only on proton states, the corresponding one-body reduction can be simplified into

$$\begin{aligned}\langle\sigma|\overline{v}^{(p)}_{\rm Coul}(\mathbf{k},\mathbf{k}')|\sigma'\rangle = 8\sum_{\sigma_1,\sigma_2}\frac{1}{N_k}\int d^3\mathbf{p}\;\widetilde{\rho}^{(p)}(\mathbf{k}'-2\mathbf{p},\sigma_2;\mathbf{k}'-2\mathbf{p}-\mathbf{q},\sigma_1)\\ \Big(\delta_{\sigma\sigma'}\delta_{\sigma_1\sigma_2}\widetilde{V}_{\rm Coul}(\mathbf{q})-\delta_{\sigma\sigma_2}\delta_{\sigma'\sigma_1}\widetilde{V}_{\rm Coul}(\mathbf{q}+2\mathbf{p})\Big)\end{aligned} \tag{III.15}$$

with $\widetilde{V}_{\rm Coul}(\mathbf{q}) = \dfrac{N_k}{(2\pi)^3}\dfrac{4\pi e^2}{\|\mathbf{k}-\mathbf{k}'\|^2}$. After replacing the silent variable $\mathbf{p}$ with $\mathbf{k}'-2\mathbf{p}$, we are left with a principal value integral

$$\langle\sigma|\overline{v}^{(p)}_{\rm Coul}(\mathbf{k},\mathbf{k}')|\sigma'\rangle = (2\pi)^{-3}\,4\pi e^2\,\mathcal{P}\int d^3\mathbf{p}\left(\sum_{\sigma''}\frac{\widetilde{\rho}^{(p)}(\mathbf{p},\sigma'';\mathbf{p}-\mathbf{q},\sigma'')}{\|\mathbf{q}\|^2}-\frac{\widetilde{\rho}^{(p)}(\mathbf{p},\sigma;\mathbf{p}-\mathbf{q},\sigma')}{\|\mathbf{k}-\mathbf{p}\|^2}\right). \tag{III.16}$$

To deal with the singularity at the origin, let us consider the action of $\overline{v}_{\rm Coul}$ onto a single-proton state $|i\rangle$

$$\begin{aligned}\langle\mathbf{k}\sigma|\overline{v}_{\rm Coul}|i\rangle = \frac{(2\pi)^{-3}}{N_k}\,4\pi e^2\sum_{\sigma'}\Bigg[\int d^3\mathbf{k}'\int d^3\mathbf{p}\Big(\sum_{\sigma''}\widetilde{\rho}^{(p)}(\mathbf{p}\sigma'';\mathbf{p}+\mathbf{k}'-\mathbf{k},\sigma'')\Big)\frac{\widetilde{\psi}_i^{(\sigma')}(\mathbf{k}')}{\|\mathbf{k}'-\mathbf{k}\|^2}\\ -\int d^3\mathbf{k}'\int d^3\mathbf{p}\;\widetilde{\rho}^{(p)}(\mathbf{p},\sigma;\mathbf{p}+\mathbf{k}'-\mathbf{k},\sigma')\frac{\widetilde{\psi}_i^{(\sigma')}(\mathbf{k}')}{\|\mathbf{p}-\mathbf{k}\|^2}\Bigg]\end{aligned} \tag{III.17}$$

After translating by $\mathbf{k}$ the integral variables,

$$\begin{aligned}\langle\mathbf{k}\sigma|\overline{v}_{\rm Coul}|i\rangle = \frac{(2\pi)^{-3}}{N_k}\,4\pi e^2\Bigg[\sum_{\sigma'}\int d^3\mathbf{k}'\left(\int d^3\mathbf{p}\sum_{\sigma''}\widetilde{\rho}^{(p)}(\mathbf{p}\sigma'';\mathbf{p}+\mathbf{k}',\sigma'')\right)\frac{\widetilde{\psi}_i^{(\sigma')}(\mathbf{k}'+\mathbf{k})}{\|\mathbf{k}'\|^2}\\ -\sum_{\sigma'}\int d^3\mathbf{k}'\left(\int d^3\mathbf{p}\;\frac{\widetilde{\rho}^{(p)}(\mathbf{p}+\mathbf{k},\sigma;\mathbf{p}+\mathbf{k}',\sigma')}{\|\mathbf{p}\|^2}\right)\widetilde{\psi}_i^{(\sigma')}(\mathbf{k}')\Bigg].\end{aligned} \tag{III.18}$$

Hence, in the spherical coordinates of $\mathbf{k}'$ and $\mathbf{p}$, the singularity at the origin is regularized

$$\boxed{\begin{aligned}\langle\mathbf{k}\sigma|\overline{v}_{\rm Coul}|i\rangle = \frac{(2\pi)^{-3}}{N_k}\,4\pi e^2\Bigg[\sum_{\sigma'}\int d\hat{k}'\left(\int d^3\mathbf{p}\sum_{\sigma''}\widetilde{\rho}^{(p)}(\mathbf{p}\sigma'';\mathbf{p}+\mathbf{k}',\sigma'')\right)\widetilde{\psi}_i^{(\sigma')}(\mathbf{k}'+\mathbf{k})\\ -\sum_{\sigma'}\int d^3\mathbf{k}'\left(\int d\hat{p}\;\widetilde{\rho}^{(p)}(\mathbf{p}+\mathbf{k},\sigma;\mathbf{p}+\mathbf{k}',\sigma')\right)\widetilde{\psi}_i^{(\sigma')}(\mathbf{k}')\Bigg].\end{aligned}} \tag{III.19}$$

III.2.3 One-body reduction of the kinetic energy correction

For the two-body kinetic energy correction contribution to the Hartree-Fock potential, its matrix elements in the 3D momentum-spin-isospin takes a simple analytical form

$$\langle \mathbf{k}_1\sigma_1\tau_1, \mathbf{k}_2\sigma_2\tau_2|\hat{K}_2|\mathbf{k}'_1\sigma'_1\tau'_1, \mathbf{k}'_2\sigma'_2\tau'_2\rangle = \frac{1}{Am}\delta_{\sigma_1\sigma'_1}\delta_{\sigma_2\sigma'_2}\delta_{\tau_1\tau'_1}\delta_{\tau_2\tau'_2}\Big(\langle \mathbf{k}_1|\hat{\mathbf{p}}|\mathbf{k}'_1\rangle \cdot \langle \mathbf{k}_2|\hat{\mathbf{p}}|\mathbf{k}'_2\rangle\Big), \tag{III.20}$$

with

$$\langle \mathbf{k}_1|\hat{\mathbf{p}}|\mathbf{k}'_1\rangle \cdot \langle \mathbf{k}_2|\hat{\mathbf{p}}|\mathbf{k}'_2\rangle = N_k^2\ \hbar^2\ \Big(\mathbf{k}_1 \cdot \mathbf{k}_2\Big)\,\delta(\mathbf{k}_1 - \mathbf{k}'_1)\delta(\mathbf{k}_2 - \mathbf{k}'_2). \tag{III.21}$$

The one-body reduction of the two-body kinetic energy correction $\langle \mathbf{k}\sigma|\overline{K_2}^{(\tau_i)}|\mathbf{k}'\sigma'\rangle$ thus becomes

$$\begin{aligned}
\langle \mathbf{k}\sigma|\overline{K_2}^{(\tau_i)}|\mathbf{k}'\sigma'\rangle &= \frac{1}{N_k^2}\,\frac{\hbar^2}{Am}\,N_k^2 \sum_{\tau,\sigma_1,\sigma_2}\int d^3\mathbf{k}_1 \int d^3\mathbf{k}_2\ \widetilde{\rho}^{(\tau)}(\mathbf{k}_2\sigma_2, \mathbf{k}_1\sigma_1)\times \\
&\Big(\delta_{\sigma\sigma'}\,\delta_{\sigma_1\sigma_2}\,\mathbf{k}\cdot\mathbf{k}_1\,\delta(\mathbf{k}-\mathbf{k}')\,\delta(\mathbf{k}_1-\mathbf{k}_2) - \delta_{\sigma\sigma_2}\,\delta_{\sigma'\sigma_1}\,\delta_{\tau\tau_i}\,\mathbf{k}\cdot\mathbf{k}'\,\delta(\mathbf{k}-\mathbf{k}_2)\,\delta(\mathbf{k}_1-\mathbf{k}')\Big) \\
&= \frac{\hbar^2}{Am}\Big[\delta_{\sigma\sigma'}\,\delta(\mathbf{k}-\mathbf{k}')\int d^3\mathbf{k}_1\,(\mathbf{k}\cdot\mathbf{k}_1)\sum_\tau\Big(\sum_{\sigma_1}\widetilde{\rho}^{(\tau)}(\mathbf{k}_1\sigma_1,\mathbf{k}_1\sigma_1)\Big) \\
&\qquad - \mathbf{k}\cdot\mathbf{k}'\,\widetilde{\rho}^{(\tau_i)}(\mathbf{k}\sigma,\mathbf{k}'\sigma')\Big],
\end{aligned} \tag{III.22}$$

that is, with the notation $\widetilde{\rho}(\mathbf{k}) = \sum_\tau\Big(\sum_\sigma \widetilde{\rho}^{(\tau)}(\mathbf{k}\sigma,\mathbf{k}\sigma)\Big)$

$$\langle \mathbf{k}\sigma|\overline{K_2}^{(\tau_i)}|\mathbf{k}'\sigma'\rangle = \frac{\hbar^2}{Am}\Big[\delta_{\sigma\sigma'}\,\delta(\mathbf{k}-\mathbf{k}')\int d^3\mathbf{k}''\,\widetilde{\rho}(\mathbf{k}'')\,(\mathbf{k}\cdot\mathbf{k}'') - (\mathbf{k}\cdot\mathbf{k}')\,\widetilde{\rho}^{(\tau_i)}(\mathbf{k}\sigma,\mathbf{k}'\sigma')\Big]. \tag{III.23}$$

Let us consider now the average momentum of the nucleus $\hat{\mathbf{P}}_{\rm cm} = \sum_{i=1}^{A}\hat{\mathbf{p}}_i$ in the Slater determinant $|\Phi\rangle$. In the momentum-spin basis,

$$\begin{aligned}
\langle\Phi|\hat{\mathbf{P}}_{\rm cm}|\Phi\rangle &= \sum_{i\in|\Phi\rangle}\langle i|\hat{\mathbf{p}}|i\rangle \qquad\qquad (\text{III.24})\\
&= \sum_{i\in|\Phi\rangle}\frac{1}{N_k}\int d^3\mathbf{k}\,\sum_\sigma\langle i\,|\,\mathbf{k}\sigma\rangle\,\langle\mathbf{k}\sigma|\hat{\mathbf{p}}|i\rangle \\
&= \frac{1}{N_k}\int d^3\mathbf{k}\,(\hbar\mathbf{k})\,\Big(\underbrace{\sum_\tau\sum_\sigma\sum_{i\in\Phi}\delta_{\tau\tau_i}\,\langle\mathbf{k}\sigma|\hat{\rho}^{(\tau)}|\mathbf{k}\sigma\rangle}_{\widetilde{\rho}(\mathbf{k})}\Big).
\end{aligned}$$

The direct term of $\langle \mathbf{k}\sigma|\overline{K}_2^{(\tau_i)}|\mathbf{k}'\sigma'\rangle$ is thus proportional to the average total momentum which, in the center-of-mass frame, should identically vanish if the one-body density matrix is invariant under parity. In the following we assume that this is always the case. Therefore, only the exchange term remains

$$\boxed{\langle \mathbf{k}\sigma|\overline{K_2}^{(\tau_i)}|\mathbf{k}'\sigma'\rangle = -\frac{\hbar^2}{Am}\,(\mathbf{k}\cdot\mathbf{k}')\,\widetilde{\rho}^{(\tau_i)}(\mathbf{k}\sigma,\mathbf{k}'\sigma').} \tag{III.25}$$

III.2.4 Hartree-Fock equation

Choice of imposed symmetries. As mentioned earlier, it is preferable to choose a symmetry that, at a moderate numerical cost, allows to incorporate correlations related to shape deformation. For this purpose, following Ref. [55], let us consider the subgroup $\mathbf{G}_{sc} = \mathrm{Gr}\{\hat{\Pi}, \hat{R}_z, \hat{S}_y^T\}$ of the dihedral double point-group $\mathbf{D}_{2h}^{DT} = \mathrm{Gr}\{\hat{\Pi}, \hat{R}_z, \hat{R}_y, \hat{T}\}$. An in-depth analysis of the latter in the Hartree-Fock approach is presented in Refs. [56]. The subgroup $\mathbf{G}_{sc}$ generated by the parity, the z-signature (the rotation of an angle π about the z-axis) and the anti-unitary y-time-simplex symmetry is a double group that allows to describe a triaxial shape and that is relevant to the description of an odd-fermion number system. In the one-nucleon Hilbert space, the action of the group elements in coordinate representation [55] is given by

$$\hat{\Pi}|\mathbf{r},\sigma\rangle = |-\mathbf{r},\sigma\rangle, \tag{III.26}$$
$$\hat{R}_z|\mathbf{r},\sigma\rangle = e^{-i\pi\sigma}|-x,-y,z,\sigma\rangle, \tag{III.27}$$
$$\hat{S}_y^T|\mathbf{r},\sigma\rangle = -|x,-y,z,\sigma\rangle. \tag{III.28}$$

In momentum representation, one has

$$\hat{\Pi}|\mathbf{k},\sigma\rangle = |-\mathbf{k},\sigma\rangle, \tag{III.29}$$
$$\hat{R}_z|\mathbf{k},\sigma\rangle = e^{-i\pi\sigma}|-k_x,-k_y,k_z,\sigma\rangle, \tag{III.30}$$
$$\hat{S}_y^T|\mathbf{k},\sigma\rangle = -|-k_x,k_y,-k_z,\sigma\rangle. \tag{III.31}$$

On the practical side, we note that to benefit from a "triaxial" reduction of the spatial domain in momentum space, $\hat{S}_y^T$ is not the suitable generator. The required generator should represent the symmetry with respect to the momentum k_x- or k_y-plane. Since the momentum changes sign under both time-reversal and parity symmetries, the y-time-signature operator $\hat{R}_y^T = \hat{\Pi}\hat{S}_y^T$ can be chosen to do the task. Indeed, its action onto a momentum-spin ket vector is given by

$$\hat{R}_y^T|\mathbf{k},\sigma\rangle = -|k_x,-k_y,k_z,\sigma\rangle, \tag{III.32}$$

which, together with the parity and z-signature, thus forms the counterpart of the case in coordinate representation. To realize the symmetry defined by $\mathbf{G}_{sc}$ in the single-particle states $\{|i\rangle\}$, let us impose the conditions

$$\hat{\Pi}|i\rangle = p|i\rangle, \;\; \hat{R}_z|i\rangle = r_z|i\rangle, \;\; \hat{R}_y^T|i\rangle = e^{i\theta}|i\rangle, \tag{III.33}$$

where p and r_z are parity and signature quantum numbers labelling the single-particle states whereas the anti-unitary symmetry does not give additional quantum number but leaves the state invariant. The phase $e^{i\theta}$ can be chosen to be unity. In the momentum representation, those

conditions imply that the wavefunction $\widetilde{\psi}_i^{(\sigma)}(\mathbf{k}) = \langle \mathbf{k}, \sigma \,|\, i \rangle$ is subjected to

$$\boxed{\begin{aligned} \widetilde{\psi}_i^{(\sigma)}(-\mathbf{k}) &= p\, \widetilde{\psi}_i^{(\sigma)}(\mathbf{k}), \\ \widetilde{\psi}_i^{(\sigma)}(-k_x, -k_y, k_z) &= e^{i\pi(\sigma-\eta_z)}\, \widetilde{\psi}_i^{(\sigma)}(k_x, k_y, k_z), \\ \widetilde{\psi}_i^{(\sigma)}(k_x, -k_y, k_z) &= -\Big(\widetilde{\psi}_i^{(\sigma)}(k_x, k_y, k_z)\Big)^*, \end{aligned}} \tag{III.34}$$

where the signature number η_z is defined by $r_z = e^{-i\pi\eta_z}$. With the relations (III.34) at our disposal, the Hartree-Fock equation (III.11) can be rewritten in the form

$$\boxed{\left(1 - \frac{1}{A}\right) \frac{(\hbar\mathbf{k})^2}{2m} \Big[\Psi\Big](\mathbf{k}) + \frac{1}{N_k} \int_{\mathbb{R}^3_+} d^3\mathbf{k}'\, \mathcal{V}^{(\tau,p,\eta_z)}(\mathbf{k}, \mathbf{k}') \Big[\Psi\Big](\mathbf{k}') = E \Big[\Psi\Big](\mathbf{k}),} \tag{III.35}$$

where $\mathbf{k}, \mathbf{k}' \in \mathbb{R}^3_+$, i.e. (III.34) was used to reduce the integral over $\mathbf{k}'$ in (III.11) into a one-eight momentum space. In (III.35), $\mathcal{V}^{(\tau,p,\eta_z)}$ is a four-by-four matrix and $\Big[\Psi\Big](\mathbf{k})$ a 4-component vector that is expressed in terms of the wave function $\widetilde{\psi}_i^{(\sigma)}(\mathbf{k})$. In practice, one can arrange the components of $\Big[\Psi\Big](\mathbf{k})$ to be complex or real functions. They can be defined as follows.

Case of complex component. In this case, $\Big[\Psi\Big](\mathbf{k})$ takes the form

$$\Big[\Psi\Big](\mathbf{k}) = \begin{bmatrix} \widetilde{\psi}_i^{(+)}(\mathbf{k}) \\ \widetilde{\psi}_i^{(-)}(\mathbf{k}) \\ \Big(\widetilde{\psi}_i^{(+)}(\mathbf{k})\Big)^* \\ \Big(\widetilde{\psi}_i^{(-)}(\mathbf{k})\Big)^* \end{bmatrix}. \tag{III.36}$$

The 4×4 matrix $\mathcal{V}^{(\tau,p,\eta_z)}$ is given by

$$\mathcal{V}^{(\tau,p,\eta_z)} = \begin{pmatrix} S_1 & -S_2 \\ -S_2^* & S_1^* \end{pmatrix}, \tag{III.37}$$

where the 2×2 (in spin space) matrices S_1, S_2 are determined through the Hartree-Fock potential $\widetilde{v}_{\mathrm{HF}}^{(\tau)}(\mathbf{k}, \mathbf{k}')$

$$\begin{aligned} S_1 &= \widetilde{v}_{\mathrm{HF}}^{(\tau)}(\mathbf{k}, \mathbf{k}') + p\, \widetilde{v}_{\mathrm{HF}}^{(\tau)}(\mathbf{k}, -\mathbf{k}') \\ &\quad + (-1)^{1/2-\eta_z} \Big(\widetilde{v}_{\mathrm{HF}}^{(\tau)}(\mathbf{k}, -k_x', -k_y', k_z') + p\, \widetilde{v}_{\mathrm{HF}}^{(\tau)}(\mathbf{k}, k_x', k_y', -k_z')\Big)\, \hat{\sigma}_z \end{aligned} \tag{III.38a}$$

$$\begin{aligned} S_2 &= \widetilde{v}_{\mathrm{HF}}^{(\tau)}(\mathbf{k}, k_x', -k_y', k_z') + p\, \widetilde{v}_{\mathrm{HF}}^{(\tau)}(\mathbf{k}, -k_x', k_y', -k_z') \\ &\quad + (-1)^{1/2-\eta_z} \Big(\widetilde{v}_{\mathrm{HF}}^{(\tau)}(\mathbf{k}, -k_x', k_y', k_z') + p\, \widetilde{v}_{\mathrm{HF}}^{(\tau)}(\mathbf{k}, k_x', -k_y', -k_z')\Big)\, \hat{\sigma}_z. \end{aligned} \tag{III.38b}$$

Furthermore, from the invariance of $\hat{v}_{\rm HF}$ under $\mathbf{G}_{sc}$, it can be shown that S_1 is hermitian and S_2 is symmetric under the interchange of momentum-spin variables,

$$\langle \mathbf{k}'\sigma'|S_1|\mathbf{k}\sigma\rangle = \langle \mathbf{k}\sigma|S_1|\mathbf{k}'\sigma'\rangle^*, \quad \langle \mathbf{k}'\sigma'|S_2|\mathbf{k}\sigma\rangle = \langle \mathbf{k}\sigma|S_2|\mathbf{k}'\sigma'\rangle. \tag{III.39}$$

It follows that $\mathcal{V}^{(\tau,p,\eta_z)}$ is hermitian.

Case of real component. By separating the real and imaginary parts of the wave function $\widetilde{\psi}_i^{(\sigma)}(\mathbf{k})$, $\Big[\Psi\Big](\mathbf{k})$ can be arranged into

$$\Big[\Psi\Big](\mathbf{k}) = \begin{pmatrix} \mathrm{Re}\,\widetilde{\psi}_i^{(+)}(\mathbf{k}) \\ \mathrm{Re}\,\widetilde{\psi}_i^{(-)}(\mathbf{k}) \\ \mathrm{Im}\,\widetilde{\psi}_i^{(+)}(\mathbf{k}) \\ \mathrm{Im}\,\widetilde{\psi}_i^{(-)}(\mathbf{k}) \end{pmatrix}. \tag{III.40}$$

The 4×4 matrix $\mathcal{V}^{(\tau,p,\eta_z)}$ is now a real symmetric matrix of the form

$$\mathcal{V}^{(\tau,p,\eta_z)} = \begin{pmatrix} \mathrm{Re}\,S_1 - \mathrm{Re}\,S_2 & -\mathrm{Im}\,S_1 - \mathrm{Im}\,S_2 \\ \mathrm{Im}\,S_1 - \mathrm{Im}\,S_2 & \mathrm{Re}\,S_1 + \mathrm{Re}\,S_2 \end{pmatrix}. \tag{III.41}$$

III.3 Momentum partial-wave representation

Let us now examine the spherical momentum partial-wave representation $\{|klm\sigma\rangle, k \in \mathbb{R}_+, l \in \mathbb{N}, -l \leq m \leq l, \sigma = \pm 1/2\}$. There are two differences in this representation in comparison with the 3D plane-wave:

- it can be directly adapted to the case of axial symmetry;
- the separation of the center-of-mass motion in a two-body system must be carried out via a transformation similar to the Moshinsky transformation [57] ;

Following the method described in Refs. [58], [59] in coordinate space, we first address the center-of-mass transformation in momentum space and discuss next the realization of the Hartree-Fock method in the partial-wave representation.

III.3.1 Two-body momentum partial-wave basis

In the two-body system, the two-body partial-wave basis vector is defined from the tensor product

$$|k_1 l_1 m_1, k_2 l_2 m_2\rangle = i^{-l_1-l_2} \int d^3\mathbf{k}_1' \int d^3\mathbf{k}_2' \frac{\delta(k_1'-k_1)}{k_1^2} \frac{\delta(k_2'-k_2)}{k_2^2} Y_{l_1 m_1}(\hat{k}_1') Y_{l_2 m_2}(\hat{k}_2') |\mathbf{k}_1'\mathbf{k}_2'\rangle. \tag{III.42}$$

By angular momentum coupling,

$$|(k_1 l_1, k_2 l_2)\lambda\mu\rangle = \sum_{m_1=-l_1}^{l_1} \sum_{m_2=-l_2}^{l_2} C^{\lambda\mu}_{l_1 m_1 l_2 m_2} |k_1 l_1 m_1, k_2 l_2 m_2\rangle, \tag{III.43}$$

the coupled angular momentum two-body state reads

$$\boxed{|(k_1 l_1, k_2 l_2)\lambda\mu\rangle = i^{-l_1-l_2} \int d^3\mathbf{k}_1' \int d^3\mathbf{k}_2' \frac{\delta(k_1'-k_1)}{k_1^2} \frac{\delta(k_2'-k_2)}{k_2^2} \{Y_{l_1}(\hat{k}_1') \otimes Y_{l_2}(\hat{k}_2')\}_{\lambda\mu} |\mathbf{k}_1'\mathbf{k}_2'\rangle.} \tag{III.44}$$

Let consider an other two-body partial-wave state $|klm, KLM\rangle$

$$|klm, KLM\rangle = i^{-l-L} \int d^3\mathbf{k}' \int d^3\mathbf{K}' \frac{\delta(k'-k)}{k^2} \frac{\delta(K'-K)}{K^2} Y_{lm}(\hat{k}') Y_{LM}(\hat{K}') |\mathbf{k}'\mathbf{K}'\rangle. \tag{III.45}$$

By performing the transformation

$$\begin{cases} \mathbf{k}' = s_1\mathbf{k}_1'' + t_1\mathbf{k}_2'' \\ \mathbf{K}' = s_2\mathbf{k}_1'' + t_2\mathbf{k}_2'' \end{cases}, \qquad \begin{cases} \mathbf{k}_1'' = p_1\mathbf{k}' + q_1\mathbf{K}' \\ \mathbf{k}_2'' = p_2\mathbf{k}' + q_2\mathbf{K}' \end{cases} \tag{III.46}$$

with the coefficients

$$\begin{aligned} p_1 &= \frac{t_2}{s_1 t_2 - s_2 t_1}, \quad & q_1 &= -\frac{t_1}{s_1 t_2 - s_2 t_1} \\ p_2 &= -\frac{s_2}{s_1 t_2 - s_2 t_1}, \quad & q_2 &= \frac{s_1}{s_1 t_2 - s_2 t_1}, \end{aligned} \tag{III.47}$$

the expression (III.45) is rewritten as

$$|klm, KLM\rangle = i^{-l-L} \int d^3\mathbf{k}_1'' \int d^3\mathbf{k}_2'' \, |J(s_1 s_2, t_1 t_2)| \frac{\delta(||s_1\mathbf{k}_1'' + t_1\mathbf{k}_2''|| - k)}{k^2} \frac{\delta(||s_2\mathbf{k}_1'' + t_2\mathbf{k}_2''|| - K)}{K^2} \times Y_{lm}(\widehat{s_1\mathbf{k}_1'' + t_1\mathbf{k}_2''}) Y_{LM}(\widehat{s_2\mathbf{k}_1'' + t_2\mathbf{k}_2''}) \, |\mathbf{k}_1''\mathbf{k}_2''\rangle \tag{III.48}$$

where $|J(s_1 s_2, t_1 t_2)|$ is the Jacobian of (III.46). By angular momentum coupling,

$$|(kl, KL)\lambda\mu\rangle = \sum_{m=-l}^{l} \sum_{M=-L}^{L} C^{\lambda\mu}_{lmLM} |klm, KLM\rangle, \tag{III.49}$$

we obtain

$$\boxed{\begin{aligned} |(kl, KL)\lambda\mu\rangle = i^{-l-L} \int d^3\mathbf{k}_1'' \int d^3\mathbf{k}_2'' \, |J(s_1 s_2, t_1 t_2)| \frac{\delta(||s_1\mathbf{k}_1'' + t_1\mathbf{k}_2''|| - k)}{k^2} \times \\ \frac{\delta(||s_2\mathbf{k}_1'' + t_2\mathbf{k}_2''|| - K)}{K^2} \left\{ Y_{lm}(\widehat{s_1\mathbf{k}_1'' + t_1\mathbf{k}_2''}) \otimes Y_{LM}(\widehat{s_2\mathbf{k}_1'' + t_2\mathbf{k}_2''}) \right\}_{\lambda\mu} |\mathbf{k}_1''\mathbf{k}_2''\rangle \end{aligned}}. \tag{III.50}$$

To separate the center-of-mass motion, the quantity of interest is the overlap $\langle (k_1 l_1, k_2 l_2)\lambda'\mu' \,|\, (kl, KL)\lambda\mu\rangle$ which will be referred to as vector bracket.

III.3.2 Vector bracket in momentum space

III.3.2.1 Expression of the vector bracket

Due to the Wigner-Eckart theorem, the vector bracket $\langle (k_1 l_1, k_2 l_2)\lambda'\mu' \,|\, (kl, KL)\lambda\mu\rangle$ is proportional to $\delta_{\lambda\lambda'}\delta_{\mu\mu'}$ and independent of μ. Moreover, because of (III.46), it is preferable to adopt the notation

$$\langle (s_1 s_2)k_1 l_1, (t_1 t_2)k_2 l_2; \lambda \,|\, kl, KL; \lambda\rangle = \langle (p_1 p_2)kl, (q_1 q_2)KL; \lambda \,|\, k_1 l_1, k_2 l_2; \lambda\rangle.$$

From the definitions (III.44),(III.50), one has

$$\begin{aligned}
&\langle (s_1 s_2)k_1 l_1, (t_1 t_2)k_2 l_2; \lambda \,|\, kl, KL; \lambda\rangle = i^{l_1+l_2-l-L} \times \int d^3\mathbf{k}_1'' \int d^3\mathbf{k}_2'' \;\; |J(s_1 s_2, t_1 t_2)| \\
&\int d^3\mathbf{k}_1' \int d^3\mathbf{k}_2' \frac{\delta(k_1' - k_1)}{k_1^2} \frac{\delta(k_2' - k_2)}{k_2^2} \frac{\delta(||s_1\mathbf{k}_1'' + t_1\mathbf{k}_2''|| - k)}{k^2} \frac{\delta(||s_2\mathbf{k}_1'' + t_2\mathbf{k}_2''|| - K)}{K^2} \times \\
&\{Y_{l_1}(\hat{k}_1') \otimes Y_{l_2}(\hat{k}_2')\}^*_{\lambda\mu} \cdot \left\{ Y_{lm}(s_1\widehat{\mathbf{k}_1'' + t_1}\mathbf{k}_2'') \otimes Y_{LM}(s_2\widehat{\mathbf{k}_1'' + t_2}\mathbf{k}_2'') \right\}_{\lambda\mu} \langle \mathbf{k}_1'\mathbf{k}_2' \,|\, \mathbf{k}_1''\mathbf{k}_2''\rangle
\end{aligned} \tag{III.51}$$

By averaging over the quantum number μ, the scalar product of two bipolar spherical harmonics thus depends on the angle of two vectors $(\mathbf{k}_1', \mathbf{k}_2')$. The last two delta functions fixes this angle while the first two delta functions eliminate the radial integrals over k_1', k_2'. We are left with two double integrals over the solid angles $\hat{k}_1', \hat{k}_2'$, which yield a factor $(4\pi)^2$. The closed form of the vector bracket thus reads

$$\boxed{\begin{aligned}
\langle (s_1 s_2)k_1 l_1, (t_1 t_2)k_2 l_2; \lambda \,|\, kl, KL; \lambda\rangle = N_k^2 i^{l_1+l_2-l-L} \frac{(4\pi)^2}{kKk_1k_2} \delta(w)\, \Theta(1-x^2) \times \\
|J(s_1 s_2, t_1 t_2)| \frac{1}{2\lambda+1} \sum_\mu \{Y_{l_1}(\hat{k}_1) \otimes Y_{l_2}(\hat{k}_2)\}^*_{\lambda\mu} \cdot \left\{ Y_{lm}(s_1\widehat{\mathbf{k}_1 + t_1}\mathbf{k}_2) \otimes Y_{LM}(s_2\widehat{\mathbf{k}_1 + t_2}\mathbf{k}_2) \right\}_{\lambda\mu}
\end{aligned}} \tag{III.52}$$

with

$$\begin{aligned}
w &= s_2 t_2 k^2 - s_1 t_1 K^2 + (t_1 s_2 - t_2 s_1)(s_1 s_2 k_1^2 - t_1 t_2 k_2^2), \\
x &= \cos(\widehat{\mathbf{k}_1, \mathbf{k}_2}) = \frac{K^2 - (s_2 k_1)^2 - (t_2 k_2)^2}{2 s_2 t_2 k_1 k_2}.
\end{aligned} \tag{III.53}$$

In the expression (III.52),

- the angles $\hat{k}_1, \hat{k}_2$ can be arbitrarily chosen;
- the delta function $\delta(w)$ expresses the "kinetic energy conservation" in laboratory and center-of-mass references;
- the Heaviside function $\Theta(1-x^2)$ restricts the center-of-mass variables (k, K) to their physical range

$$\boxed{\left| |s_1|k_1 - |t_1|k_2 \right| \le k \le |s_1|k_1 + |t_1|k_2, \;\; \left| |s_2|k_1 - |t_2|k_2 \right| \le K \le |s_2|k_1 + |t_2|k_2;} \tag{III.54}$$

- the vector bracket is real and even under parity, i.e. $(-)^{l_1+l_2+l+L} = 1$.

For a two-body system where $s_1 = -t_1 = 1/2, s_2 = t_2 = 1$, the vector bracket has an useful symmetry property under permutation $\hat{P}_{12}$,

$$\langle k_1 l_1, k_2 l_2; \lambda | \hat{P}_{12} | kl, KL; \lambda \rangle = (-)^l \langle k_1 l_1, k_2 l_2; \lambda \,|\, kl, KL; \lambda \rangle. \tag{III.55}$$

In the following, we will not refer to the coefficients s_1, s_2, t_1, t_2 for a two-body system and simply denote in that case $\langle k_1 l_1, k_2 l_2; \lambda \,|\, kl, KL; \lambda \rangle$.

III.3.2.2 Reduced vector bracket

In practice, it is convenient to express the vector bracket (III.52) as

$$\langle (s_1 s_2) k_1 l_1, (t_1 t_2) k_2 l_2; \lambda \,|\, kl, KL; \lambda \rangle = \frac{N_k^2}{k_1 k_2 K k} \delta(w)\, \Theta(1-x^2)\, ((s_1 s_2) k_1 l_1, (t_1 t_2) k_2 l_2; \lambda || kl, KL; \lambda) \tag{III.56}$$

with the reduced vector bracket

$$\boxed{\begin{aligned} &((s_1 s_2) k_1 l_1, (t_1 t_2) k_2 l_2; \lambda || kl, KL; \lambda) = i^{l_1+l_2-l-L}\, (4\pi)^2\, |J(s_1 s_2, t_1 t_2)| \times \\ &\frac{1}{(2\lambda+1)} \sum_\mu \{Y_{l_1}(\hat{k}_1) \otimes Y_{l_2}(\hat{k}_2)\}^*_{\lambda\mu} \cdot \left\{ Y_{lm}(s_1 \widehat{\mathbf{k}_1 + t_1 \mathbf{k}_2}) \otimes Y_{LM}(s_2 \widehat{\mathbf{k}_1 + t_2 \mathbf{k}_2}) \right\}_{\lambda\mu}. \end{aligned}} \tag{III.57}$$

Similarly, we define the corresponding quantity in the uncoupled scheme

$$\langle k_1 l_1 m_1, k_2 l_2 m_2 \,|\, klm, KLM \rangle = \frac{N_k^2}{k_1 k_2 K k}\, \delta(w)\, \Theta(1-x^2)\, (k_1 l_1 m_1, k_2 l_2 m_2 || klm, KLM) \tag{III.58}$$

with the uncoupled reduced vector bracket

$$(k_1 l_1 m_1, k_2 l_2 m_2 || klm, KLM) = \sum_{\lambda=\lambda_{\min}}^{\lambda_{\max}} C^{\lambda m+M}_{lmLM}\; C^{\lambda m_1+m_2}_{l_1 m_1 l_2 m_2} ((s_1 s_2) k_1 l_1, (t_1 t_2) k_2 l_2; \lambda || kl, KL; \lambda). \tag{III.59}$$

The lower and upper bounds of λ are respectively

$$\lambda_{\min} = \max(|\mathrm{l}_1 - \mathrm{l}_2|, |\mathrm{l} - \mathrm{L}|), \quad \lambda_{\max} = \min(\mathrm{l}_1 + \mathrm{l}_2, \mathrm{l} + \mathrm{L}).$$

III.3.2.3 Calculation of reduced vector bracket

The reduced vector bracket as defined above can be written explicitly as

$$\begin{aligned} &((s_1 s_2) k_1 l_1, (t_1 t_2) k_2 l_2; \lambda || kl, KL; \lambda) = i^{l_1+l_2-l-L}\, (4\pi)^2\, |J(s_1 s_2, t_1 t_2)| \times \\ &\frac{1}{(2\lambda+1)} \sum_\mu \sum_{m_1 m_2} \sum_{mM} C^{\lambda\mu}_{l_1 m_1 l_2 m_2}\, C^{\lambda\mu}_{lmLM}\, Y^*_{l_1 m_1}(\theta_1, \phi_1) Y^*_{l_2 m_2}(\theta_2, \phi_2) Y_{lm}(\theta, \phi) Y_{LM}(\Theta, \Phi). \end{aligned} \tag{III.60}$$

If we fix $(\theta_1, \phi_1) = (0, 0)$ and $\phi_2 = 0$, together with (III.46) we have

$$\cos\theta_2 = \cos(\widehat{\mathbf{k}_2, \mathbf{k}_1}) = \frac{K^2 - (s_2k_1)^2 - (t_2k_2)^2}{2s_2t_2k_1k_2} \tag{III.61}$$

$$\cos\theta = \cos(\widehat{\mathbf{k}, \mathbf{k}_1}) = \frac{k^2 + (s_1k_1)^2 - (t_1k_2)^2}{2s_1kk_1} \tag{III.62}$$

$$\cos\Theta = \cos(\widehat{\mathbf{K}, \mathbf{k}_1}) = \frac{K^2 + (s_2k_1)^2 - (t_2k_2)^2}{2s_2k_1K} \tag{III.63}$$

$$\cos\theta_a = \cos(\widehat{\mathbf{k}, \mathbf{k}_2}) = \frac{k^2 + (t_1k_2)^2 - (s_1k_1)^2}{2t_1k_2k} \tag{III.64}$$

$$\cos\theta_b = \cos(\widehat{\mathbf{K}, \mathbf{k}_2}) = \frac{K^2 + (t_2k_2)^2 - (s_2k_1)^2}{2t_2k_2K}. \tag{III.65}$$

There are thus two possibilities to find the angles (ϕ, Φ)

$$\phi = \begin{cases} 0 & \text{if } \theta = |\theta_a - \theta_2| \\ \pi & \text{if } \theta = |\theta_a + \theta_2| \end{cases}, \qquad \Phi = \begin{cases} 0 & \text{if } \Theta = |\theta_b - \theta_2| \\ \pi & \text{if } \Theta = |\theta_b + \theta_2| \end{cases}.$$

The choice of (θ_1, ϕ_1) means $m_1 = 0$. Since $m_2 = \mu = m + M$, only the sums over m, M remains

$$\boxed{\begin{aligned} &((s_1s_2)k_1l_1, (t_1t_2)k_2l_2; \lambda||kl, KL; \lambda) = i^{l_1+l_2-l-L}\,(4\pi)^2\ |J(s_1s_2, t_1t_2)| \times \\ &\frac{1}{2\lambda+1} \sum_{m=-l}^{l} \sum_{M=-L}^{L} C^{\lambda m+M}_{l_1 0 l_2 m+M}\, C^{\lambda m+M}_{lmLM}\, Y_{l_1 0}(0,0)\, Y_{l_2 m+M}(\theta_2, 0)\, Y_{lm}(\theta, \phi)\, Y_{LM}(\Theta, \Phi), \end{aligned}} \tag{III.66}$$

with $Y_{l_1 0}(0, 0) = \sqrt{\dfrac{2l_1 + 1}{4\pi}}$.

III.3.3 Axial symmetry in the partial-wave basis

In the case of parity and axial symmetry, that is to assume the Hartree-Fock mean-field is invariant under rotation about the z-axis and the inversion through the origin, eigenstates of parity $\hat{\Pi}$ and the z-component of the angular momentum operator $\hat{j}_z$ can be constructed with the projectors

$$\hat{P}(p) = \frac{1}{2}\Big(1 + \frac{\hat{\Pi}}{p}\Big), \quad \hat{P}(\Omega) = \prod_{\Omega' \neq \Omega} \frac{\hat{j}_z - \Omega'}{\Omega - \Omega'}, \tag{III.67}$$

with Ω', Ω denoting the quantum numbers of $\hat{j}_z$ and $p = \pm 1$ the parity quantum number. Applying these projectors onto a partial-wave-spin state $|klm\sigma\rangle$, a basis state having good parity and good angular momentum projection is given by

$$|\Omega, p(klm\sigma)\rangle = \frac{1}{2}\Big(1 + \frac{(-)^l}{p}\Big)\, \delta_{\Omega, m+\sigma}\, |klm\sigma\rangle. \tag{III.68}$$

With the notation

$$\Omega^p = \{(l,m,\sigma)|\ (-)^l = p,\ \ m+\sigma = \Omega,\ \ l \geq 0,\ m \in [-l,l],\ \sigma = \pm\frac{1}{2}\}, \tag{III.69}$$

a single-particle state $|i\rangle$ of definite isospin is then decomposed as

$$\boxed{|i\rangle = \frac{1}{N_k} \sum_{\Omega \in \mathbb{Z}+1/2} \sum_{p=-1}^{1} \sum_{(l,m,\sigma)\in\Omega^p} \int_0^{+\infty} dk\, k^2\, \widetilde{\psi}^{(\Omega,p)}_{lm\sigma}(k)\, |\Omega, p(klm\sigma)\rangle.} \tag{III.70}$$

III.3.4 Two-body matrix elements

We address now the matrix elements calculation of a two-body interaction $\hat{V}$ in the two-body partial-wave basis. By translational invariance, it can be shown that

$$\begin{aligned}
&\langle k_1' l_1' m_1' \sigma_1' \tau_1'; k_2' l_2' m_2' \sigma_2' \tau_2' | \hat{V} | k_1 l_1 m_1 \sigma_1 \tau_1; k_2 l_2 m_2 \sigma_2 \tau_2 \rangle \\
&= \frac{1}{N_k^3} \sum_{LM} \int_0^{+\infty} dK\, K^2 \sum_{l'm'} \int_0^{+\infty} dk'\, k'^2 \sum_{lm} \int_0^{+\infty} dk\, k^2 \langle k'l'm', \sigma_1'\sigma_2', \tau_1'\tau_2' | \hat{V} | klm, \sigma_1\sigma_2, \tau_1\tau_2 \rangle \times \\
&\quad \langle klm, KLM \,|\, k_1 l_1 m_1, k_2 l_2 m_2 \rangle \langle k_1' l_1' m_1', k_2' l_2' m_2' \,|\, k'l'm', KLM \rangle
\end{aligned} \tag{III.71}$$

where k, k' are the relative momenta in the center-of-mass reference and K the total momentum. To simplify this expression, let us express the delta functions of the vector bracket (III.52) as follows

$$\delta\Big(k'^2 + \frac{K^2}{4} - \frac{k_1'^2 + k_2'^2}{2}\Big) = \frac{1}{2k_0'}\, \delta(k' - k_0') \quad \text{with} \quad \begin{cases} k_0' = \sqrt{\dfrac{k_1'^2 + k_2'^2}{2} - \dfrac{K^2}{4}}, \\ \dfrac{K^2}{4} \leq \dfrac{k_1'^2 + k_2'^2}{2}. \end{cases} \tag{III.72}$$

Similarly for the incoming relative momentum k,

$$\delta\Big(k^2 + \frac{K^2}{4} - \frac{k_1^2 + k_2^2}{2}\Big) = \frac{1}{2k_0}\, \delta(k - k_0) \quad \text{with} \quad \begin{cases} k_0 = \sqrt{\dfrac{k_1^2 + k_2^2}{2} - \dfrac{K^2}{4}}, \\ \dfrac{K^2}{4} \leq \dfrac{k_1^2 + k_2^2}{2}. \end{cases} \tag{III.73}$$

From (III.54), the center-of-mass radial variables are restricted into

$$|k_1' - k_2'| \leq K \leq k_1' + k_2' \quad \text{and} \quad |k_1 - k_2| \leq K \leq k_1 + k_2. \tag{III.74}$$

III.3.4.1 General expression of two-body matrix elements

Using the delta function as expressed above, we can suppress the integrals over relative momenta (k', k) and the sums over (m', m). (III.71) is reduced to

$$\boxed{\begin{aligned}&\langle k_1' l_1' m_1' \sigma_1' \tau_1'; k_2' l_2' m_2' \sigma_2' \tau_2' | \hat{V} | k_1 l_1 m_1 \sigma_1 \tau_1; k_2 l_2 m_2 \sigma_2 \tau_2 \rangle = N_k \frac{1}{k_1' k_2' k_1 k_2} \cdot \frac{1}{4} \times \\ &\sum_{l'=0}^{+\infty} \sum_{l=0}^{+\infty} \sum_{L=L_{\min}}^{L_{\max}} \sum_{M=-L}^{L} \int_{K_{\min}}^{K_{\max}} dK \, \langle k_0' l' m', \sigma_1' \sigma_2', \tau_1' \tau_2' | \hat{V} | k_0 l m, \sigma_1 \sigma_2, \tau_1 \tau_2 \rangle \times \\ &\qquad (k_1' l_1' m_1', k_2' l_2' m_2' || k_0' l' m', KLM) \, (k_0 l m, KLM || k_1 l_1 m_1, k_2 l_2 m_2).\end{aligned}} \tag{III.75}$$

Because of the conservation of total momentum K, we have the restriction

$$\begin{cases} |k_1' - k_2'| \leq k_1 + k_2 \\ |k_1 - k_2| \leq k_1' + k_2' \end{cases} \quad \text{with} \quad \begin{cases} K_{\min} = \max(|k_1' - k_2'|, |k_1 - k_2|) \\ K_{\max} = \min(k_1' + k_2', k_1 + k_2). \end{cases} \tag{III.76}$$

From the angular momentum coupling relation (III.59), the center-of-mass angular momentum L varies from $L_{\min}$ to $L_{\max}$ by step of 2 (because of the vector bracket parity) where

$$\begin{cases} L_a = \max(0, |l_1' - l_2'| - l', l' - l_1' - l_2') \\ L_b = \max(0, |l_1 - l_2| - l, l - l_1 - l_2) \\ L_a \leq l_1 + l_2 + l \text{ and } L_b \leq l_1' + l_2' + l', \\ P_a = (-)^{l' + l_1' + l_2' + L_a}, \quad P_b = (-)^{l + l_1 + l_2 + L_b}, \\ L_1 = L_a + \frac{1}{2}\big(1 - P_a\big), \quad L_2 = L_b + \frac{1}{2}\big(1 - P_b\big), \\ P = (-)^{l + l_1 + l_2}, \quad L_0 = \max(L_1, L_2), \end{cases} \implies \begin{cases} L_{\min} = L_0 + \frac{1}{2}\big(1 - P \cdot (-)^{L_0}\big) \\ L_{\max} = \min(l_1' + l_2' + l', l_1 + l_2 + l). \end{cases} \tag{III.77}$$

Moreover, the third quantum numbers m', m and the variables k_0', k_0 are fixed by

$$\begin{cases} m' = m_1' + m_2' - M, & m = m_1 + m_2 - M \\ k_0' = \sqrt{\dfrac{k_1'^2 + k_2'^2}{2} - \dfrac{K^2}{4}}, & k_0 = \sqrt{\dfrac{k_1^2 + k_2^2}{2} - \dfrac{K^2}{4}}. \end{cases} \tag{III.78}$$

III.3.4.2 Anti-symmetrized two-body matrix elements

Due to the Pauli principle, we need to consider only anti-symmetrized two-body matrix elements. Upon coupling spin and isospin, the anti-symmetrized two-body matrix element is given by

$$\begin{aligned}\langle k_1' l_1' m_1' \sigma_1' \tau_1; k_2' l_2' m_2' \sigma_2' \tau_2 | \hat{V}(1-\hat{P}_{12}) | k_1 l_1 m_1 \sigma_1 \tau_1; k_2 l_2 m_2 \sigma_2 \tau_2 \rangle = N_k \frac{1}{k_1' k_2' k_1 k_2} \cdot \frac{1}{2} \times \\ \sum_{T=T_{\min}}^{1} (C^{T\tau_1+\tau_2}_{\frac{1}{2}\tau_1\frac{1}{2}\tau_2})^2 \sum_{l'=0}^{l_{\max}} \sum_{\substack{l= \\ \max(l'-2,l_{\max})}}^{\min(l'+2,l_{\max})} \sum_{S=S_{\min}}^{1} \sum_{J=J_{\min}}^{J_{\max}} C^{S\sigma_1'+\sigma_2'}_{\frac{1}{2}\sigma_1'\frac{1}{2}\sigma_2'} C^{S\sigma_1+\sigma_2}_{\frac{1}{2}\sigma_1\frac{1}{2}\sigma_2} \times \\ \sum_{L=L_{\min}}^{L_{\max}} \sum_{M=-L}^{L} C^{Jm'+\sigma_1'+\sigma_2'}_{l'm'S\sigma_1'+\sigma_2'} C^{Jm+\sigma_1+\sigma_2}_{lmS\sigma_1+\sigma_2} \int_{K_{\min}}^{K_{\max}} dK \, \langle k_0'(l'S)J, TT_z | \hat{V} | k_0(lS)J, TT_z \rangle \times \\ \left(\sum_{\lambda'=\lambda'_{\min}}^{\lambda'_{\max}} C^{\lambda' m'+M}_{l'm'LM} \; C^{\lambda' m_1'+m_2'}_{l_1' m_1' l_2' m_2'} (k_1' l_1', k_2' l_2'; \lambda' || k_0' l', KL; \lambda') \right) \times \\ \left(\sum_{\lambda=\lambda_{\min}}^{\lambda_{\max}} C^{\lambda m+M}_{lmLM} \; C^{\lambda m_1+m_2}_{l_1 m_1 l_2 m_2} (k_1 l_1, k_2 l_2; \lambda || k_0 l, KL; \lambda) \right),\end{aligned} \tag{III.79}$$

with the odd-partial-wave condition $(-)^{l+S+T} = -1$, where $T_z = \tau_1 + \tau_2$. The lower and upper bounds of S, T, J respectively reads

$$\begin{aligned} S_{\min} &= \max(|\sigma_1' + \sigma_2'|, |\sigma_1 + \sigma_2|), T_{\min} = \max(|\tau_1' + \tau_2'|, |\tau_1 + \tau_2|), \\ J_{\min} &= \max(|l' - S|, |l - S|, |m + \sigma_1 + \sigma_2|), \\ J_{\max} &= \min(l' + S, l + S) \\ \lambda'_{\min} &= \max(|l_1' - l_2'|, |l' - L|) \\ \lambda'_{\max} &= \min(l_1' + l_2', l' + L), \\ \lambda_{\min} &= \max(|l_1 - l_2|, |l - L|) \\ \lambda_{\max} &= \min(l_1 + l_2, l + L). \end{aligned} \tag{III.80}$$

In (III.79), $l_{\max}$ is the truncation value on the relative orbital quantum numbers l', l which satisfy $|l' - l| \leq 2$.

III.3.5 Discretized Hartree-Fock equation

The discretization of the Hartree-Fock equation in the partial-wave basis is now performed using the Lagrange-mesh method. To do so, we briefly recall the main ingredients of this method following Ref. [60] (for more details, see e.g. [61] and references therein). It is an approximate Ritz variational method using a specific set of the so-called Lagrange-functions $\{f_i(x)\}$ that are associated to a set of mesh points $\{x_i \in [a, b],\ i = 1, 2, ..., n\}$ and satisfy two conditions

$$f_i(x_j) = \lambda_i^{-1/2} \, \delta_{ij} \tag{III.81}$$

and

$$\int_a^b dx\, f_i^*(x) f_j(x) \approx \delta_{ij}. \tag{III.82}$$

While with the first condition, one can approximate any function $\Phi(x)$ based on its values at the mesh points, i.e.

$$\Phi(x) = \sum_{i=1}^{n} \Phi(x_i)\, f_i(x), \tag{III.83}$$

the second condition allows one to define the scalar product of functions that are expanded in the form (III.83). The values $\Phi(x_i)$ of the function $\Phi(x)$ at the mesh points $\{x_i\}$ could be regarded as variational expansion coefficients when one needs to solve Schrödinger-like equations of the form $H\Phi(x) = E\Phi(x)$. This is why the Lagrange-mesh method is considered as a Ritz variational method. Its approximate character often comes from the evaluation of matrix elements of the Hamiltonian H using the Lagrange functions $\{f_i(x)\}$. In practice, one has various choices of meshes that are usually taken from a Gauss quadrature rule (e.g. Hermite, Laguerre or Legendre). The coefficients $\{\lambda_i\}$ in that case are simply the associated weights of the considered Gauss quadrature. The essential feature of the Lagrange-mesh method is its simplicity since only matrix elements and wavefunctions at the mesh points are needed. In coordinate space, the accuracy of this method in mean-field calculations is studied for example in Ref. [62] using an equidistant mesh. Here, we consider the Legendre quadrature in the discretization of the Hartree-Fock equation in the partial-wave basis.

With the decomposition (III.70), the Hartree-Fock equation (III.7) is brought into

$$\begin{aligned}\sum_{(l_1,m_1,\sigma_1)\in\Omega_1^{p_1}} \Bigg[\Big(1-\frac{1}{A}\Big)\frac{(\hbar k_1')^2}{2m}\, \widetilde{\psi}^{(\Omega_1,p_1)}_{l_1 m_1\sigma_1}(k_1')\, \delta_{l_1' l_1}\delta_{m_1' m_1}\delta_{\sigma_1'\sigma_1} + \frac{1}{N_k}\int_0^{+\infty} dk_1\ k_1^2\ \times \\ \langle \Omega_1 p_1(k_1' l_1' m_1' \sigma_1')\tau_1 | \hat{v}_{\rm HF} | \Omega_1 p_1(k_1 l_1 m_1 \sigma_1)\tau_1\rangle \widetilde{\psi}^{(\Omega_1,p_1)}_{l_1 m_1\sigma_1}(k_1) \Bigg] = e_i\, \widetilde{\psi}^{(\Omega_1,p_1)}_{l_1' m_1' \sigma_1'}(k_1').\end{aligned} \tag{III.84}$$

Let us introduce the momentum truncation $k_{\rm max}^{\rm (sp)}$ and perform a change of variable

$$k = \frac{k_{\rm max}^{\rm (sp)}}{2}(\kappa+1), \quad \kappa \in [-1,1]. \tag{III.85}$$

By expanding the wavefunction onto n Lagrange-Legendre functions $f_\alpha(\kappa)$ defined in the interval $[-1,1]$ with the mesh points and weights $\{\kappa_\alpha, \lambda_\alpha\}$,

$$\widetilde{\psi}^{(\Omega_1,p_1)}_{l_1 m_1\sigma_1}(k_1) = \sum_{\alpha_1=1}^{n} C^{(\Omega_1,p_1)}_{l_1 m_1\sigma_1\alpha_1}\ \frac{f_{\alpha_1}(\kappa)}{k}, \tag{III.86}$$

one obtains the discretized equation

$$\boxed{\sum_{i_1=1}^{\mathcal{N}_{b_1}} \Bigg[\Big(1-\frac{1}{A}\Big)\frac{(\hbar k_{\alpha_1})^2}{2m}\, \delta_{i_1' i_1} + \frac{1}{N_k}\sqrt{w_{\alpha_1'} w_{\alpha_1}}\, k_{\alpha_1'} k_{\alpha_1}\ \times\ \widetilde{v}^{(b_1,\tau_1)}_{i_1' i_1} \Bigg] C^{(b_1)}_{i_1} = e_i\ C^{(b_1)}_{i_1'}} \tag{III.87}$$

with $w_{\alpha_1} = \dfrac{k_{\max}^{(\mathrm{sp})}}{2}\,\lambda_{\alpha_1}$. In (III.87), we have defined $\mathcal{N}_{b_1} = n \times \mathrm{card}(\Omega_1^{p_1})$ and the mappings

$$I_b : (\Omega, p) \longmapsto b \in \mathbb{N}_+, \quad I_{id} : (l, m, \sigma, \alpha) \longmapsto i \in \mathbb{N}_+. \tag{III.88}$$

Moreover, it is necessary to impose a truncation on the angular momentum projection Ω and the orbital angular momentum quantum number l which can be done as follows

$$\Omega_{\max} = l_{\max}^{(\mathrm{sp})} - \frac{1}{2}, \quad b_{\max} = 2\Omega_{\max} + 1 \quad (l_{\max}^{(\mathrm{sp})} \geq 1). \tag{III.89}$$

$b_{\max}$ is the number of diagonal blocks of the one-body discretized HF Hamiltonian.

III.3.6 Hartree-Fock potential in the partial-wave basis

The Hartree-Fock equation in the partial-wave representation, once discretized (III.87), takes a very simple form with the Lagrange-mesh method. The main source of complication lies in the preparation of the two-body matrix elements which, as we have seen, involves the vector bracket transformation. In what follows, we present an algorithm to calculate the Hartree-Fock potential for the two-body nuclear interaction. The main idea of this implementation is to exploit

- the radial-angular separation of the single-particle basis $\{|klm\sigma\rangle\}$;
- the symmetries of the two-body interaction: hermiticity, translation, parity, time-reversal, permutation and the convervation of nucleon number.

More precisely, the anti-symmetrized TBME (III.79) depends on the isospin, $\{\Omega\}$ quantum numbers of $\hat{j}_z$, the angular quantum numbers $\{(l, m, \sigma)\}$ and the radial momenta. So one needs to define appropriate sets associated to each of these variables. The role of each symmetry mentioned above is as follows:

- the time-reversal and permutation symmetries determine all possible combinations of $\hat{j}_z$ quantum numbers;
- the parity and the axial self-consistent symmetry limit the variation range of $\{l, m, \sigma\}$;
- the translation symmetry allows to store necessary quadruplet of single-particle momenta without redundancy;
- the hermiticity of the Hartree-Fock potential reduces further the involved two-body states $\{|k_1 l_1 m_1 \sigma_1, k_2 l_2 m_2 \sigma_2\rangle\}$ in (III.79).

Using these properties, we describe now the calculation of the one-body reduction of $\hat{V}$, which in the axial momentum basis takes the form

$$\begin{aligned}
&\langle\Omega_1 p_1(k_1' l_1' m_1' \sigma_1')\tau_1|\overline{v}|\Omega_1 p_1(k_1 l_1 m_1 \sigma_1)\tau_1\rangle = \frac{1}{N_k^2} \quad \times \\
&\sum_{\tau_2} \sum_{(l_2' m_2' \sigma_2')\in\Omega_2^{p_2}} \int_0^{+\infty} dk_2'\, k_2'^2 \sum_{(l_2 m_2 \sigma_2)\in\Omega_2^{p_2}} \int_0^{+\infty} dk_2\, k_2^2 \langle\Omega_2 p_2(k_2 l_2 m_2 \sigma_2)|\hat{\rho}^{(\tau_2)}|\Omega_2 p_2(k_2' l_2' m_2' \sigma_2')\rangle \quad \text{(III.90)} \\
&\langle\Omega_1 p_1(k_1' l_1' m_1' \sigma_1')\tau_1, \Omega_2 p_2(k_2' l_2' m_2' \sigma_2')\tau_2|\hat{V}(1-\hat{P}_{12})|\Omega_1 p_1(k_1 l_1 m_1 \sigma_1)\tau_1, \Omega_2 p_2(k_2 l_2 m_2 \sigma_2)\tau_2\rangle.
\end{aligned}$$

III.3.6.1 Discretized Hartree-Fock potential

In discretizing the radial integrals appearing in (III.90) with the conventions (III.88), we obtain the more compact form of the one-body reduction matrix element

$$\overline{v}^{(b_1,\tau_1)}_{i_1' i_1} = \frac{1}{N_k^2} \sum_{\tau_2} \sum_{b_2=1}^{b_{\max}} \sum_{i_2'=1}^{\mathcal{N}_{b_2}} \sum_{i_2=1}^{\mathcal{N}_{b_2}} w_{\alpha_2'} w_{\alpha_2}\, k_{\alpha_2'}^2 k_{\alpha_2}^2\, \widetilde{\rho}^{(b_2,\tau_2)}_{i_2 i_2'}\, \langle i_1' i_2', \tau_1\tau_2|\hat{V}(1-\hat{P}_{12})|i_1 i_2, \tau_1\tau_2\rangle. \quad \text{(III.91)}$$

As mentioned previously, with the symmetries of $\hat{V}$ and the vector bracket (III.55)

- first, since $C^{T\tau_2+\tau_1}_{\frac{1}{2}\tau_2\frac{1}{2}\tau_1} = (-)^{1-T}\, C^{T\tau_1+\tau_2}_{\frac{1}{2}\tau_1\frac{1}{2}\tau_2}$,

  $$\langle i_1' i_2', \tau_2\tau_1|\hat{V}(1-\hat{P}_{12})|i_1 i_2, \tau_2\tau_1\rangle = \langle i_1' i_2', \tau_1\tau_2|\hat{V}(1-\hat{P}_{12})|i_1 i_2, \tau_1\tau_2\rangle, \quad \text{(III.92)}$$

  the anti-symmetrized matrix element depends on the total isospin projection $T_z = \tau_1 + \tau_2$ alone;

- second, by vector bracket property (III.55) and $(-)^{l'} = (-)^{l}$ (parity symmetry of the interation in the center-of-mass frame),

  $$\langle i_2' i_1', \tau_1\tau_2|\hat{V}(1-\hat{P}_{12})|i_2 i_1, \tau_1\tau_2\rangle = \langle i_1' i_2', \tau_1\tau_2|\hat{V}(1-\hat{P}_{12})|i_1 i_2, \tau_1\tau_2\rangle, \quad \text{(III.93)}$$

  hence we can perform the permutation on the spin-momentum and isospin degree of freedoms separately;

- and third, the anti-symmetrized matrix element is real, hence using time-reversal symmetry,

  $$\begin{aligned}
  &\langle k_1' l_1' m_1' \sigma_1', k_2' l_2' m_2' \sigma_2'|\hat{V}(\mathbb{1}-\hat{P}_{12})|k_1 l_1 m_1 \sigma_1, k_2 l_2 m_2 \sigma_2\rangle = (-)^{\Omega_1'+\Omega_2'+\Omega_1+\Omega_2} \times \\
  &\langle k_1' l_1' - m_1' - \sigma_1', k_2' l_2' - m_2' - \sigma_2'|\hat{V}(\mathbb{1}-\hat{P}_{12})|k_1 l_1 - m_1 - \sigma_1, k_2 l_2 - m_2 - \sigma_2\rangle
  \end{aligned} \quad \text{(III.94)}$$

  with the definition $\Omega = m + \sigma$. Because of the axial self-consistent symmetry, $\Omega_1' = \Omega_1, \Omega_2' = \Omega_2$, hence $(-)^{\Omega_1'+\Omega_2'+\Omega_1+\Omega_2} = 1$.

Combining the permutation and time reversal, we can limit ourselves to the anti-symmetrized two-body matrix elements calculated for the axial quantum numbers (Ω_1, Ω_2) satisfying

$$\boxed{\begin{cases} \Omega_2 > 0, \quad \text{if} \quad \Omega_1 < 0, \\ \Omega_2 \geq \max(\frac{1}{2}, \Omega_1), \quad \text{if} \quad \Omega_1 > 0. \end{cases}} \tag{III.95}$$

In terms of the block indices (b_1, b_2),

$$\boxed{\begin{cases} b_1 = 1, ..., b_{\max}, \quad b_2 \geq \max\Big(b_1, \dfrac{b_{\max}}{2} + 1\Big), \\ n_{(b_1,b_2)} = \dfrac{3}{8}\, b_{\max}^2 + \dfrac{b_{\max}}{4}, \end{cases}} \tag{III.96}$$

where $n_{(b_1,b_2)}$ is the corresponding number of pair (b_1, b_2).

III.3.6.2 Use of NN interaction symmetries

The correspondences (III.88) are defined as follows

$$\begin{cases} p = \text{sign}\Big(b - \dfrac{b_{\max}}{2} - 1\Big) \times (-)^b, \\ \Omega = -\Omega_{\max} + \dfrac{2b - \Big(3 + (-)^b\Big)}{4}. \end{cases} \tag{III.97}$$

For example, $\Omega_{\max} = 5/2$,

Ω^p	$-\frac{5}{2}^+$	$-\frac{5}{2}^-$	$-\frac{3}{2}^+$	$-\frac{3}{2}^-$	$-\frac{1}{2}^+$	$-\frac{1}{2}^-$	$\frac{1}{2}^-$	$\frac{1}{2}^+$	$\frac{3}{2}^-$	$\frac{3}{2}^+$	$\frac{5}{2}^-$	$\frac{5}{2}^+$
b	1	2	3	4	5	6	7	8	9	10	11	12

By time-reversal transformation, the index b' associated to $-\Omega^p$ is thus

$$b' = b_{\max} + 1 - b. \tag{III.98}$$

Moreover, we have an useful property

$$b_1 \leq b_2 \leq b_{\max}/2 \iff b_1' \geq b_2' \geq b_{\max}/2 + 1. \tag{III.99}$$

With those relations, we can now specify how to use the interaction symmetries in the calculation of the HF potential (III.91). We distinguish five cases.

Case 1: $\Omega_1 = -\Omega_{\max}$, $b_1 = 1$.

$$\begin{cases} b_2 \in \left[1, \dfrac{b_{\max}}{2}\right]: \quad (b_1, b_2) \xrightarrow{\hat{\mathcal{T}}} (b_1', b_2') \xrightarrow{\hat{P}_{12}} (b_2', b_1'), \\ b_2 \in \left[\dfrac{b_{\max}}{2} + 1, b_{\max}\right]: \quad (b_1, b_2) \longrightarrow (b_1, b_2). \end{cases} \tag{III.100}$$

Case 2: $-\Omega_{\max} < \Omega_1 < -\frac{1}{2}$, $1 < b_1 < \frac{b_{\max}}{2}$.

$$\begin{cases} b_2 \in \left[1, b_1\right]: \quad (b_1, b_2) \xrightarrow{\hat{\mathcal{T}}} (b_1', b_2'), \\ b_2 \in \left[b_1 + 1, \dfrac{b_{\max}}{2}\right]: \quad (b_1, b_2) \xrightarrow{\hat{\mathcal{T}}} (b_1', b_2') \xrightarrow{\hat{P}_{12}} (b_2', b_1'), \\ b_2 \in \left[\dfrac{b_{\max}}{2} + 1, b_{\max}\right]: \quad (b_1, b_2) \longrightarrow (b_1, b_2). \end{cases} \tag{III.101}$$

Case 3: $\Omega_1 = -\frac{1}{2}$, $b_1 = \frac{b_{\max}}{2}$.

$$\begin{cases} b_2 \in \left[1, \dfrac{b_{\max}}{2}\right]: \quad (b_1, b_2) \xrightarrow{\hat{\mathcal{T}}} (b_1', b_2'), \\ b_2 \in \left[\dfrac{b_{\max}}{2} + 1, b_{\max}\right]: \quad (b_1, b_2) \longrightarrow (b_1, b_2). \end{cases} \tag{III.102}$$

Case 4: $\frac{1}{2} \leq \Omega_1 < \Omega_{\max}$, $\frac{b_{\max}}{2} + 1 \leq b_1 < b_{\max}$.

$$\begin{cases} b_2 \in \left[1, b_1\right]: \quad (b_1, b_2) \xrightarrow{\hat{P}_{12}} (b_2, b_1), \\ b_2 \in \left[b_1 + 1, b_{\max}\right]: \quad (b_1, b_2) \longrightarrow (b_1, b_2). \end{cases} \tag{III.103}$$

Case 5: $\Omega_1 = \Omega_{\max}$, $b_1 = b_{\max}$.

$$b_2 \in \left[1, b_{\max}\right]: \quad (b_1, b_2) \xrightarrow{\hat{P}_{12}} (b_2, b_1). \tag{III.104}$$

Translational invariant momenta set. To exploit the translation invariance, let us define the set of momenta obeying this symmetry

$$\mathcal{K} = \{(k_1', k_2', k_1, k_2), \quad |k_1' - k_2'| \leq k_1 + k_2 \text{ and } |k_1 - k_2| \leq k_1' + k_2'\}, \tag{III.105}$$

which can be partitioned into equivalence classes $\{\mathcal{K}_c\}$ as

$$\mathcal{K} = \bigcup_{c \in \mathbf{I}} \mathcal{K}_c. \tag{III.106}$$

The set $\mathbf{I}$ defines all distinct intervals $[K_{\min}, K_{\max}]$ over which one performs the integration in the anti-symmetrized matrix elements. Because of the radial-angular separable form of the axial basis,

it is desirable to define the sets

$$\mathbf{L} = \{(l_1', l_2', l_1, l_2), \quad (-)^{l_1'} = (-)^{l_1}, \quad (-)^{l_2'} = (-)^{l_2}\}, \tag{III.107}$$

and

$$\mathbf{S} = \{(\sigma_1', \sigma_2', \sigma_1, \sigma_2), \quad \sigma_i, \sigma_i' = \pm\frac{1}{2}, \quad i = 1, 2\}. \tag{III.108}$$

Therefore, to combine with the axial symmetry, one needs to determine the set of pairs (Ω_1, Ω_2) for each element of $\mathbf{L}$. Then the magnetic quantum numbers (m_1', m_2', m_1, m_2) satisfying the axial symmetry are determined by the definition $\Omega = m + \sigma,\ |m| \leq l$.

Relative NN matrix elements. To each interval $c \in \mathbf{I}$, suppose that each of them is discretized onto a mesh consisting of $N_K^{(c)}$ points. The number of corresponding relative matrix elements $\langle k'(l'S)JTT_z|\hat{V}|k(lS)JTT_z\rangle$ is therefore

$$n_{\mathrm{ME}} = 3 \times 6(J_{\max} + 1) \sum_{c\in\mathbf{I}} N_K^{(c)}\, \mathrm{card}(\mathcal{K}_c), \tag{III.109}$$

with $J_{\max} + 1 = l_{\max}$ which defines the odd partial waves set

$$\mathbf{Q} = \{(l, S, J, T, T_z)\}, \text{ such that } \begin{cases} S \in \{0,\ 1\},\ l \geq 0,\ |l - S| \leq J \leq l + S, \\ T_z \in \{-1, 0, +1\},\ T = \dfrac{1 + (-)^{l+S}}{2},\ T \geq |T_z|. \end{cases} \tag{III.110}$$

Reduced vector bracket. To calculate only necessary vector bracket, it is desirable to define the set

$$\mathcal{L} = \{(l_1, l_2, l, L, \lambda)\}, \text{ such that } \begin{cases} (-1)^{l_1+l_2+l+L} = 1, \\ \max(0, |l_1 - l_2| - l, l - l_1 - l_2) \leq L \leq l_1 + l_2 + l, \\ \max(|l_1 - l_2|, |l - L|) \leq \lambda \leq \min(l_1 + l_2, l + L). \end{cases} \tag{III.111}$$

To each equivalent class $\mathcal{K}_c$, one can extract its generating set $\mathbf{G}_c$ which contains distinct single-particle momentum pairs (k_1, k_2). Hence, the number of corresponding reduced vector bracket is given by

$$n_{\mathrm{VB}} = \mathrm{card}(\mathcal{L})\ \times \sum_{c\in\mathbf{I}} N_K^{(c)} \cdot \mathrm{card}(\mathbf{G}_c). \tag{III.112}$$

In practice, we use $N_K^{(c)} = const\ \forall c \in \mathbf{I}$.

Chapter IV

Hartree-Fock method in confined plane-wave basis

In this chapter, we revisit the 3D plane-wave representation considered previously. First, we construct a discrete basis by confining the continuous 3D plane-wave in a cubic box. The obtained discrete basis will be referred to as the confined plane-wave basis. Starting from the latter, we construct the single-particle basis adapted to the symmetry group $\mathbf{G}_{sc} = \mathrm{Gr}\{\hat{\Pi}, \hat{R}_z, \hat{R}_y^T\}$.

IV.1 Confined plane-wave representation

IV.1.1 Definition

Let us consider the one-dimensional plane-wave equation

$$\frac{d^2}{dx^2}\varphi(x) + k^2\,\varphi(x) = 0 \tag{IV.1}$$

with $k \in \mathbb{R}$. The plane-wave $\varphi(x)$ is required to satisfy the confinement condition

$$\varphi(x) = \begin{cases} A\,e^{ikx},\ x \in \big[-\frac{L}{2}, \frac{L}{2}\big] \\ 0,\ |x| > \frac{L}{2} \end{cases} \tag{IV.2}$$

where $L > 0$ defines the cubic edge length. Moreover, let us impose that the plane-waves $\{\varphi(x)\}$ are orthonormal in $[-L/2, L/2]$, hence,

$$A^2 \int_{-L/2}^{L/2} dx\, e^{i(k_1-k_2)x} = \delta_{k_1 k_2},\ k_1, k_2 \in \mathbb{R}. \tag{IV.3}$$

This condition implies $A = \dfrac{1}{\sqrt{L}}$ and

$$k_1 - k_2 = m\,\frac{2\pi}{L},\ m \in \mathbb{Z}. \tag{IV.4}$$

In particular, we note that there are two disjoint sets of orthornormal confined plane-waves verifying (IV.4) of the form

$$\varphi_m(x) = \frac{1}{\sqrt{L}}\,e^{ik_m x},\ x \in [-L/2, L/2] \tag{IV.5}$$

with $k_m = m\dfrac{2\pi}{L}$. The first set is characterized by $m \in \mathbb{Z}$ and the second by $m \in \mathbb{Z} + 1/2$.[1] For convenience, let us introduce the Dirac notation and define the confined plane-wave state with the coordinate representation

$$\langle x \,|\, \varphi_m \rangle = \varphi_m(x). \tag{IV.6}$$

Accordingly, in the three-dimensional case, one can define the state of momentum $\mathbf{k}_\alpha = \frac{2\pi}{L}(\alpha_x, \alpha_y, \alpha_z)$ as

$$\langle \mathbf{r} \,|\, \varphi_\alpha \rangle = \begin{cases} \dfrac{1}{L^{3/2}}\,e^{i\mathbf{k}_\alpha \cdot \mathbf{r}}, & \mathbf{r} \in [-L/2, L/2]^3 \\ \quad 0 \qquad , & \text{otherwise.} \end{cases} \tag{IV.7}$$

with the orthogonality relation

$$\langle \varphi_{\alpha'} \,|\, \varphi_\alpha \rangle = \delta_{\alpha'\alpha}. \tag{IV.8}$$

The index α thus refers to the triplet of indices $(\alpha_x, \alpha_y, \alpha_z)$. In the following sections, we will consider the states including spin $\{|\varphi_\alpha \sigma\rangle\}$ ($\sigma = \pm 1/2$) and denote it as the confined plane-wave basis.

IV.1.2 Properties

We examine now the properties of the confined plane-wave basis and the calculation of matrix elements (dropping the spin index).

Large box approximation. When the box size $L \to +\infty$, it can be shown that the confined plane-wave tends to the exact one of the same momentum, i.e we can write approximately

$$|\varphi_\alpha\rangle \approx \left(\frac{2\pi}{L}\right)^{3/2} \cdot \frac{1}{N_k^{3/2}}\,|\mathbf{k}_\alpha\rangle \tag{IV.9}$$

[1] We note that the sets of integer and half-integer values of the momentum index m can be alternatively found by imposing the boundary conditions $\varphi(-L/2) = \varphi(L/2)$ and $\varphi(-L/2) = -\varphi(L/2)$ respectively.

Kinetic matrix element. Due to the confinement condition (IV.2), the matrix element of the square momentum operator $\hat{\mathbf{p}}^2$ is proportional to a delta kronecker

$$\langle\varphi_{\alpha'}|\hat{\mathbf{p}}^2|\varphi_\alpha\rangle = (\hbar\mathbf{k}_\alpha)^2\,\delta_{\alpha\alpha'}. \tag{IV.10}$$

Two-body matrix elements. In the coordinate representation of the confined plane-wave basis, the matrix element of a Galilean- and translational-invariant two-body interaction $\hat{V}$ is given by

$$\begin{aligned}\langle\varphi_{\alpha_1'}\varphi_{\alpha_2'}|\hat{V}|\varphi_{\alpha_1}\varphi_{\alpha_2}\rangle = \int_{\mathbb{R}^3} d^3\mathbf{R}\int_{\mathbb{R}^3} d^3\mathbf{r}'\int_{\mathbb{R}^3} d^3\mathbf{r}\langle\varphi_{\alpha_1'}\,|\,\mathbf{R}+\frac{\mathbf{r}'}{2}\rangle\,\langle\varphi_{\alpha_2'}\,|\,\mathbf{R}-\frac{\mathbf{r}'}{2}\rangle\,\langle\mathbf{r}'|\hat{V}|\mathbf{r}\rangle \\ \langle\mathbf{R}+\frac{\mathbf{r}}{2}\,|\,\varphi_{\alpha_1}\rangle\,\langle\mathbf{R}-\frac{\mathbf{r}}{2}\,|\,\varphi_{\alpha_2}\rangle.\end{aligned} \tag{IV.11}$$

Let us denote the cubic domain $\mathcal{D}=[-L,L]^3$. Then, the confinement condition (IV.2) leads to the following restriction on integration variables: $\mathbf{r}',\mathbf{r}\in\mathcal{D}$ and $\mathbf{R}\in\mathcal{D}_{\mathbf{r}'}\cap\mathcal{D}_{\mathbf{r}}$ where $\mathcal{D}_{\mathbf{r}}=\mathcal{D}_x\times\mathcal{D}_y\times\mathcal{D}_z$ with, for instance,

$$\mathcal{D}_x=\Big[-\frac{L}{2}+\frac{|x|}{2},\frac{L}{2}-\frac{|x|}{2}\Big]. \tag{IV.12}$$

This peculiarity of the confined plane-wave basis will be used to simplify the calculation of matrix elements when combining with the short range property of the nuclear force and the specific local form of the Coulomb interaction.

IV.1.3 Approximate separation of the center-of-mass motion

When the box size is large enough compared to the range of the nuclear interaction, the variation domain of the center-of-mass coordinate $\mathbf{R}$ can be considered independent of the relative distances, i.e. $\mathcal{D}_x\approx[-L/2,L/2]$. This allows us to write (IV.11) in the coordinate representation of 3D confined plane-wave basis as

$$\langle\varphi_{\alpha_1'}\varphi_{\alpha_2'}|\hat{V}|\varphi_{\alpha_1}\varphi_{\alpha_2}\rangle \approx \Big(\frac{1}{L^3}\int\limits_{[-\frac{L}{2},\frac{L}{2}]^3} d^3\mathbf{R}e^{i(\mathbf{K}_{\alpha'}-\mathbf{K}_\alpha)\cdot\mathbf{R}}\Big)\,\frac{1}{L^3}\int\limits_{\mathcal{D}} d^3\mathbf{r}'e^{-i\mathbf{k}_{\alpha'}\cdot\mathbf{r}'}\int\limits_{\mathcal{D}} d^3\mathbf{r}e^{i\mathbf{k}_\alpha\cdot\mathbf{r}}\langle\mathbf{r}'|\hat{V}|\mathbf{r}\rangle, \tag{IV.13}$$

with the relative and center-of-mass momenta

$$\begin{cases}\mathbf{k}_\alpha=\frac{1}{2}(\mathbf{k}_{\alpha_1}-\mathbf{k}_{\alpha_2})\\ \mathbf{K}_\alpha=\mathbf{k}_{\alpha_1}+\mathbf{k}_{\alpha_2}.\end{cases}\qquad\begin{cases}\mathbf{k}_{\alpha'}=\frac{1}{2}(\mathbf{k}_{\alpha_1'}-\mathbf{k}_{\alpha_2'})\\ \mathbf{K}_{\alpha'}=\mathbf{k}_{\alpha_1'}+\mathbf{k}_{\alpha_2'}.\end{cases} \tag{IV.14}$$

Note that in (IV.13), the integral over the center-of-mass coordinate $\mathbf{R}$ can be identified with the scalar product of confined plane-wave states with momenta $\mathbf{K}_{\alpha'},\mathbf{K}_\alpha$. Moreover, because of the large box size in comparison with the force range, the remaining integrals in the coordinate space can be approximated by the momentum representation of $\hat{V}$. Therefore,

$$\boxed{\langle\varphi_{\alpha_1'}\varphi_{\alpha_2'}|\hat{V}|\varphi_{\alpha_1}\varphi_{\alpha_2}\rangle \approx \delta_{\alpha_1'+\alpha_2',\alpha_1+\alpha_2}\;\frac{1}{N_k^3}\Big(\frac{2\pi}{L}\Big)^3\,\langle\mathbf{k}_{\alpha'}|\hat{V}|\mathbf{k}_\alpha\rangle.} \tag{IV.15}$$

IV.1.4 Treatment of the Coulomb interaction

Since the Coulomb force has an infinite range, the approximation above no longer holds. The center-of-mass motion will be directly integrated. Because of the locality of the Coulomb interaction, (IV.11) is simplified into

$$\langle\varphi_{\alpha_1'}\varphi_{\alpha_2'}|\hat{V}_{\text{Coul}}|\varphi_{\alpha_1}\varphi_{\alpha_2}\rangle = \frac{1}{L^6}\int_{\mathcal{D}} d^3\mathbf{r}\, e^{i\mathbf{q}\cdot\mathbf{r}}\ \frac{e^2}{\|\mathbf{r}\|}\ \int_{\mathcal{D}_{\mathbf{r}}} d^3\mathbf{R}\, e^{i\mathbf{Q}\cdot\mathbf{R}} \tag{IV.16}$$

with the notation

$$\begin{cases} \mathbf{q} = \frac{1}{2}(\mathbf{k}_{\alpha_1'} - \mathbf{k}_{\alpha_2'}) - \frac{1}{2}(\mathbf{k}_{\alpha_1} - \mathbf{k}_{\alpha_2}) \\ \mathbf{Q} = (\mathbf{k}_{\alpha_1'} + \mathbf{k}_{\alpha_2'}) - (\mathbf{k}_{\alpha_1} + \mathbf{k}_{\alpha_2}). \end{cases} \tag{IV.17}$$

The integral over the center-of-mass coordinates takes a simple analytical form

$$\int_{\mathcal{D}_{\mathbf{r}}} d^3\mathbf{R}\, e^{i\mathbf{Q}\cdot\mathbf{R}} = f(Q_x, |x|)\, f(Q_y, |y|)\, f(Q_z, |z|) \tag{IV.18}$$

where

$$f(Q, |x|) = \Big(L - |x|\Big)\ \text{sinc}\Big(\frac{Q(L-|x|)}{2}\Big). \tag{IV.19}$$

Indeed, since the domain $\mathcal{D}_{\mathbf{r}}$ that depends on $\mathbf{r}$ is easily expressed in cartesian coordinates, it is sufficient to consider the one-dimensional integral, e.g. in the x-direction, $\int_{\mathcal{D}_x} dX\, e^{iQ_x X}$ which is straightforwardly given by (IV.19). In addition, because $f(Q, |x|)$ is an even function of x, the integral kernel of (IV.16) is symmetric under three plane-reflections with respect to the relative distance $\mathbf{r}$. As a consequence, one can reduce the full cubic domain $\mathcal{D}$ into $\mathcal{D}_c = [0, L]^3$. Adopting now the spherical coordinates, we are left with the following expression of the two-body Coulomb matrix element

$$\boxed{\begin{aligned}\langle\varphi_{\alpha_1'}\varphi_{\alpha_2'}|\hat{V}_{\text{Coul}}|\varphi_{\alpha_1}\varphi_{\alpha_2}\rangle = 8 \times \frac{e^2}{L^6}\int_{\mathcal{D}_c} d\varphi\ d\theta\ \sin\theta\ dr\, r\cos(x\,q_x)\ \cos(y\,q_y)\ \cos(z\,q_z)\times \\ f(Q_x, |x|)\, f(Q_y, |y|)\, f(Q_z, |z|),\end{aligned}} \tag{IV.20}$$

with the reduced cubic domain represented in spherical coordinates $(\varphi, \theta, r) \in \mathcal{D}_c = \bigcup_{i=1}^{4} \mathcal{D}_i$

$$\begin{cases} \mathcal{D}_1 = [0, \frac{\pi}{4}] \times [0, \arctan(\frac{1}{\cos\varphi})] \times [0, \frac{L}{\cos\theta}], \\ \mathcal{D}_2 = [0, \frac{\pi}{4}] \times [\arctan(\frac{1}{\cos\varphi}), \frac{\pi}{2}] \times [0, \frac{L}{\sin\theta\cos\varphi}], \\ \mathcal{D}_3 = [\frac{\pi}{4}, \frac{\pi}{2}] \times [0, \arctan(\frac{1}{\sin\varphi})] \times [0, \frac{L}{\cos\theta}], \\ \mathcal{D}_4 = [\frac{\pi}{4}, \frac{\pi}{2}] \times [\arctan(\frac{1}{\sin\varphi}), \frac{\pi}{2}] \times [0, \frac{L}{\sin\theta\sin\varphi}]. \end{cases} \tag{IV.21}$$

The singularity of the Coulomb interaction is therefore exactly regularized in the confined plane-wave basis. This is in contrast to the continuous 3D plane-wave representation where the regularization is done in the context of the Hartree-Fock method. In practice, to compute the matrix element (IV.20), we discretize the domain $\mathcal{D}_c$ using the Legendre quadrature rule. More specifically, a Legendre mesh in the θ-direction is associated with each tabulated value in the φ-direction. The size of the θ-mesh is fixed independently of the value of φ. Similarly, each tabulated value of θ corresponds to a r-mesh whose size is independent of θ. For all Hartree-Fock calculations involving the Coulomb interaction in this work, we use 20 points for the angular variables and 30 points for the radial one.

IV.2 Symmetry-adapted confined plane-wave basis

IV.2.1 Construction

The symmetry group $\mathbf{G}_{sc}$ generated by $(\hat{\Pi})$, z-signature $(\hat{R}_z)$ and the involutive anti-unitary y-time-signature $(\hat{R}_y^T)$ can be expressed as a coset partition

$$\mathbf{G}_{sc} = \mathbf{C}_{2h}^D \cup \hat{R}_y^T \mathbf{C}_{2h}^D \tag{IV.22}$$

where $\mathbf{C}_{2h}^D = \mathrm{Gr}\{\hat{\Pi}, \hat{R}_z\}$ is a double subgroup composed solely of linear operators. It is a double group because we are dealing with spin one-half particles requiring that [63]

$$\hat{R}_z^2 = \hat{R}_y^2 = -\mathbb{1}. \tag{IV.23}$$

The irreducible representation basis of $\mathbf{G}_{sc}$, following the method exposed in [64], is defined as the corresponding irreducible co-representations of $\mathbf{C}_{2h}^D$ with respect to the anti-unitary symmetry $\hat{R}_y^T$. Since $\mathbf{C}_{2h}^D$ is a abelian group, its irreducible representations are of dimension 1. The representation basis can be constructed through the use of projection operators [65]

$$\hat{P}(p) = \frac{1}{2}(\mathbb{1} + \frac{\hat{\Pi}}{p}), \;\; \hat{P}(r_z) = \frac{1}{2}(\mathbb{1} + \frac{\hat{R}_z}{r_z}) \tag{IV.24}$$

with the parity and signature $p = \pm 1$, $r_z = \pm i$. Starting from a confined plane-wave state $|\varphi_\alpha, \sigma\rangle$, the irreducible representation basis of $\mathbf{C}_{2h}^D$ is thus given by

$$|p, r_z(\alpha\sigma)\rangle = \hat{P}(p)\hat{P}(r_z)\,|\varphi_\alpha, \sigma\rangle. \tag{IV.25}$$

In this case of the anti-unitary symmetry $\hat{R}_y^T$, the Dimmock test shows that the irreducible representations of C_{2h}^D falls into type I according to Wigner classification. The vectors $\{|p, r_z(\alpha, \sigma)\rangle$, $\hat{R}_y^T|p, r_z(\alpha, \sigma)\rangle\}$ therefore form a reducible representation of C_{2h}^D that can be decomposed into two

equivalent one-dimensional irreducible representations

$$\mathrm{Vect}\{|p, r_z(\alpha,\sigma)\rangle, \hat{R}_y^T|p, r_z(\alpha,\sigma)\rangle\} = \bigoplus_{c\in\{-1,1\}} \mathrm{Vect}\{|p, r_z(c,\alpha,\sigma)\rangle\} \tag{IV.26}$$

with (A_0 is a normalization factor)

$$|p, r_z(c,\alpha,\sigma)\rangle = A_0\, \hat{Q}_c|p, r_z(\alpha,\sigma)\rangle, \tag{IV.27}$$

and

$$\hat{Q}_c = \frac{1}{2}(\mathbb{1} + c\hat{R}_y^T). \tag{IV.28}$$

Because $\hat{R}_y^T$ commutes with $\hat{\Pi}$ and anticommutes with $\hat{R}_z$, as a consequence, the following commutations hold

$$[\hat{Q}_c, \hat{P}(r_z)] = 0, \;\; [\hat{Q}_c, \hat{P}(p)] = 0. \tag{IV.29}$$

In addition, using the projector properties,

$$\begin{aligned} \hat{\Pi}\hat{P}(p) &= p\hat{P}(p), \\ \hat{R}_z\hat{P}(r_z) &= r_z\hat{P}(r_z), \\ \hat{R}_y^T\hat{Q}_c &= c\hat{Q}_c, \end{aligned} \tag{IV.30}$$

it follows that, under the action of the generators, the state $|p, r_z(c,\alpha,\sigma)\rangle$ transforms as

$$\hat{\Pi}|p, r_z(c,\alpha,\sigma)\rangle = p|p, r_z(c,\alpha,\sigma)\rangle \tag{IV.31a}$$
$$\hat{R}_z|p, r_z(c,\alpha,\sigma)\rangle = r_z|p, r_z(c,\alpha,\sigma)\rangle \tag{IV.31b}$$
$$\hat{R}_y^T|p, r_z(c,\alpha,\sigma)\rangle = c|p, r_z(c,\alpha,\sigma)\rangle. \tag{IV.31c}$$

Note that starting from two different confined plane-wave states of e.g. opposite momenta, the corresponding symmetry-adapted states obtained by projection are proportional. Indeed, owing to the transformation of confined plane-wave states,

$$\hat{\Pi}|\varphi_\alpha\sigma\rangle = |\varphi_{-\alpha}\sigma\rangle \tag{IV.32a}$$
$$\hat{R}_z|\varphi_\alpha\sigma\rangle = e^{-i\pi\sigma}|\varphi_{-\alpha_x,-\alpha_y,\alpha_z}\sigma\rangle \tag{IV.32b}$$
$$\hat{R}_y^T|\varphi_\alpha\sigma\rangle = -|\varphi_{\alpha_x,-\alpha_y,\alpha_z}\sigma\rangle, \tag{IV.32c}$$

and using (IV.30), it can be shown that

$$\begin{aligned} |p, r_z(c,-\alpha,\sigma)\rangle &= p|p, r_z(c,\alpha,\sigma)\rangle \\ |p, r_z(c,-\alpha_x,-\alpha_y,\alpha_z,\sigma)\rangle &= r_z\, e^{i\pi\sigma}|p, r_z(c,\alpha,\sigma)\rangle \\ |p, r_z(c,\alpha_x,-\alpha_y,\alpha_z,\sigma)\rangle &= -c\,|p, r_z(c,\alpha,\sigma)\rangle. \end{aligned} \tag{IV.33}$$

Therefore, to obtain the set of linear independent states $\{|p, r_z(c\,\alpha\sigma\rangle\}$, it is necessary to restrict the individual momenta $\{\mathbf{k}_\alpha\}$ into an one eight of $\mathbb{R}^3$. In the following, we use the notation $\mathbf{k}_\gamma$

with $\gamma = \{\gamma_x, \gamma_y, \gamma_z \geq 0\}$ whereas α refers to momenta $\{\mathbf{k}_\alpha\}$ without the restriction imposed by the symmetry group $\mathbf{G}_{sc}$. Moreover, let us adopt the notation $\lambda = (p, r_z)$. Then, by expanding the product of projectors in (IV.25), (IV.27), the symmetry-adapted state $|\lambda(c\gamma\sigma)\rangle$ is a linear combination of confined plane-waves

$$|\lambda(c\gamma\sigma)\rangle = \sum_\mu a_\mu^{(\lambda, c\gamma\sigma)} |\varphi_{S_\mu(\gamma)}\sigma\rangle, \tag{IV.34}$$

where the index μ labels the element $\hat{S} \in \mathbf{G}_{sc}$ which is present in the expansion of the projectors product. The corresponding mapping S_μ represents the action of $\hat{S}$ onto the momentum part

$$S_\mu(\gamma) \to (\epsilon_x^{(\mu)}\gamma_x, \epsilon_y^{(\mu)}\gamma_y, \epsilon_z^{(\mu)}\gamma_z), \quad \epsilon_m^{(\mu)} = \pm 1 \ \ (m = x, y, z). \tag{IV.35}$$

The symmetry-adapted states obtained for each momentum $\mathbf{k}_\gamma = \frac{2\pi}{L}(\gamma_x, \gamma_y, \gamma_z)$ respectively takes the following form for the groups $\mathbf{C}_{2h}^D$ and $\mathbf{G}_{sc}$.

$\mathbf{C}_{2h}^D = \mathrm{Gr}\{\hat{\Pi}, \hat{R}_z\}$.

$$|p, r_z(0,0,0,\sigma)\rangle = \frac{1}{2}\left(1 + \frac{e^{-i\pi\sigma}}{r_z}\right)\left(\frac{1+p}{2}\right) \ |\varphi_{0,0,0}, \sigma\rangle; \tag{IV.36a}$$

$$|p, r_z(0,0,\gamma_z,\sigma)\rangle = \begin{cases} \sqrt{2}\left(\frac{1+\frac{e^{-i\pi\sigma}}{r_z}}{2}\right)\hat{P}(p)|\varphi_{0,0,\gamma_z}, \sigma\rangle, & \gamma_z > 0 \\ 0, & \gamma_z < 0 \end{cases} \tag{IV.36b}$$

$$|p, r_z(\gamma_x,0,0,\sigma)\rangle = \begin{cases} \sqrt{2}\left(\frac{1+p\cdot\frac{e^{-i\pi\sigma}}{r_z}}{2}\right)\hat{P}(p)|\varphi_{\gamma_x,0,0}, \sigma\rangle, & \gamma_x > 0 \\ 0, & \gamma_x < 0 \end{cases} \tag{IV.36c}$$

$$|p, r_z(0,\gamma_y,0,\sigma)\rangle = \begin{cases} \sqrt{2}\left(\frac{1+p\cdot\frac{e^{-i\pi\sigma}}{r_z}}{2}\right)\hat{P}(p)|\varphi_{0,\gamma_y,0}, \sigma\rangle, & \gamma_y > 0 \\ 0, & \gamma_y < 0 \end{cases} \tag{IV.36d}$$

$$|p, r_z(\gamma_x,\gamma_y,0,\sigma)\rangle = \begin{cases} \sqrt{2}\left(\frac{1+p\cdot\frac{e^{-i\pi\sigma}}{r_z}}{2}\right)\hat{P}(p)|\varphi_{\gamma_x,\gamma_y,0}, \sigma\rangle, & \gamma_x > 0 \\ 0, & \gamma_x < 0 \end{cases} \tag{IV.36e}$$

$$|p, r_z(0,\gamma_y,\gamma_z,\sigma)\rangle = \begin{cases} \sqrt{4} \ \ \hat{P}(p)\hat{P}(r_z)|\varphi_{0,\gamma_y,\gamma_z}, \sigma\rangle, & \gamma_y, \gamma_z > 0 \\ 0, & \text{otherwise} \end{cases} \tag{IV.36f}$$

$$|p, r_z(\gamma_x,0,\gamma_z,\sigma)\rangle = \begin{cases} \sqrt{4} \ \ \hat{P}(p)\hat{P}(r_z)|\varphi_{\gamma_x,0,\gamma_z}, \sigma\rangle, & \gamma_x, \gamma_z > 0 \\ 0, & \text{otherwise} \end{cases} \tag{IV.36g}$$

$$|p, r_z(\gamma_x, \gamma_y, \gamma_z, \sigma)\rangle = \begin{cases} \sqrt{4}\ \hat{P}(p)\hat{P}(r_z)|\varphi_{\gamma_x,\gamma_y,\gamma_z}, \sigma\rangle, & \gamma_z > 0 \\ 0, & \gamma_z < 0. \end{cases} \tag{IV.36h}$$

$\mathbf{G}_{sc} = \mathrm{Gr}\{\hat{\Pi}, \hat{R}_z, \hat{R}_y^T\}$.

$$|p, r_z(c, 0, 0, 0, \sigma)\rangle = \frac{1}{8}(1+p)(1+\frac{e^{-i\pi\sigma}}{r_z})(1-c)|\varphi_{0,0,0}, \sigma\rangle, \tag{IV.37a}$$

$$|p, r_z(c, \gamma_x, 0, 0, \sigma)\rangle = \sqrt{2}\ \frac{(1-c)(1+p\cdot\frac{e^{-i\pi\sigma}}{r_z})}{4}\ \hat{P}(p)|\varphi_{\gamma_x,0,0}, \sigma\rangle, \tag{IV.37b}$$

$$|p, r_z(c, 0, \gamma_y, 0, \sigma)\rangle = \sqrt{2}\ \frac{(1-c\cdot\frac{e^{-i\pi\sigma}}{r_z})(1-c\cdot p)}{4}\hat{P}(p)|\varphi_{0,\gamma_y,0}, \sigma\rangle, \tag{IV.37c}$$

$$|p, r_z(c, 0, 0, \gamma_z, \sigma)\rangle = \sqrt{2}\ \frac{(1-c)(1+\frac{e^{-i\pi\sigma}}{r_z})}{4}\ \hat{P}(p)|\varphi_{0,0,\gamma_z}, \sigma\rangle, \tag{IV.37d}$$

$$|p, r_z(c, \gamma_x, \gamma_y, 0, \sigma)\rangle = \sqrt{4}\ \frac{(1+p\cdot\frac{e^{-i\pi\sigma}}{r_z})}{2}\hat{P}(p)\hat{Q}_c|\varphi_{\gamma_x,\gamma_y,0}, \sigma\rangle, \tag{IV.37e}$$

$$|p, r_z(c, 0, \gamma_y, \gamma_z, \sigma)\rangle = \sqrt{4}\ \frac{(1-c\cdot\frac{e^{-i\pi\sigma}}{r_z})}{2}\hat{P}(p)\hat{Q}_c|\varphi_{0,\gamma_y,\gamma_z}, \sigma\rangle, \tag{IV.37f}$$

$$|p, r_z(c, \gamma_x, 0, \gamma_z, \sigma)\rangle = \sqrt{4}\ \frac{(1-c)}{2}\ \hat{P}(p)\hat{P}(r_z)|\varphi_{\gamma_x,0,\gamma_z}, \sigma\rangle, \tag{IV.37g}$$

$$|p, r_z(c, \gamma_x, \gamma_y, \gamma_z, \sigma)\rangle = \sqrt{8}\ \hat{P}(p)\hat{P}(r_z)\hat{Q}_c|\varphi_{\gamma}, \sigma\rangle. \tag{IV.37h}$$

IV.2.2 One-body Hartree-Fock Hamiltonian

In the symmetry-adapted confined plane-wave basis, the one-body HF Hamiltonian (III.8) invariant under $\mathbf{G}_{sc}$ is of block diagonal form $\langle\lambda_1'(c_1'\gamma_1'\sigma_1')|\hat{h}^{(\tau_1)}|\lambda_1(c_1\gamma_1\sigma_1)\rangle = \delta_{\lambda_1'\lambda_1} h^{(\tau_1,\lambda_1)}_{c_1'\gamma_1'\sigma_1',c_1\gamma_1\sigma_1}$. This allows us to solve the HF equation by diagonalizing the Hamiltonian $h^{(\tau_1,\lambda_1)}$ for each block labeled by λ_1,

$$\sum_{c_1\gamma_1\sigma_1} h^{(\tau_1,\lambda_1)}_{c_1'\gamma_1'\sigma_1',c_1\gamma_1\sigma_1} C^{(i)}_{\lambda_1,c_1\gamma_1\sigma_1} = E\, C^{(i)}_{\lambda_1,c_1'\gamma_1'\sigma_1'}, \tag{IV.38}$$

with (A_0 is the normalization factor in (IV.27))

$$h^{(\tau_1,\lambda_1)}_{c_1'\gamma_1'\sigma_1',c_1\gamma_1\sigma_1} = A_0\left(1-\frac{1}{A}\right)\frac{(\hbar\mathbf{k}_{\gamma_1})^2}{2m}\,\delta_{\sigma_1'\sigma_1}\delta_{\gamma_1'\gamma_1} + \langle\lambda_1(c_1'\gamma_1'\sigma_1')|\hat{v}^{(\tau_1)}_{\mathrm{HF}}|\lambda_1(c_1\gamma_1\sigma_1)\rangle \tag{IV.39}$$

The corresponding single-particle HF state $|i\rangle$ is expanded onto the symmetry-adapted basis as

$$|i\rangle = \sum_{c_1\gamma_1\sigma_1} C^{(i)}_{\lambda_1,c_1\gamma_1\sigma_1}\,|\lambda_1(c_1\gamma_1\sigma_1)\rangle. \tag{IV.40}$$

Owing to the anti-unitary symmetry $\hat{R}_y^T$, the HF potential matrix element is such that

$$\boxed{\langle\lambda_1(c_1'\gamma_1'\sigma_1')|\hat{v}_{\rm HF}^{(\tau_1)}|\lambda_1(c_1\gamma_1\sigma_1)\rangle = \frac{A_0}{2}\Big(\langle\varphi_{\gamma_1'}\sigma_1'|\hat{v}_{\rm HF}^{(\tau_1)}|\lambda_1(c_1\gamma_1\sigma_1)\rangle + c_1'c_1\,\langle\varphi_{\gamma_1'}\sigma_1'|\hat{v}_{\rm HF}^{(\tau_1)}|\lambda_1(c_1\gamma_1\sigma_1)\rangle^*\Big).} \tag{IV.41}$$

To compute the HF potential in the symmetry-adapted basis, we first consider the "mixed" matrix element $\langle\varphi_{\gamma_1'}\sigma_1'|\hat{v}_{\rm HF}^{(\tau_1)}|\lambda_1(c_1\gamma_1\sigma_1)\rangle$ and then use (IV.41).

IV.2.3 Hartree-Fock potential in the symmetry-adapted basis

Let us consider the mixed matrix element of the one-body reduction $\overline{v}$ of a two-body interaction $\hat{V}$. Upon inserting (IV.40) and (IV.34) into (III.9), we obtain

$$\begin{aligned}\langle\varphi_{\gamma_1'}\sigma_1'|\overline{v}^{(\tau_1)}|\lambda_1(c_1\gamma_1\sigma_1)\rangle = \sum_{\tau_2}\sum_{\lambda_2}\sum_{c_2'\gamma_2'\sigma_2'}\sum_{c_2\gamma_2\sigma_2}\rho^{(\lambda_2,\tau_2)}_{c_2\gamma_2\sigma_2,c_2'\gamma_2'\sigma_2'}\sum_{\mu_2'\mu_1\mu_2} a_{\mu_2'}^{(\lambda_2,c_2'\gamma_2'\sigma_2')}\,a_{\mu_2}^{(\lambda_2,c_2\gamma_2\sigma_2)}\\ a_{\mu_1}^{(\lambda_1,c_1\gamma_1\sigma_1)}\,\langle\varphi_{\gamma_1'}\varphi_{S_{\mu_2'}(\gamma_2')},\sigma_1'\sigma_2',\tau_1\tau_2|\hat{V}(\mathbb{1}-\hat{P}_{12})|\varphi_{S_{\mu_1}(\gamma_1)}\varphi_{S_{\mu_2}(\gamma_2)},\sigma_1\sigma_2,\tau_1\tau_2\rangle\end{aligned} \tag{IV.42}$$

where $\rho^{(\lambda_2,\tau_2)}_{c_2\gamma_2\sigma_2,c_2'\gamma_2'\sigma_2'}$ is the matrix element of the one-body density (III.5).

One-body reduction of the NN interaction. The approximate center-of-mass motion (IV.11) due to the short range of nuclear force provides an additional simplification when calculating the nuclear HF potential. In this case, we can define the set

$$\mathcal{K} = \bigcup_{\gamma_1',\gamma_1}\mathcal{K}_{\gamma_1'\gamma_1} = \{(\mu_1,\gamma_2',\gamma_2,\mu_2',\mu_2,\alpha',\alpha)\ \ |\gamma_1' + S_{\mu_2'}(\gamma_2') = S_{\mu_1}(\gamma_1) + S_{\mu_2}(\gamma_2)\} \tag{IV.43}$$

which verify the translational invariance. The indices α',α define the corresponding relative momenta

$$\begin{cases}\mathbf{k}_{\alpha'} = \dfrac{1}{2}(\mathbf{k}_{\gamma_1'} - \mathbf{k}_{S_{\mu_2'}(\gamma_2')})\\ \mathbf{k}_{\alpha} = \dfrac{1}{2}(\mathbf{k}_{S_{\mu_1}(\gamma_1)} - \mathbf{k}_{S_{\mu_2}(\gamma_2)}).\end{cases} \tag{IV.44}$$

So that the nuclear HF potential can be re-arranged into

$$\begin{aligned}\langle\varphi_{\gamma_1'}\sigma_1'|\overline{v}_{\rm NN}^{(\tau_1)}|\lambda_1(c_1\gamma_1\sigma_1)\rangle = \sum_{\tau_2\sigma_2'\sigma_2}\sum_{\substack{i\in\\ \mathcal{K}_{\gamma_1'\gamma_1}}}\sum_{\mu_1} a_{\mu_1}^{(\lambda_1,c_1\gamma_1\sigma_1)}\Big(\sum_{\lambda_2\,c_2'c_2} a_{\mu_2'}^{(\lambda_2,c_2'\gamma_2'\sigma_2')}\,a_{\mu_2}^{(\lambda_2,c_2\gamma_2\sigma_2)}\,\rho^{(\lambda_2,\tau_2)}_{c_2\gamma_2\sigma_2,c_2'\gamma_2'\sigma_2'}\Big)\times\\ \langle\mathbf{k}_{\alpha'},\sigma_1'\sigma_2',\tau_1\tau_2|\hat{V}_{\rm NN}(\mathbb{1}-\hat{P}_{12})|\mathbf{k}_{\alpha},\sigma_1\sigma_2,\tau_1\tau_2\rangle\end{aligned} \tag{IV.45}$$

with $i = (\mu_1,\gamma_2',\gamma_2,\mu_2',\mu_2,\alpha',\alpha)$.

One-body reduction of the Coulomb interaction. On the other hand, in the case of the Coulomb force, the approximate treatment of the center-of-mass motion is no longer valid. However, by separating $\overline{v}_{\rm Coul}$ in (III.10) into direct and exchange contributions, the expression (IV.42)

becomes for the direct term

$$\langle\varphi_{\gamma_1'}\sigma_1'|\overline{v}^{(\mathrm{dir})}_{\mathrm{Coul}}|\lambda_1(c_1\gamma_1\sigma_1)\rangle = \delta_{\sigma_1\sigma_1'}\sum_{\mu_1}\Big(a^{(\lambda_1,c_1\gamma_1\sigma_1)}_{\mu_1}\sum_{\substack{\gamma_2'\mu_2'\\ \gamma_2\mu_2}}\langle\varphi_{\gamma_1'}\varphi_{S_{\mu_2'}(\gamma_2')}|\hat{V}_{\mathrm{Coul}}|\varphi_{S_{\mu_1}(\gamma_1)}\varphi_{S_{\mu_2}(\gamma_2)}\rangle\Big)\times \Big(\sum_{\lambda_2,\sigma_2'\sigma_2,c_2'c_2}\delta_{\sigma_2'\sigma_2}a^{(\lambda_2,c_2'\gamma_2'\sigma_2')}_{\mu_2'}\,a^{(\lambda_2,c_2\gamma_2\sigma_2)}_{\mu_2}\,\rho^{(\lambda_2,p)}_{c_2\gamma_2\sigma_2,c_2'\gamma_2'\sigma_2'}\Big), \tag{IV.46}$$

whereas the exchange term is defined as

$$\langle\varphi_{\gamma_1'}\sigma_1'|\overline{v}^{(\mathrm{exch})}_{\mathrm{Coul}}|\lambda_1(c_1\gamma_1\sigma_1)\rangle = \sum_{\mu_1}\Big(a^{(\lambda_1,c_1\gamma_1\sigma_1)}_{\mu_1}\sum_{\substack{\gamma_2'\mu_2'\\ \gamma_2\mu_2}}\langle\varphi_{\gamma_1'}\varphi_{S_{\mu_2'}(\gamma_2')}|\hat{V}_{\mathrm{Coul}}|\varphi_{S_{\mu_2}(\gamma_2)}\varphi_{S_{\mu_1}(\gamma_1)}\rangle\Big)\times \Big(\sum_{\lambda_2,\sigma_2'\sigma_2,c_2'c_2}\delta_{\sigma_1'\sigma_2}\delta_{\sigma_2'\sigma_1}a^{(\lambda_2,c_2'\gamma_2'\sigma_2')}_{\mu_2'}\,a^{(\lambda_2,c_2\gamma_2\sigma_2)}_{\mu_2}\,\rho^{(\lambda_2,p)}_{c_2\gamma_2\sigma_2,c_2'\gamma_2'\sigma_2'}\Big), \tag{IV.47}$$

so that $\overline{v}_{\mathrm{Coul}} = \overline{v}^{(\mathrm{dir})}_{\mathrm{Coul}} - \overline{v}^{(\mathrm{exch})}_{\mathrm{Coul}}$.

One-body reduction of the two-body kinetic energy correction. For the two-body kinetic energy correction $\hat{K}_2$ (III.3), we calculate its matrix element directly in the symmetry-adapted basis. It can be shown that the direct contribution is proportional to the center-of-mass momentum

$$\langle\lambda_1(c_1'\gamma_1'\sigma_1'),\tau_1|\overline{K}^{(\mathrm{dir})}_2|\lambda_1(c_1\gamma_1\sigma_1),\tau_1\rangle = \frac{1}{Am}\,\langle\lambda_1(c_1'\gamma_1'\sigma_1')|\hat{\mathbf{p}}|\lambda_1(c_1\gamma_1\sigma_1)\rangle\cdot\langle\Phi|\hat{\mathbf{P}}_{\mathrm{cm}}|\Phi\rangle \tag{IV.48}$$

which therefore vanishes in the center-of-mass frame attached to the nucleus due to the parity symmetry of the one-body density matrix. The corresponding one-body reduction of $\hat{K}_2$ is thus given by the exchange term

$$\langle\lambda_1(c_1'\gamma_1'\sigma_1'),\tau_1|\overline{K}^{(\tau_1)}_2|\lambda_1(c_1\gamma_1\sigma_1),\tau_1\rangle = -\frac{1}{Am}\,\delta_{\tau_1\tau_2}\delta_{\sigma_1'\sigma_2}\,\delta_{\sigma_2'\sigma_1}\delta_{\gamma_1'\gamma_2}\,\delta_{\gamma_2'\gamma_1} \sum_{\lambda_2}\sum_{c_2'c_2}\rho^{(\lambda_2,\tau_2)}_{c_2\gamma_2\sigma_2,c_2'\gamma_2'\sigma_2'}\,\Big(\langle\lambda_1(c_1'\gamma_1'\sigma_1')|\hat{\mathbf{p}}|\lambda_2(c_2\gamma_2\sigma_2)\rangle\cdot\langle\lambda_2(c_2'\gamma_2'\sigma_2')|\hat{\mathbf{p}}|\lambda_1(c_1\gamma_1\sigma_1)\rangle\Big). \tag{IV.49}$$

IV.3 Truncation scheme in confined plane-waves

The confined plane-wave basis $\{|\varphi_\alpha\sigma\rangle\}$ is characterized by the discrete equidistant momenta

$$\mathbf{k}_\alpha = \frac{2\pi}{L}(\alpha_x\mathbf{e}_x + \alpha_y\mathbf{e}_y + \alpha_z\mathbf{e}_z) \tag{IV.50}$$

which in turn are defined by the triplets of integers or half-integers $\alpha = (\alpha_x, \alpha_y, \alpha_z)$. To work with a finite set of states, we will first restrict the triplets $\{\alpha\}$ into a cubic mesh point centered at the origin, $\alpha \in \mathcal{A}^3_{1D}$ where

$$\mathcal{A}_{1D} = \{-\frac{N-1}{2}, ..., \frac{N-1}{2}\} \tag{IV.51}$$

which defines the equidistant one-dimensional mesh of size N. Hence odd values of N correspond to integer triplets and even values to the half-integer triplets. Second, we introduce a parameter Λ_b so as to select basis states of momenta $\|\mathbf{k}_\alpha\| \leq \Lambda_b$. Then for a given value of the box size L, N is chosen to retain all momenta inside the sphere of radius Λ_b. Let us denote the set of these momenta by

$$\mathcal{D}(\Lambda_b, L) = \{\mathbf{k}_\alpha,\ \|\mathbf{k}_\alpha\| \leq \Lambda_b,\ \ \alpha \in \mathcal{A}^3_{1D}\}. \tag{IV.52}$$

Owing to the triaxial symmetry group $\mathbf{G}_{sc}$, the single-particle momenta set $\mathcal{D}(\Lambda_b, L)$ is reduced to

$$\mathcal{D}_G(\Lambda_b, L) = \{\mathbf{k}_\gamma \in \mathcal{D}(\Lambda_b, L),\ \ \gamma_x, \gamma_y, \gamma_z \geq 0\}. \tag{IV.53}$$

In particular, for N-even, we have a simple relation $\mathrm{card}(\mathcal{D}_G(\Lambda_b, L)) = \mathrm{card}(\mathcal{D}(\Lambda_b, L))/8$ whereas for N-odd, due to the zero point, one needs a specific treatment of points lying on different axes and planes. Therefore, the overall factor 8 is not possible.

Within this truncation and owing to the equidistant property, the set of relative momenta generated by the single-particle basis $\{|\varphi_\alpha \sigma\rangle\}$ is given by definition (IV.14)

$$\begin{cases} \mathbf{k}_\alpha = \dfrac{\pi}{L}(\alpha_x, \alpha_y, \alpha_z),\ \|\mathbf{k}_\alpha\| \leq \Lambda_b \\ \alpha_x, \alpha_y, \alpha_z \in \{-N+1, ..., N-1\} \end{cases} \tag{IV.54}$$

Similarly, the set of transfer momenta (IV.17) is determined by

$$\begin{cases} \mathbf{q}_\alpha = \dfrac{\pi}{L}(\alpha_x, \alpha_y, \alpha_z),\ \|\mathbf{q}_\alpha\| \leq 2\Lambda_b \\ \alpha_x, \alpha_y, \alpha_z \in \{-2(N-1), ..., 2(N-1)\} \end{cases} \tag{IV.55}$$

and

$$\begin{cases} \mathbf{Q}_\alpha = \dfrac{2\pi}{L}(\alpha_x, \alpha_y, \alpha_z),\ \|\mathbf{Q}_\alpha\| \leq 4\Lambda_b \\ \alpha_x, \alpha_y, \alpha_z \in \{-2(N-1), ..., 2(N-1)\}. \end{cases} \tag{IV.56}$$

These relations show that truncating the confined plane-wave basis will induce a corresponding truncation in relative quantities defined in the center-of-mass frame. As we shall present later, this is numerically advantageous in the calculation of matrix elements in comparison with the exact plane-wave and partial-wave representations which are studied in the previous chapter. Moreover, since the individual momentum and relative momentum sets are bounded with the same cut-off Λ_b (IV.54), this parameter can be used to explore the influence of the two-body nuclear interaction's cut-off on the single-particle basis. This point will be discussed in chapter V. Regarding the choice between integer and half-integer cubic mesh (IV.51), we will work with the latter case (N-even) which is more convenient to handle as the extra treatment of the zero point in $\mathcal{A}_{1D}$ is excluded. Finally, we note that without the spherical truncation introduced above, the confined plane-wave basis can be considered as a "discrete variable representation" basis discussed in Ref. [66].

IV.4 Numerical aspects

IV.4.1 Description of algorithm

Starting from a one-body potential of Wood-Saxon type, the resolution of the HF eigenvalue equation (IV.38) is performed iteratively by diagonalizing the Hamiltonian matrix (IV.39). We use a simple linear mixing of iterations and apply the convergence condition on the total binding energy $E_{\rm HF} = \langle\Phi|\hat{H}|\Phi\rangle$ and the expectation value of the quadrupole moment $Q_{20} = \langle\Phi|\hat{Q}_{20}|\Phi\rangle$. In this iterative process, the main part lies in i) the preparation of two-body matrix elements and ii) the HF potential calculation (IV.42). We use the symmetries of the nuclear interaction and the properties of the confined plane-wave basis to restrict the number of necessary matrix elements before parallelizing the processes i) and ii) using Open MP.

IV.4.1.1 Anti-symmetrized TBME

Since nucleons obey the Pauli principle, two-body matrix elements of the interaction are always anti-symmetrized. In the confined plane-wave basis $\{|\varphi_\alpha\sigma\rangle\}$, one thus needs to calculate the matrix elements $\langle\varphi_{\alpha'_1}\varphi_{\alpha'_2},\sigma'_1\sigma'_2,\tau'_1\tau'_2|\hat{V}_{\rm NN}(\mathbb{1}-\hat{P}_{12})|\varphi_{\alpha_1}\varphi_{\alpha_2},\sigma_1\sigma_2,\tau_1\tau_2\rangle$ where $\tau'_1,\tau'_2,\tau_1,\tau_2$ are isospin quantum numbers. By means of the expansions (IV.34) and (IV.40), we can then find the corresponding matrix elements in the Hartree-Fock basis needed for beyond mean-field calculations

$$\langle i'_1 i'_2|\hat{V}_{\rm NN}(\mathbb{1}-\hat{P}_{12})|i_1 i_2\rangle = \sum_{\lambda'_1,c'_1\gamma'_1\sigma'_1}\sum_{\lambda'_2,c'_2\gamma'_2\sigma'_2}\sum_{\lambda_1,c_1\gamma_1\sigma_1}\sum_{\lambda_2,c_2\gamma_2\sigma_2} C^{(i'_1)}_{\lambda'_1,c'_1\gamma'_1\sigma'_1}C^{(i'_2)}_{\lambda'_2,c'_2\gamma'_2\sigma'_2}C^{(i_1)}_{\lambda_1,c_1\gamma_1\sigma_1}C^{(i_2)}_{\lambda_2,c_2\gamma_2\sigma_2}$$
$$\langle\lambda'_1(c'_1\gamma'_1\sigma'_1)\tau'_1,\lambda'_2(c'_2\gamma'_2\sigma'_2)\tau'_2|\hat{V}_{\rm NN}(\mathbb{1}-\hat{P}_{12})|\lambda_1(c_1\gamma_1\sigma_1)\tau_1,\lambda_2(c_2\gamma_2\sigma_2)\tau_2\rangle. \tag{IV.57}$$

Momentum dependence. The confined plane-wave basis provides us with two features:

- the approximate center-of-mass momentum conservation (IV.15);
- an equidistant bounded set of relative momenta (IV.54) when truncating the individual basis by Λ_b.

As a consequence, for the nuclear force, we need therefore to determine anti-symmetrized matrix elements $\langle\mathbf{k}_{\alpha'},\sigma'_1\sigma'_2,\tau'_1\tau'_2|\hat{V}_{\rm NN}(\mathbb{1}-\hat{P}_{12})|\mathbf{k}_\alpha,\sigma_1\sigma_2,\tau_1\tau_2\rangle$ with the set of pairs $\mathcal{D}_J(\Lambda_b) = (\mathbf{k}_{\alpha'},\mathbf{k}_\alpha)$ constructed from the quadruplets $\{(\alpha'_1,\alpha'_2,\alpha_1,\alpha_2)\}$ verifying

$$\begin{cases} \alpha'_1+\alpha'_2=\alpha_1+\alpha_2, \\ \|\mathbf{k}_{\alpha'}\|\leq\Lambda_b,\ \|\mathbf{k}_\alpha\|\leq\Lambda_b. \end{cases} \tag{IV.58}$$

Isospin dependence. Among 16 combinations of isospin projections $(\tau'_1,\tau'_2,\tau_1,\tau_2)$, the ones allowed by T_z-conservation are

- $T_z = -1$ (pp matrix element): $\tau_1' = \tau_2' = \tau_1 = \tau_2 = -\frac{1}{2}$;
- $T_z = 0$ (np matrix element): $(\tau_1', \tau_2') \in \left\{(-\frac{1}{2}, \frac{1}{2}), (\frac{1}{2}, -\frac{1}{2})\right\}$ and $(\tau_1', \tau_2') \in \left\{(-\frac{1}{2}, \frac{1}{2}), (-\frac{1}{2}, \frac{1}{2})\right\}$
- $T_z = 1$ (nn matrix element): $\tau_1' = \tau_2' = \tau_1 = \tau_2 = \frac{1}{2}$.

Because of the anti-symmetrization

$$(\mathbb{1} - \hat{P}_{12})|\mathbf{k}_\alpha, \sigma_1\sigma_2, \tau_1\tau_2\rangle = -(\mathbb{1} - \hat{P}_{12})|\mathbf{k}_{-\alpha}, \sigma_2\sigma_1, \tau_2\tau_1\rangle \tag{IV.59}$$

hence

$$\langle \mathbf{k}_{\alpha'}, \sigma_1'\sigma_2', \tau_1'\tau_2'|\hat{V}_{\mathrm{NN}}(\mathbb{1} - \hat{P}_{12})|\mathbf{k}_\alpha, \sigma_1\sigma_2, \tau_1\tau_2\rangle = -\langle \mathbf{k}_{\alpha'}, \sigma_1'\sigma_2', \tau_1'\tau_2'|\hat{V}_{\mathrm{NN}}(\mathbb{1} - \hat{P}_{12})|\mathbf{k}_{-\alpha}, \sigma_2\sigma_1, \tau_2\tau_1\rangle. \tag{IV.60}$$

Furthermore, owing to the permutation symmetry

$$\langle \mathbf{k}_{\alpha'}, \sigma_1'\sigma_2', \tau_1'\tau_2'|\hat{V}_{\mathrm{NN}}(\mathbb{1} - \hat{P}_{12})|\mathbf{k}_\alpha, \sigma_1\sigma_2, \tau_1\tau_2\rangle = \langle \mathbf{k}_{-\alpha'}, \sigma_2'\sigma_1', \tau_2'\tau_1'|\hat{V}_{\mathrm{NN}}(\mathbb{1} - \hat{P}_{12})|\mathbf{k}_{-\alpha}, \sigma_2\sigma_1, \tau_2\tau_1\rangle \tag{IV.61}$$

Combining the two last identities with the total isospin conservation $\tau_1' + \tau_2' = \tau_1 + \tau_2$ and because $\tau_i', \tau_i = \pm 1/2$, it is possible to restrict ourselves to matrix elements of isospin

$$\tau_1' = \tau_1 \geq \tau_2 = \tau_2'. \tag{IV.62}$$

The corresponding number of two-body anti-symmetrized matrix elements $\langle \mathbf{k}_{\alpha'}, \sigma_1'\sigma_2', \tau_1'\tau_2'|\hat{V}_{\mathrm{NN}}(\mathbb{1} - \hat{P}_{12})|\mathbf{k}_\alpha, \sigma_1\sigma_2, \tau_1\tau_2\rangle$ is thus given by

$$n_{\mathrm{aTBME}} = 3 \times 16 \times \mathrm{card}(\mathcal{D}_J). \tag{IV.63}$$

For the Coulomb interaction, the situation is simpler for isospin and spin parts such that only the momentum dependence has to be addressed. It is clear that the integral kernel of (IV.20) is even with respect to transfer momenta variables $\mathbf{q}$ and $\mathbf{Q}$. Combining this property and the truncation induced by the single-particle basis (IV.55), (IV.56), the transfer momenta at play for the Coulomb force are those belonging to

$$\begin{cases} \mathcal{D}_q(\Lambda_b, L) = \{\mathbf{q}_\alpha,\ \|\mathbf{q}_\alpha\| \leq 2\Lambda_b\},\ \ \alpha = (\alpha_x, \alpha_y, \alpha_z) \in \{0, 1, ..., 2(N-1)\}^3, \\ \mathcal{D}_Q(\Lambda_b, L) = \{\mathbf{Q}_\alpha,\ \|\mathbf{Q}_\alpha\| \leq 4\Lambda_b\},\ \ \alpha = (\alpha_x, \alpha_y, \alpha_z) \in \{0, 1, ..., 2(N-1)\}^3. \end{cases} \tag{IV.64}$$

IV.4.1.2 Hartree-Fock potential calculation algorithm

Having determined the matrix elements to be calculated, we can specify now how to use them when calculating the Hartree-Fock potential according to (IV.45), (IV.46) and (IV.47). To optimize the calculation of each Hartree-Fock potential matrix element, one identifies the independent quantities and prepares them preliminarily. Finally, one can define a partition of the total number of one-body Hartree-Fock matrix elements to perform the parallelization where each subset of the partition is

calculated independently. In practice, we perform this step based on the reduced single-particle momenta set $\mathcal{D}_G(\Lambda_b, L)$ defined in (IV.53).

In the case of the nuclear Hartree-Fock potential, the algorithm outlined above is based on the definition of the set (IV.43). For each subset $\mathcal{K}_{\gamma_1'\gamma_1}$, as we can see in (IV.45), the sum over co-representation index and quantum numbers defined by the self-consistent symmetry group can be prepared in advance. In parallel, only two-body anti-symmetrized matrix elements relevant for that pair (γ_1', γ_1) are selected. In the case of the Coulomb force, because of its spin independence, in the direct (IV.46) and exchange terms (IV.47), we can further average over the spin projections in the one-body density. Once the mixed matrix element is calculated, the anti-symmetry relation (IV.41) is used to obtain the HF potential in the symmetry-adapted basis.

IV.4.2 Comparison to other momentum bases

Table (IV.1) presents the corresponding time and resources needed to apply the above-described algorithm. For ^{48}Cr, the convergence in the three calculations in (IV.1) is reached after about thirty iterations with the linear mixing method. We note that while adding the two-body kinetic energy correction requires a negligeable time, computing the exchange Hartree-Fock Coulomb potential costs a factor of 4 with respect to the Coulomb direct term alone. Overall, the main factor governing the calculation time of the HF potential per iteration is the size of the reduced single-particle momenta set $\mathcal{D}_G(\Lambda_b, L)$ and is practically independent of the nucleus under consideration.

Λ_b	L	card($\mathcal{D}_G$)	nuclear TBME		Coulomb TBME		HF potential	
			RAM	time	RAM	time	nuclear	Coulomb direct
2.0	12.5	35	203 Mb	4m25s	20.5 Mb	1min28s	2.5s	4.4s
	15.0	60	645 Mb	14min	62 Mb	4min30s	11.6s	33.1s
	17.5	90	1.47 Gb	33min	154 Mb	9min	4min	2min40

Table IV.1 Memory and calculation time for different box size (L in fm) with ^{48}Cr nucleus using the evolved block diagonal EM17+SRG(2.0) interaction that allows to fix $\Lambda_b = 2.0$ fm^{-1}. The columns 4-7 indicate the memory and initialization time of nuclear and Coulomb two-body matrix elements. The last two columns show the calculation time per iteration of the corresponding Hartree-Fock potential.

To make a comparison with the partial-wave representation, we perform in this representation the HF calculation of ^{16}O based on the Skyrme (SV) force alone with different number of discretized radial momentum mesh points n (cf. (III.86)). Table (IV.2) shows the initialization time of anti-symmetrized two-body matrix elements. The main difference of this representation with respect to 3D plane-wave basis is the center-of-mass transformation. The second factor is the truncation parameter $\Omega_{\max}$ (III.89) defining the highest single-particle total angular momentum j that can be

occupied. For instance, taking $\Omega_{\max} = 11/2$ with a number of points $n = 15$, the corresponding number of anti-symmetrized TBME to be calculated is $\sim 4.5 \times 10^9$ (~ 33.5 Gb). The third factor driving the calculation time of anti-symmetrized TBME is the total angular momentum quantum number $J_{\max}$ and the center-of-mass integration number of point (N_K) in (III.79). Even with parallelization, it becomes difficult, within our available resources, in this representation to go beyond ^{16}O or perform HF calculation with other non-empirical interactions requiring higher $J_{\max}$ values.

In summary, the confined plane-wave representation essentially solves two problems that we encountered in the exact 3D plane-wave and partial-wave bases. The first is the direct separation of the center-of-mass motion while reducing at the same time the numerical cost with respect to the exact 3D plane-wave. The second is the regularization of the Coulomb singularity as a result of the confinement. The latter feature is very interesting if we look at the other two momentum bases where, for instance, in the partial-wave representation, the singularity manifests itself in an inextricable dependence on the quadruplet of single-particle momenta (cf. EQs. (III.75), (III.78)).

$\Omega_{\max}$	$(J_{\max}, N_K)$	n	nuclear TBME		HF potential
			RAM	time	
3/2	(2, 12)	20	455 Mb	6h35min	1min
		24	940 Mb	13h30min	2min15s
		28	1.7 Gb	25h	4min36s

Table IV.2 HF calculation time in the axial partial-wave representation for ^{16}O with the Skyrme (SV) force. The fifth column correspond to the total calculation time of all anti-symmetrized two-body matrix elements in the partial-wave basis whereas the last column shows the calculation time of the Hartree-Fock potential per iteration.

Chapter V

First results of Hartree-Fock calculations

In this chapter, we study the Hartree-Fock convergence with respect to the confined plane-wave truncation parameters, i.e. the box size L and the spherical momentum cut-off Λ_b. The Hartree-Fock calculations presented below are performed with the phenomenological Skyrme force [67] and the chiral N^{3}LO force developed by D. Entem and collaborators in Refs [12], [13].

V.1 Determination of basis parameters

V.1.1 Cubic box size L

Validation. To validate our implementation of the Hartree-Fock method in the confined plane-wave basis, the phenomenological Skyrme parametrization SV (in Ref. [67]) is used since it is free from any density dependence. The benchmark calculation is performed with ^{16}O and compared to two other representations: the spherical harmonic oscillator (SHO) and the axial partial-wave (PW) that has been discussed in chapter III. In this calculation, we do not include the Coulomb and kinetic energy correction terms. Table (V.1) shows the binding energy E_b (in MeV) and the nuclear mean squared radius $\langle \mathbf{r}^2 \rangle$ (in fm^2) for various box size value L (fm). We fix here the spherical momentum cut-off Λ_b at 2 fm^{-1}. A priori, the box size L should be large enough as compared to the nuclear radius.

Force: SV - ^{16}O ($\Lambda_b = 2.0$ fm^{-1})

L (fm)	10.0	12.5	15.0	17.5	20.0	22.5
E_b (MeV)	-128.552	-126.787	-126.685	-126.675	-126.669	-126.671
$\langle \mathbf{r}^2 \rangle$ (fm^2)	7.081	6.950	6.930	6.927	6.927	6.927

Table V.1 Variation of binding energy (E_b) and nuclear mean squared radius ($\langle \mathbf{r}^2 \rangle$) of ^{16}O with the box size L.

As the SHO and PW are characterized by their proper truncation parameters, a similar variation of the basis size is performed. While the truncation in SHO basis is defined solely by the number of hamornic oscillator shells for fixed $\hbar\omega$, we recall that in Table (V.2), $\Omega_{\max}$ defines the highest total single-particle angular momentum that the basis can describe. Because $J_{\max}$ and N_K control the precision with which the interaction is represented in the partial-wave basis (III.79), the convergence of the Hartree-Fock solution is essentially governed by the discretization of the radial momentum mesh defined in (III.85), i.e. the momentum truncation parameter $k_{\max}^{(\mathrm{sp})}$ and the number of points n. One thus expects to observe the convergence when increasing $k_{\max}^{(\mathrm{sp})}$ and accordingly n.

$\Omega_{\max} = 3,\ J_{\max} = 2,\ N_K = 12,\ k_{\max}^{(\mathrm{sp})} = 2.5\ \mathrm{fm}^{-1}$				
n	20	24	28	32
E_b (MeV)	-129.1	-128.2	-127.8	-127.5
$\langle \mathbf{r}^2 \rangle$ (fm^2)	6.72	6.72	6.72	6.72

Table V.2 Same as Table (V.1) with the partial-wave basis.

Table (V.3) shows the binding energy and mean squared radius of ^{16}O using the HF-Skyrme code in the spherical harmonic oscillator basis. In these calculations, we choose a large number of major shells so as to minimize the dependence of the HF solution on $\hbar\omega$, which is chosen to be 8 MeV. This value approximately corresponds to the optimal value that minimizes the binding energy for fixed basis size.

Number of major shells	17	21	27
E_b (MeV)	-126.9	-127.1	-127.3
$\langle \mathbf{r}^2 \rangle$ (fm^2)	6.91	6.90	6.88

Table V.3 Same as Table (V.1) with the spherical harmonic oscillator basis ($\hbar\omega = 8$ MeV).

In the confined plane-wave basis as shown in Table (V.1), we observe that a 10-keV level convergence is reached with a box size $L \sim 15.0$ fm. With the experimental nuclear charge radius of ^{16}O about ~ 2.7 fm, the edge-length-to-charge-radius ratio L/r_c is of the order of 4 to 5. Compared to the SHO and PW bases, the binding energy obtained in the confined plane-wave basis can be considered to be consistent within a few hundreds of keV.

Box size variation with chiral (initial and transformed) EM17 potentials. With the N^{3}LO chiral potential (regularized at 450 MeV) developed in Ref. [13] (dubbed as EM17), we perform the SRG evolution using the diagonal block generator to obtain a low momentum potential (dubbed as EM17+SRG(2.0)) with a decoupling at 2.0 fm^{-1} in relative momentum. By construction,

we are only interested in the momentum region below 2.0 fm^{-1}. Matrix elements of relative momenta larger than the momentum decoupling are set to zero. Furthermore, we exclude the Coulomb interaction and look at the variation of binding energy as a function of the confinement box size for EM17 and EM17+SRG(2.0) potentials.

Force: EM17 ($\Lambda_b = 2.5$ fm^{-1})

Nucleus	L	10.0	12.5	15.0	15.5	17.5
^{16}O	E_b	−41.073	−39.481	−39.516		−39.415
	r_c	3.378	3.350	3.335		3.338
^{48}Cr	E_b	−347.890	−335.634		−337.720	−337.010
	r_c	3.844	3.841		3.817	3.823
	Q_{20}	136.900	120.720		117.377	117.745
	β_2	0.32	0.28		0.28	0.28

Table V.4 Variation of binding energy (E_b in MeV) and nuclear charge radius (r_c in fm) with the confinement box size. The third column shows results obtained for ^{16}O with $L = 15.0$ fm whereas for ^{48}Cr we have used $L = 15.5$ fm.

Force: EM17+SRG(2.0) ($\Lambda_b = 2.0$ fm^{-1})

Nucleus	L	12.5	15.0	17.5	20.0
^{16}O	E_b	−82.909	−82.179	−79.947	−79.704
	r_c	3.230	3.247	3.290	3.301
^{48}Cr	E_b	−518.131	−512.052	−493.088	−491.112
	r_c	4.003	4.035	4.115	4.134
	Q_{20}	127.177	126.454	134.217	133.681
	β_2	0.27	0.27	0.27	0.27
^{98}Sr	E_b		−1309.121	−1241.578	−1237.075
	r_c		5.486	5.683	5.709
	Q_{20}		369.625	587.647	588.487
	β_2		0.26	0.39	0.38

Table V.5 Same as Table. (V.4) with the diagonal block evolved EM17+SRG(2.0) force. Q_{20} is in fm^2.

The binding energy and nuclear charge radius obtained with these potentials are shown respectively in Tables (V.4) and (V.5). For the heavier nuclei ^{48}Cr and ^{98}Sr, the convergence in binding energy is observed when L reaches about 17.5 fm, although there is a larger absolute difference for these nuclei than in ^{16}O. In contrast, the deformation parameter β_2 remains rather stable in both initial and renormalized potentials.

Coulomb interaction and the box size. To see how the Coulomb energy varies with the box size, we include the Coulomb direct contribution into the nuclear Hartree-Fock potential obtained with the EM17+SRG(2.0) interaction. By construction, this interaction allows to fix $\Lambda_b = 2.0$ fm^{-1} since we are only interested in the low-momentum region below 2.0 fm^{-1}. Table (V.6) shows the contribution of the Coulomb direct one-body reduction (E_{Coul} in MeV), which turns out to be practically unchanged versus the box size. This can be explained owing to the one-body density that should vanish outside the cubic box (once the box size is chosen large enough compared to the nuclear radius). Indeed, the direct contribution to the Coulomb energy is given by

$$E_{\text{Coul}} = \frac{1}{2}\int_{\mathbb{R}^3} d^3\mathbf{r}\,\rho_p(\mathbf{r})\,\overline{v}_{\text{Coul}}(\mathbf{r}), \quad \overline{v}_{\text{Coul}}(\mathbf{r}) = \int_{\mathbb{R}^3} d^3\mathbf{r}'\,\rho_p(\mathbf{r}')\,\frac{e^2}{\|\mathbf{r}-\mathbf{r}'\|} \tag{V.1}$$

where $\rho_p(\mathbf{r})$ is the proton one-body density. These relations show that despite the infinite range of the Coulomb interaction, due to the Hartree-Fock self-consistency, one can estimate the box size by the typical nuclear size driven by the one-body density matrix. Finally, we note that the deformation β_2 seems unaffected by the Coulomb presence compared to Table (V.5) in ^{48}Cr.

Force: EM17+SRG(2.0) and direct Coulomb ($\Lambda_b = 2.0$ fm^{-1})

Nucleus	L	12.5	15.0	17.5	20.0
^{16}O	E_b	−63.027	−62.359	−60.367	
	E_{Coul}	19.738	19.680	19.444	
	r_c	3.263	3.278	3.320	
^{48}Cr	E_b	−375.989	−370.544	−354.043	−352.312
	E_{Coul}	141.190	140.572	138.164	137.923
	r_c	4.038	4.068	4.147	4.165
	Q_{20}	133.256	132.425	139.764	139.260
	β_2	0.28	0.27	0.28	0.27

Table V.6 Variation of binding energy and Coulomb direct contribution (E_{Coul}) with different confinement box size L.

V.1.2 Single-particle momenta cut-off Λ_b

In Tables (V.7) and (V.8), the binding energy and nuclear charge radius are calculated for ^{16}O for Λ_b ranging from 2.0 to 4.0 fm^{-1} without the Coulomb interaction and kinetic energy corrections. The binding energy is lowered as Λ_b increases for both SV and EM17 interactions. This can be understood as a result of the variational character of the HF method. Indeed, fixing L is equivalent to fixing the momentum step size $2\pi/L$ which characterizes the discrete single-particle momenta set (IV.52) $\mathcal{D}(\Lambda_b, L)$. As the cut-off Λ_b increases, we enlarge the confined plane-wave basis by adding states. It is therefore expected to lower the binding energy with increasing Λ_b. To constrain the cut-off Λ_b, there are a priori two factors. The first one is the momentum scale of the nuclear interaction (Λ_{NN}). This scale can be translated into the single-particle momentum as the confined plane-wave is characterized by discrete and bounded momenta (result of the spherical truncation). The second factor relates to the characteristic scale (a) set up by the one-body Hartree-Fock potential. For a qualitative argument, one could define the latter scale from the typical form of the Wood-Saxon potential, i.e. the diffuseness $a \sim 0.7$ fm. To be able to probe this characteristic scale, Λ_b is expected to be of order $\geq \pi/a$. So qualitatively $\Lambda_b \gtrsim \min\{\Lambda_{NN}, \pi/a\}$.

Λ_b (fm^{-1})	2.0	2.5	3.0	3.5	4.0
E_b (MeV)	−35.602	−39.481	−39.892	−39.908	−39.917
r_c (fm)	3.499	3.350	3.329	3.329	3.328

Table V.7 Variation of ^{16}O binding energy and nuclear charge radius with the single-particle momentum truncation Λ_b for the initial EM17 force with the box size $L = 12.5$ fm.

Λ_b (fm^{-1})	2.0	2.5	3.0	3.5	4.0
E_b (MeV)	−126.787	−127.000	−127.340	−127.464	−127.468
r_c (fm)	3.813	3.806	3.803	3.800	3.800

Table V.8 Same as Table (V.7) for the Skyrme force SV.

For the N^{3}LO EM17 interaction regularized at $\Lambda_{NN} = \dfrac{450 \text{ MeV}}{\hbar c} \approx 2.25$ fm^{-1} (smaller than $\pi/a \sim 4.0$ fm^{-1}), a good convergence at 0.5 MeV level is reached for $\Lambda_b \approx 2.5$ fm^{-1}, which is of the order of Λ_{NN} as expected. However, one expects Λ_{NN} rather large for the SV force because it is not regularized. So Λ_b is expected to be fixed by the one-body reduction scale π/a, as seen in Table (V.8).

As a final example, to see the impact of the Coulomb interaction and the two-body kinetic energy correction on the determination of Λ_b, Table (V.9) shows the total binding energy (E_b)

of ^{16}O, the direct contribution to the Coulomb energy (E_{Coul}) and the two-body kinetic energy correction $\langle \hat{K}_2 \rangle$ using the Daejeon16 interaction. The box size is fixed at 12.5 fm.

Λ_b (fm^{-1})	2.0	2.5	2.75	3.0
E_b (MeV)	−100.196	−101.451	−101.472	−101.475
E_{Coul} (MeV)	18.781	19.120	19.129	19.129
$\langle \hat{K}_2 \rangle$ (MeV)	−6.843	−7.050	−7.055	−7.054
r_c (fm)	3.388	3.336	3.334	3.334

Table V.9 Same as Table (V.8) using the Daejeon16 interaction with the presence of the Coulomb interaction and the two-body kinetic energy correction.

Although the Daejeon16 interaction does not have an explicit regularization momentum Λ_{NN} since it results from the original N^{3}LO EM17 transformed by SRG [52], which is subject to further phase-equivalent transformations, we find that a 20-keV level convergence for the total binding energy is reached at $\Lambda_b \approx 2.5$ fm^{-1}, which is well below the π/a scale. The Coulomb energy and the two-body kinetic energy correction converge very well when $\Lambda_b \gtrsim 2.5$ fm^{-1}.

In conclusion, we could expect that the overall behavior of the confined plane-wave basis is essentially under control. In the next section, we present a full-fledged Hartree-Fock calculation with the EM17+SRG(2.0) potential for some $N = Z$ deformed nuclei and retain the same basis parameters $\Lambda_b = 2.0$ fm^{-1} and $L = 17.5$ fm. As a final remark, overall the binding energy tends to increase with the box size, i.e. one obtains a lower energy with smaller box sizes. This is however not in contradiction to the variational principle but due to the cubic box approximation (IV.2).

V.2 Bulk properties of even-even nuclei

Table (V.10) presents different contributions to the binding energy and the nuclear charge radius of selected nuclei. One notices that the Coulomb energy in light nuclei such as ^{16}O, ^{24}Mg and ^{28}Si is close to empirical estimation in the liquid drop model: $E_{\text{Coul}} = a_C Z^2/A^{1/3}$ with $a_C = 0.7$ MeV. In the heaviest nucleus that we calculated, the non-empirical EM17+SRG(2.0) gives 284.5 MeV compared to the empirical estimate 219.2 MeV. The two-body kinetic correction $\langle \overline{K}_2 \rangle$ compensates about $50 - 60\%$ of the one-body correction and becomes important in heavier systems. Although the total absolute binding is not meant to be compared to experimental data, we note that the obtained energy is underestimated in ^{16}O or ^{24}Mg and overestimated in ^{98}Sr.

Nucleus	E_b	$E_{\rm Coul}$	$\langle \overline{K}_2 \rangle$	$\langle \hat{K} \rangle / A$	r_c
^{16}O	−77.807	16.123	−7.813	22.045	3.264
^{24}Mg	−123.022	33.936	−10.552	24.273	3.708
^{28}Si	−161.382	45.718	−11.800	25.276	3.784
^{48}Cr	−378.607	126.519	−16.037	28.653	4.135
^{98}Sr	−966.303	284.542	−21.056	31.825	5.706

Table V.10 Binding energy (E_b) and nuclear charge radius (r_c) obtained with EM17+SRG(2.0) force where we have included the full Coulomb contribution $E_{\rm Coul}$ (direct and exchange) and the one- and two-body kinetic corrections ($\hat{K}/A$ and $\hat{K}_2$).

Nucleus	β_2	γ	β_2 (with SIII)
^{24}Mg	0.39	5.6°	0.45
^{28}Si	−0.33	0	−0.30
^{32}S	0.21	15°	0.22
^{48}Cr	0.28	0	0.25
^{98}Sr	0.39	0	0.39

Table V.11 Deformation parameters (β_2, γ) obtained with HF calculations presented in Table. (V.10)

The deformation parameters (β_2, γ) are given by [68]

$$\beta_2 = \sqrt{\frac{\pi}{5}} \frac{\sqrt{\langle \hat{Q}_{20} \rangle^2 + 3 \langle \hat{Q}_{22} \rangle^2}}{A \langle \mathbf{r}^2 \rangle}, \quad \tan\gamma = \frac{\sqrt{3} \langle \hat{Q}_{22} \rangle}{\langle \hat{Q}_{20} \rangle}. \tag{V.2}$$

It is interesting to note that the deformation properties resulting from the transformed EM17+SRG(2.0) potential does not substantially differ from those obtained in a phenomenological force SIII.

Chapter VI

Many-body approaches to pairing correlations

In this chapter we address the description of pairing correlations of a nucleus in two simple approaches: the BCS approximation, which does not conserve the particle number but can be treated together with the mean field in a variational way, and the Highly Truncated Diagonalization approach (HTDA) which preserves the particle number but is not variational (see Refs. [36], [69], [70]). A fully variational treatment that starts with the HTDA formalism is realized in the framework of the multi-particle-multi-hole self-consistent configuration-mixing approach developed by the authors of Ref. [71].

VI.1 BCS approximation

As is well-known (see, e.g., Ref. [33]), the BCS approximation relies on (i) the identification of pairs of conjugate states $(|i\rangle, |\bar{i}\rangle)$, usually done via the time-reversal operator $\hat{\mathcal{T}}$

$$|\bar{i}\rangle \equiv \hat{\mathcal{T}}|i\rangle\,, \tag{VI.1}$$

and (ii) a trial wavefunction representing independent quasiparticles built from the Bogoliubov–Valatin transformation

$$|\mathrm{BCS}\rangle = \Big(\prod_{i>0} \alpha_i^\dagger \alpha_{\bar{i}}^\dagger\Big)|0\rangle \tag{VI.2}$$

with, using standard notation

$$\alpha_i^\dagger = u_i\, a_i^\dagger - v_i a_{\bar{i}} \qquad \text{and} \qquad \alpha_{\bar{i}}^\dagger = u_i\, a_{\bar{i}}^\dagger + v_i a_i\,. \tag{VI.3}$$

VI.1.1 Definition of pairs of conjugate states

As discussed in Appendix A of Ref. [72] the actual relation between the two members of a pair of conjugate single-particle states appearing in the special Bogoliubov transformation can be identified from the numerically obtained Bogoliubov transformation by the Bloch–Messiah–Zumino decomposition [73], [74]. This relation has been shown by Herbut and Vujičič [75] to be formally represented by an antilinear, unitary operator called the pairing operator $\hat{\mathcal{P}}$. When time-reversal is a selfconsistent symmetry, then this operator is the time-reversal operator $\hat{\mathcal{T}}$.

However in the present work the operator $\hat{\mathcal{T}}$ does not belong to the selected symmetry group of the nucleus and the question of defining the conjugacy relation is not obvious. To do so we follow the idea of Ref. [72]: for a given single-particle state $|i\rangle$, the like-nucleon "pairing partner" is the single-particle state $|j\rangle$ of same isospin whose time-reversed state $|\bar{j}\rangle$ has the largest overlap in absolute value with $|i\rangle$. A similar definition is retained to identify the neutron-proton pairs of conjugate states.

This definition of pairs of conjugate states will also be used in the construction of the many-body basis in the Highly Truncated Diagonalization approach.

VI.1.2 BCS equations

Because of the mixing of annihilation and creation operators, the BCS wave function breaks particle-number symmetry. Minimizing the expectation value $\langle \mathrm{BCS}|(\hat{H} - \lambda \hat{N})|\mathrm{BCS}\rangle$ with respect to v_i, where λ is a Lagrange multiplier associated with the particle-number operator $\hat{N}$, one obtains the gap equation (for $i > 0$)

$$2\,u_i v_i \Big[\langle i|\hat{K}|i\rangle + \frac{1}{2}\sum_j \left(\langle ij|\hat{V}|\widetilde{ij}\rangle + \langle \bar{i}j|\hat{V}|\widetilde{\bar{i}j}\rangle \right) v_j^2 - \lambda \Big] + \Delta_i \left(u_i^2 - v_i^2\right) = 0 \tag{VI.4}$$

where the pairing gap Δ_i is defined by

$$\Delta_i = -\sum_{j>0} \langle i\bar{i}|\hat{V}|\widetilde{j\bar{j}}\rangle\, u_j v_j \,. \tag{VI.5}$$

The matrix elements with the tilde symbol are antisymmetrized. In principle the two-body matrix elements of $\hat{V}$ are to be calculated from the same interaction as the one appearing in the mean-field equations, and this has to be done at each Hartree–Fock iteration until convergence of both BCS and Hartree–Fock equations. However this is prohibitively time-consuming within our available resources. In contrast this is tractable when using phenomenological effective nucleon-nucleon interactions–or, rather, energy-density functionals–which, to a few exceptions, is replaced by an empirical residual interaction (seniority force or zero-range local interaction). Among these exceptions let us mention the Gogny-type functionals [76] and the Skyrme functional in its SkP parametrization [77].

Before closing this section, it is worth mentioning that, because of the particle-number symmetry breaking, the BCS approximation is expected to provide a fair description of pairing correlations only in high-pairing regimes, that is for a sufficiently high level density around the Fermi level. Indeed when the single-particle spectrum around the Fermi level exhibits too low level density, the only solution to the BCS equations is the trivial one with a vanishing pairing gap and 0 or 1 occupation probabilities. In practice this translates into an application range limited to nuclei that are not too light and far from magic numbers. For example it is a good approximation in well-deformed $A \sim 100$ nuclei, in the rare-earth region and in actinides.

VI.2 Highly truncated diagonalization approach

The highly-truncated diagonalization approach (HTDA) can be viewed as a kind of shell model based on a selfconsistent mean-field solution, except that one does not seek to form a rotationally invariant many-body basis (although it may be rotationally invariant when applied to spherical nuclei).

This approach was developped by N. Pillet, P. Quentin and J. Libert in Ref. [69] for like-nucleon pairing and then extended to neutron-proton pairing by K. Sieja, P. Quentin and A. Baran [70]. It was then used in a systematic way to study how pairing correlations induce isospin-symmetry breaking in $N = Z$ nuclei by J. Le Bloas and collaborators [36], [78], [79]. In the following we summarize the HTDA Hamiltonian and basis along the lines of Ref. [36].

VI.2.1 Hamiltonian

Let us consider a Slater determinant $|\Phi_0\rangle$ built from a single-particle orthonormal basis $\{|\psi_i\rangle, i \in \mathbb{N}^*\}$ (including all degrees of freedom), with $|\psi_i\rangle = a_i^\dagger|0\rangle$, formed by eigenvectors of the one-body Hamiltonian $\hat{H}_0 = \hat{K} + \hat{U}$, where $\hat{K}$ is the kinetic energy operator and $\hat{U}$ is an arbitrary one-body (mean-field) potential. In the following we shall use the shorthand notation $|i\rangle = |\psi_i\rangle$ when it is unambiguous. In practice this potential can be selfconsistent (as in the Hartree–Fock approximation for example) or not (such as the phenomenological Woods–Saxon potential, or the harmonic-oscillator potential). It is meant to capture most of the one-body effects of correlations (saturation density, deformation, nuclear radius). The operator $\hat{K}$ can include the one-body center-of-mass correction to the kinetic energy.

Assuming the many-body Hamiltonian of the nucleus can be initially defined by $\hat{H} = \hat{K} + \hat{V}$ where $\hat{V}$ is the internucleon potential (nuclear and electromagnetic interactions) and can include the two-body center-of-mass correction to the kinetic energy. In the following we shall restrict to the case of a pure two-body operator $\hat{V}$. Then we can express $\hat{H}$ in normal-product form with respect to $|\Phi_0\rangle$ as follows

$$\hat{H} = \hat{H}_{\text{iqp}} + \hat{V}_{\text{res}} + \langle\Phi_0|\hat{H}|\Phi_0\rangle\,, \tag{VI.6}$$

where the independent quasiparticle (of particle-hole type) Hamiltonian $\hat{H}_{\rm iqp}$ is defined by

$$\hat{H}_{\rm iqp} = :\hat{H}_0:_{\Phi_0} = \hat{H}_0 - \langle\Phi_0|\hat{H}_0|\Phi_0\rangle \tag{VI.7}$$

and the residual interaction $\hat{V}_{\rm res}$ is by definition

$$\hat{V}_{\rm res} = \hat{V} - \hat{U} - \langle\Phi_0|(\hat{V}-\hat{U})|\Phi_0\rangle = :\hat{V}:_{\Phi_0} + :(\overline{V}-\hat{U}):_{\Phi_0} \tag{VI.8}$$

where $\overline{V}$ is the one-body reduction of $\hat{V}$ for $|\Phi_0\rangle$ (defined in chapter IV) and, for a two-body operator

$$:\hat{V}:_{\Phi_0} = \hat{V} - \overline{V} + \langle\Phi_0|\hat{V}|\Phi_0\rangle\,. \tag{VI.9}$$

It is worth noting that in the Hartree–Fock approximation, $\hat{U}$ can be identified with $\overline{V}$ and the residual interaction is simply the normal product of $\hat{V}$ with respect to the Hartree–Fock solution $|\Phi_0\rangle$.

Up to the constant term in Eq. (VI.6) we are left with the diagonalization of $\hat{H}_{\rm iqp} + \hat{V}_{\rm res}$ whose eigenvalues are the correlation energies

$$E_{\rm corr} = \langle\Psi|\hat{H}|\Psi\rangle - \langle\Phi_0|\hat{H}|\Phi_0\rangle\,, \tag{VI.10}$$

where $|\Psi\rangle$ is an eigenstate of $\hat{H}$

$$(\hat{H}_{\rm iqp} + \hat{V}_{\rm res})|\Psi\rangle = E_{\rm corr}|\Psi\rangle\,. \tag{VI.11}$$

As it will be presented in detail in the next subsection, the HTDA basis in which the Hamiltonian (VI.6) is diagonalized (using a Lanczos algorithm to find only the lowest-energy eigenstates) is made up with multi-particle–multi-hole excitations with respect to a reference Slater determinant built from a given single-particle orthonormal basis $\{|i\rangle\}$. In order to obtain the matrix of the above Hamiltonian in the HTDA basis, we apply Wick theorem to $\hat{V}_{\rm res}$. Because the residual interaction amounts to the normal product of a two-body operator, four cases can occur when calculating the matrix element $\langle\Phi|:\hat{V}:|\Phi'\rangle$ with $|\Phi\rangle = \prod_{\ell=1}^{n} a^\dagger_{\mu_\ell} \prod_{\ell=n}^{1} a_{m_\ell}|\Phi_0\rangle$

- $|\Phi'\rangle = |\Phi\rangle$:

$$\langle\Phi|:\hat{V}:|\Phi'\rangle = \sum_{k=1}^{n}\sum_{\ell=1}^{n}\left[\frac{1}{2}\langle\mu_k\mu_\ell|\hat{V}|\widetilde{\mu_k\mu_\ell}\rangle + \frac{1}{2}\langle m_k m_\ell|\hat{V}|\widetilde{m_k m_\ell}\rangle - \langle\mu_k m_\ell|\hat{V}|\widetilde{\mu_k m_\ell}\rangle\right]. \tag{VI.12}$$

- $|\Phi'\rangle$ is a 1p1h excitation with respect to $|\Phi\rangle$, that is $|\Phi'\rangle = \hat{a}^\dagger_\alpha a_i|\Phi\rangle$

$$\langle\Phi|:\hat{V}:|\Phi'\rangle = \sum_{\ell=1}^{n}\left[\langle\mu_\ell i|\hat{V}|\widetilde{\mu_\ell\alpha}\rangle - \langle m_\ell i|\hat{V}|\widetilde{m_\ell\alpha}\rangle\right]. \tag{VI.13}$$

- $|\Phi'\rangle$ is a 2p2h excitation with rest to $|\Phi\rangle$, that is $|\Phi'\rangle = \hat{a}^\dagger_\alpha \hat{a}^\dagger_\beta a_i a_j |\Phi\rangle$

$$\langle\Phi| :\hat{V}: |\Phi'\rangle = \langle\alpha\beta|\hat{v}|\widetilde{ij}\rangle \tag{VI.14}$$

- $|\Phi'\rangle$ is a particle-hole excitation of order 3 or larger with respect to $|\Phi\rangle$:

$$\langle\Phi| :\hat{V}: |\Phi'\rangle = 0\,. \tag{VI.15}$$

VI.2.2 Many-body basis

The HTDA model space for pairing is made up with paired Slater determinants built by multi-particle–multi-hole excitations with respect to the Hartree–Fock solution $|\Phi_0\rangle$. In practice, we account for up to a total of 4 pairs (that is 8p8h excitations). These many-body states involve single-particle states in a valence window around the Fermi level made up from N_h hole states and N_p particle states (for neutrons and for protons separately). Then pairs of pairing partners of two-body isospin projection $T_z \in \{-1, 0, 1\}$ are built and stored into sets $P^h_{T_z}$ for holes and $P^p_{T_z}$ for particles as illustrated in Figure VI.1. From these sets it is then possible to build sets of n pairs

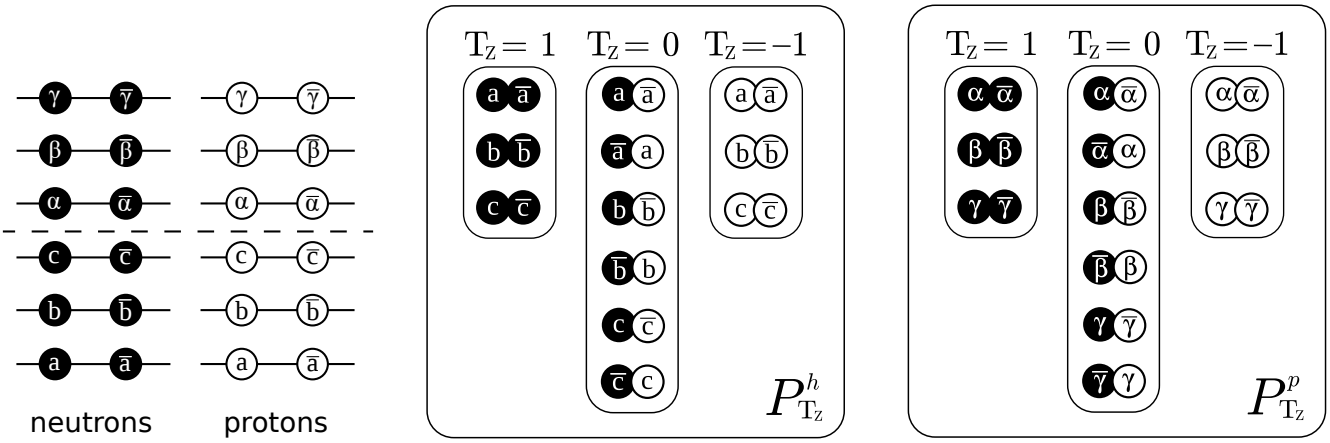

Figure VI.1 Left panel: schematic single-particle valence space around Fermi level. Center and right panels: sets of hole $P^h_{T_z}$ and particle $P^p_{T_z}$ sets of pairs of conjugate states. Figure taken from J. Le Bloas PhD thesis [36].

among hole states $\mathcal{P}^h_{n=2,T_z}$ for various values of T_z, as shown for $n = 2$ in Figure VI.2, and sets of n pairs among particle states. Finally many-body states corresponding to n pairs ($(2n)$p$(2n)$h excitations) are formed by choosing one element of P^h_{n,T_z}, for any T_z value, and one element of P^p_{n,T'_z}, where T_z and T'_z run independently over their three possible values. As shown in Figure VI.3, these excitations are not only pair transfers, but can also be breaking and recombination of pairs.

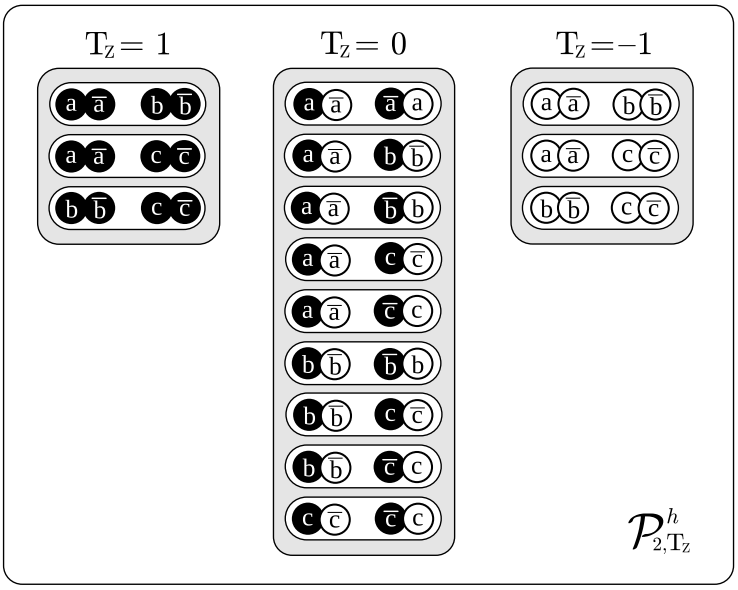

Figure VI.2 Sets $\mathcal{P}^h_{n=2,T_z}$ of two pairs among hole states. Figure taken from J. Le Bloas PhD thesis [36].

VI.3 First results

VI.3.1 Calculations settings

Ground-state pairing correlations are expected to be weak in nuclei exhibiting a low single-particle level density around the Fermi level. They are thus worth studied in well-deformed and heavy nuclei. Among those considered in the above presented mean-field calculations, ^{98}Sr is the most appropriate one. Because of the large difference between the neutron and proton numbers, like-nucleon pairing only is effective. However, this nucleus requires accordingly a confining box size $L > 20$ fm too large for our computer resources. So we limit ourselves to a smaller value $L = 15$ fm for this nucleus. In addition we study also a lighter nucleus, ^{28}Si, exhibiting an oblate and a prolate local mimimum in its potential-energy surface in order to probe two different weak-pairing regimes. In contrast to ^{98}Sr this involves neutron-proton pairing correlations in addition to like-nucleon pairing. We also use a box size $L = 15$ fm for ^{28}Si.

In these exploratory calculations aiming at a proof of principle, we consider only the nuclear force and the corresponding residual interaction while omitting the Coulomb force and kinetic energy corrections. In ^{28}Si the HTDA solution is obtained with the phenomenological Skyrme force (SHZ2) developed in Ref. [80], which is density-independent, and with the low-momentum interaction EM17+SRG(2.0), whereas in ^{98}Sr the Daejeon16 potential is chosen as an example (other interactions such as N2LOsat or even Skyrme SV provide similar level densities around Fermi level) as by construction, the effect of three-nucleon forces is minimized [52].

As explained in the previous section, we build the many-body basis from a single-particle valence window characterized by the last N_h states below Fermi level and the first N_p states above

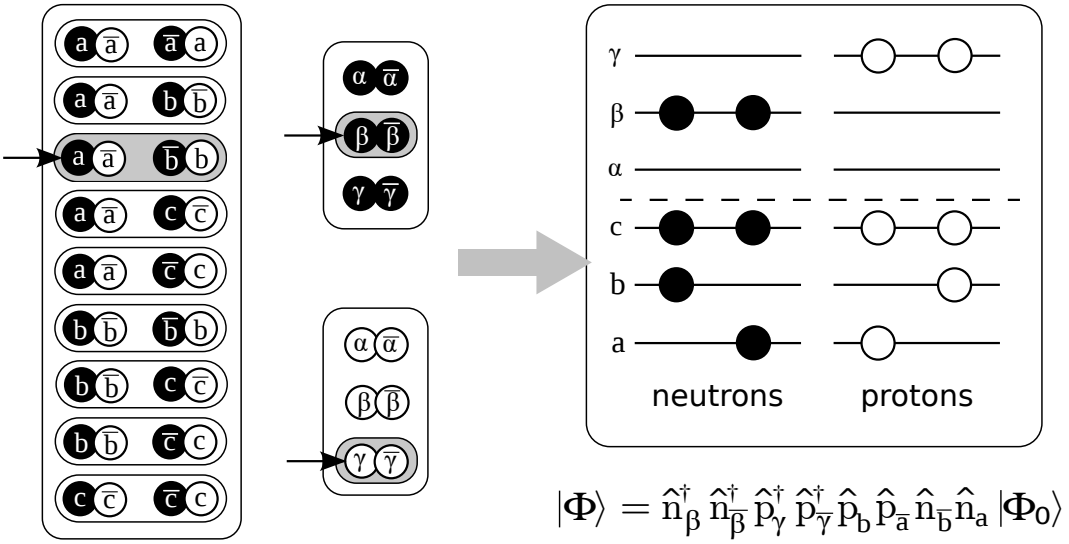

Figure VI.3 Example of a double-pair excitation (4p4h) corresponding to a breaking and recombination of pairs. Figure taken from J. Le Bloas PhD thesis [36].

the Fermi level. These values are chosen separately for neutrons and protons. In addition we impose a cutoff E_{cut} on the unperturbed excitation energy (eigenvalue of $\hat{H}_{\text{iqp}}$) of the many-body states built from this valence window. For the HTDA ground-state solution to be weakly sensitive to this valence window, one has to make sure that the lowest-energy excluded pair excitations formed with hole states below the valence window or with particle states above the window have the unperturbed excitation energy much larger than their coupling matrix elements (by the residual interaction) with other basis states and much larger than their expectation value of the residual interaction. Note that the latter, when negative, represents extra binding in the paired state provided by the residual interaction as compared to HF solution.

VI.3.2 Weak-pairing regime in ^{28}Si

The ground-state deformation of the ^{28}Si nucleus is known to be oblate. However a prolate-deformed equilibrium solution also exists, almost 10 MeV above the ground-state shape from various calculations (see, e.g., Ref. [81]). In the corresponding Hartree–Fock solutions the single-particle spectrum has different level densities around the Fermi level but they are small enough so that one can speak in both cases of weak-pairing regime.

EM17+SRG(2.0) ^{28}Si oblate ($L = 15$ fm). The single-particle spectrum obtained with this interaction is displayed in Fig. VI.4. Each energy level is twice degenerate owing to time-reversal invariance of the Hartree–Fock mean field (the two states have opposite z-signature). Next to each level the parity is indicated in parenthesis.

We retain hole states up to 30 MeV below the Fermi level (that is, the last occupied state) and virtually all bound particle states (10 states above the Fermi level with negative single-particle

energy). Typical coupling matrix elements of the residual interaction between different paired states and extra binding energies provided by the residual interaction in paired states, if any, are of the order of a few MeV at most. Therefore it is expected that the selected valence window generates a sufficiently large many-body basis for the description of pairing correlations.

Then we perform the HTDA calculation for several values of the unperturbed-excitation-energy cutoff E_{cut}. The calculated correlation energy and wave function structure are presented in Table VI.1 for the ground state. One observes very small correlation energies (below 1 MeV in absolute value) which converge for $E_{\mathrm{cut}} \sim 100$ MeV. In the same way the weights of various pair excitations in the HTDA eigenstate are very small and converge for $E_{\mathrm{cut}} \sim 70$ MeV. The HTDA ground state is thus largely dominated by the HF solution. The role of DP, TP and QP excitations is negligible in this case.

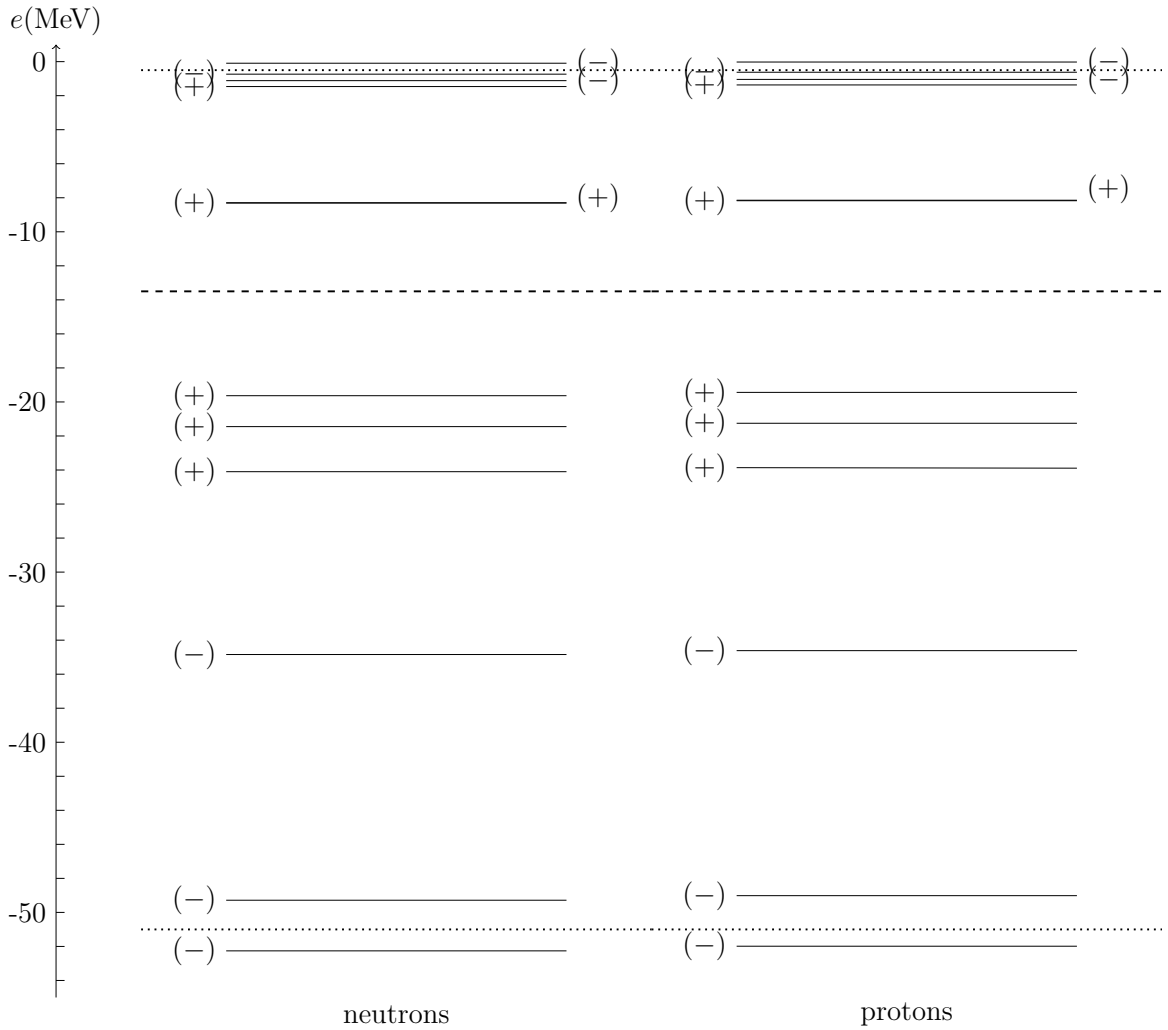

Figure VI.4 Single-particle spectrum of ^{28}Si in the oblate-deformed Hartree–Fock solution obtained with the EM17+SRG(2.0) interaction and the box size $L = 15$ fm. Note in particular the accidental quasi-degeneracy of two energy levels around -8 MeV. The dashed line separates hole levels (below) and particle levels (above), whereas the dotted lines are the boundaries of the single-particle valence window with 5 hole energy levels and 5 particle energy levels ($N_h = N_p = 10$).

Table VI.1 HTDA ground-state correlation energy and pair structure of the correlated wave function calculated as a function of E_{cut} with the EM17+SRG(2.0) residual interaction in the oblate-deformed well of ^{28}Si. The underlying single-particle spectrum and valence window are shown in Fig. VI.4. Empty entries (hyphen symbol) correspond to HTDA bases which do not contain the corresponding multiple-pair excitations (SP, DP, TP and QP stand for single-pair, double-pair, triple-pair and quadruple-pair excitations).

E_{cut} (MeV)	Basis size	E_{corr} (MeV)	$\lvert\Phi_0\rangle$ (%)	SP (%)	DP (%)	TP (%)	QP (%)
30	13	−0.1119	99.42	0.58	–	–	–
50	76	−0.3919	98.52	1.48	0.00	–	–
70	415	−0.6040	98.07	1.92	0.01	–	–
100	2216	−0.6556	97.93	2.06	0.02	0.00	0.00
120	5464	−0.6569	97.92	2.07	0.02	0.00	0.00

EM17+SRG(2.0) ^{28}Si prolate ($L = 15$ fm). This local minimum in the potential-energy surface of ^{28}Si is found to lie 6.35 MeV above the oblate HF solution and to be axially deformed with $\beta_2 = 0.39$. The single-particle spectrum obtained for this solution is shown in Fig. VI.5.

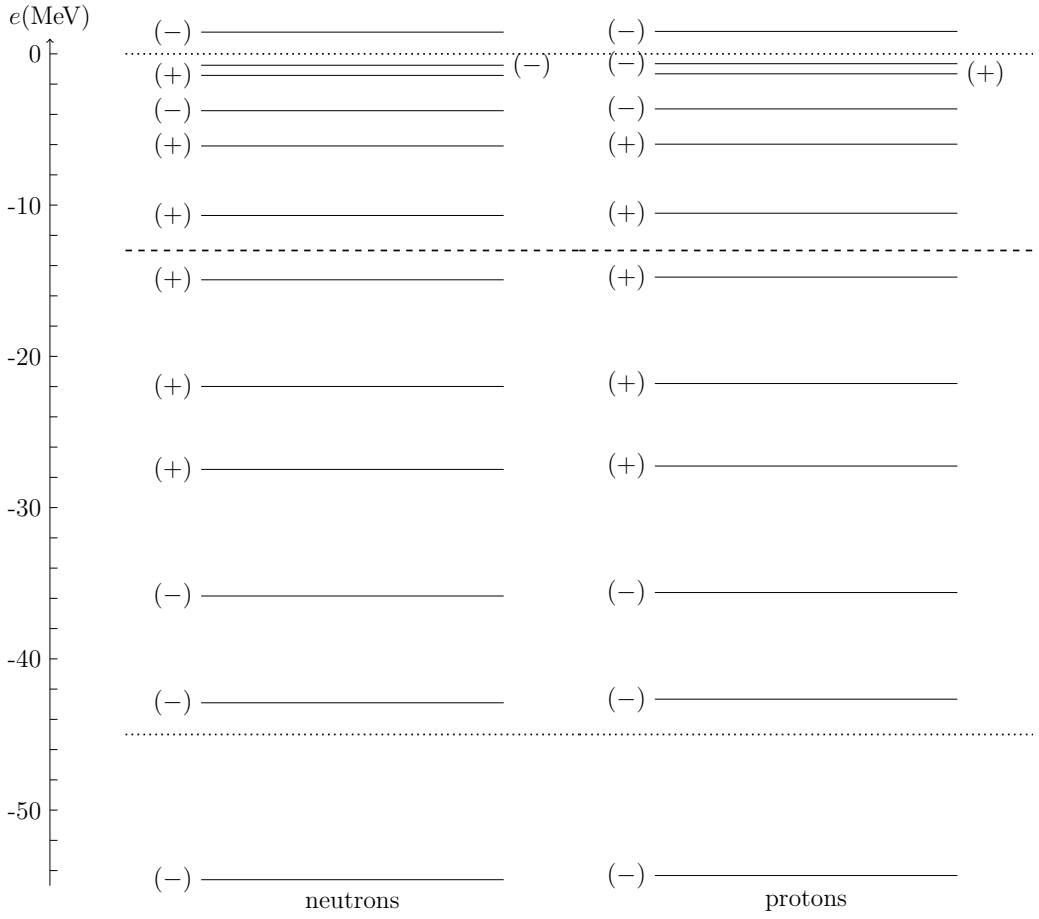

Figure VI.5 Same as Fig. VI.4 for the prolate-deformed Hartree–Fock solution in ^{28}Si with the EM17+SRG2 interaction and box size $L = 15$ fm.

One clearly sees that the level density is significantly larger than that in the oblate solution. The corresponding results for the HTDA ground-state solution are displayed in Table VI.2.

Table VI.2 Same as Table VI.1 for the prolate-deformed well of ^{28}Si. The underlying single-particle spectrum and valence window are shown in Fig. VI.5

$E_{\rm cut}$ (MeV)	Basis size	$E_{\rm corr}$ (MeV)	$\|\Phi_0\rangle$ (%)	SP (%)	DP (%)	TP (%)	QP (%)
50	137	−0.5072	96.55	3.43	0.02	–	–
70	595	−0.9243	95.48	4.49	0.03	–	–
100	3048	−1.0702	95.08	4.86	0.06	0.00	0.00
120	7773	−1.0749	95.04	4.89	0.07	0.00	0.00

A larger amount of pairing correlations is found as expected even though they remain limited. Similarly to the oblate case above, DP, TP and QP play a negligible role on the structure of the pair-correlated ground state, and convergence of the correlation energy and wave-function structure is observed around 70–100 MeV.

Skyrme SHZ2 ^{28}Si oblate ($L = 15$ fm). With the SHZ2 parametrization of the Skyrme interaction one obtains an oblate deformation $\beta_2 = -0.35$ comparable to the one obtained with the EM17+SRG(2.0) interaction. However the single-particle spectrum is slightly more compressed as can be seen on Fig. VI.6.

The valence window is made of 10 hole and 10 particle states. Despite the slightly larger level density the pairing correlations in the ground state are found to be significantly less important than those obtained with the EM17+SRG(2.0) interaction. Indeed Table VI.3 shows that, with the SHZ2 interaction, the correlation energy and the weight of different type of pair-excitations in the ground-state wave function are about half their values obtained with EM17+SRG(2.0).

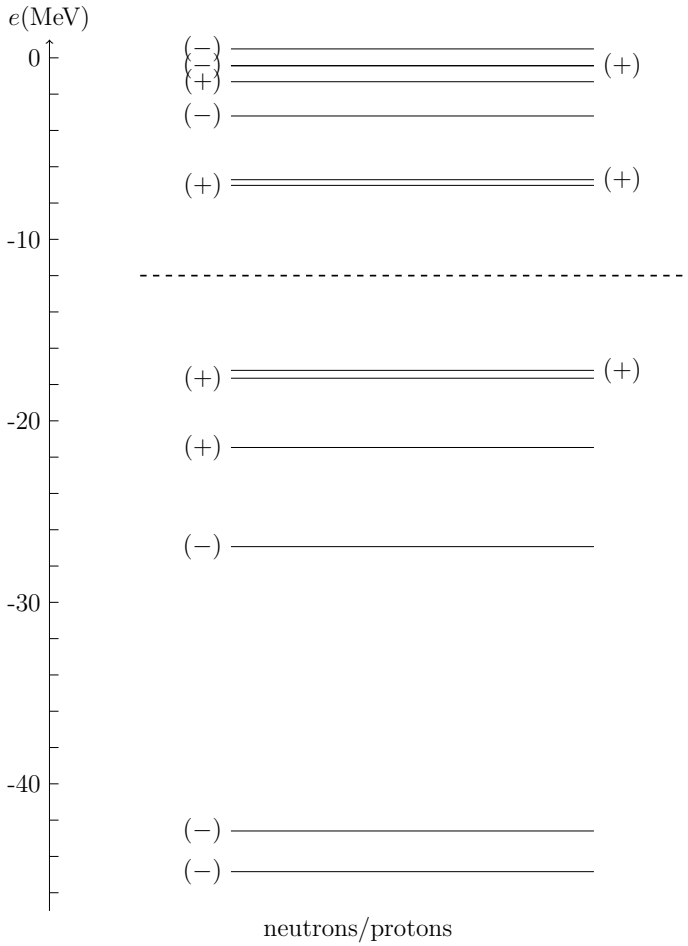

Figure VI.6 Same as Fig. VI.4 for the oblate-deformed Hartree-Fock solution in ^{28}Si with the Skyrme SHZ2 force ($\Lambda_b = 2$ fm^{-1}, $L = 15$ fm).

Table VI.3 Same as Table VI.1 for the oblate-deformed well of ^{28}Si with the Skyrme SHZ2 interaction and $N_h = N_p = 10$.

E_{cut} (MeV)	Basis size	E_{corr} (MeV)	$\|\Phi_0\rangle$ (%)	SP (%)	DP (%)	TP (%)	QP (%)
30	25	−0.1266	99.44	0.56	–	–	–
50	156	−0.2730	99.02	0.98	0.00	–	–
70	841	−0.2744	99.01	0.99	0.00	0.00	–
100	5656	−0.3007	98.94	1.05	0.00	0.00	0.00
120	14141	−0.3009	98.94	1.05	0.00	0.00	0.00

To explicitly assess the possible impact of the restriction of the valence window the same calculations have been repeated with a larger window corresponding to 12 hole and 12 particle states. As can be seen from VI.4, the pair structure of the ground state is very stable against the window size although the correlation energy decreases by about 20% when enlarging the many-body basis. This is due to the structure of the correlated state that contains many small contributions of single-pair excitations which bring extra binding to the correlation energy. One can presumably ascribe this behavior to the non–regularized character of the Skyrme interaction (dominated by the zero–range central part).

Table VI.4 Same as Table VI.3 with $N_h = N_p = 12$.

E_{cut} (MeV)	Basis size	E_{corr} (MeV)	$\|\Phi_0\rangle$ (%)	SP (%)	DP (%)	TP (%)	QP (%)
30	25	−0.1266	99.44	0.56	–	–	–
50	165	−0.2689	99.03	0.97	0.00	–	–
70	1059	−0.3090	98.94	1.06	0.00	0.00	–
100	8507	−0.3621	98.81	1.18	0.01	0.00	0.00
120	24488	−0.3626	98.81	1.18	0.01	0.00	0.00

VI.3.3 Strong-pairing regime in ^{98}Sr

The ^{98}Sr nucleus has a well-deformed prolate equilibrium shape that provides it with a fairly good rotor character. Indeed a rotational band built on its ground state has been experimentally observed. As explained above we have to limit the box size to $L = 15$ fm and we use a cutoff of 2 fm^{-1} on single-particle momenta. The results shown below may thus be affected by an unknown uncertainty. However the qualitative features that we shall analyze are expected to be robust against the variation of single-particle basis parameters.

Calculations with the Daejeon16 interaction. The obtained HF solution is such that $\beta_2 = 0.22$ and the corresponding single-particle spectrum is depicted in Fig. VI.7.

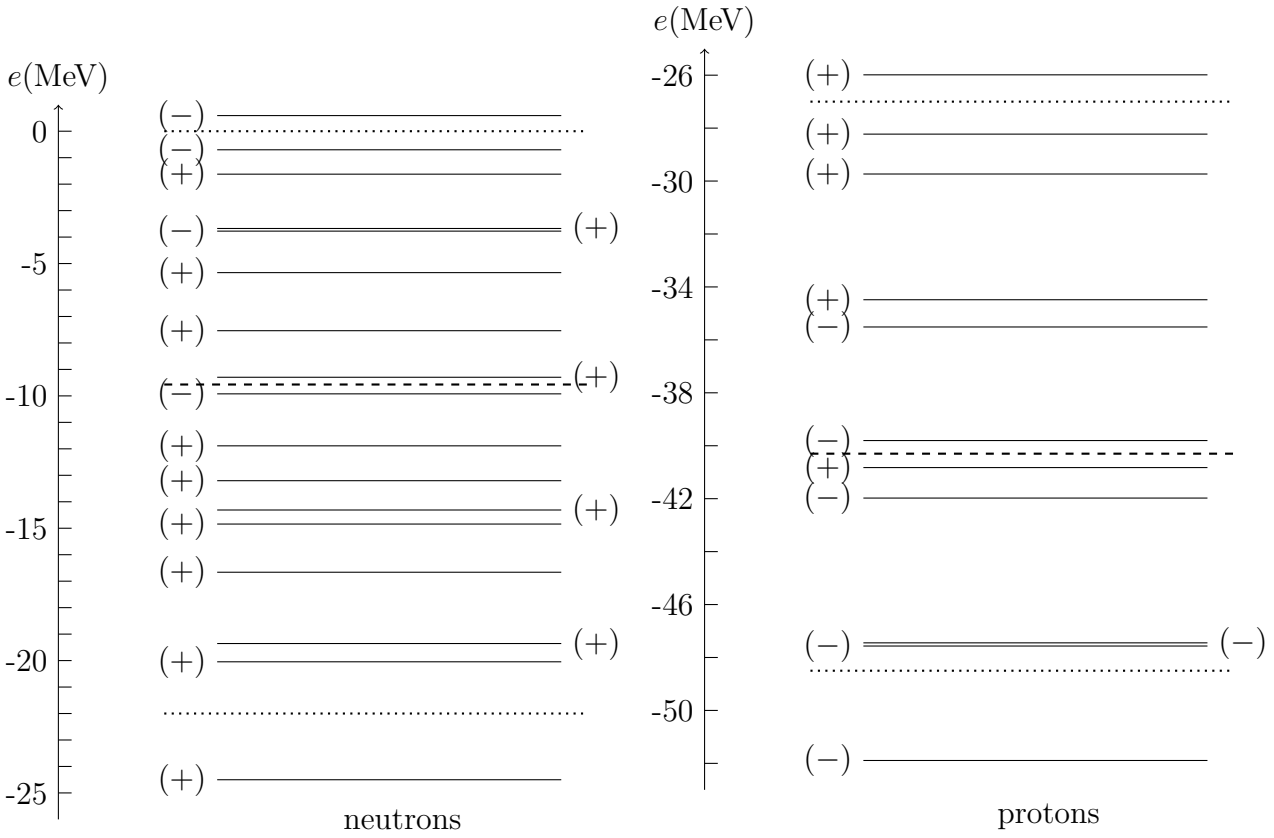

Figure VI.7 Same as Fig. VI.4 for the prolate-deformed Hartree–Fock solution in ^{98}Sr with the Daejeon16 interaction and box size $L = 15$ fm.

In addition to an overall much larger level density than in ^{28}Si we find a small energy gap across the neutron Fermi level of 0.625 MeV, and a larger gap of 1.02 MeV in the proton spectrum. Then we consider a valence window corresponding to $N_h = 16$, $N_p = 14$ for neutrons and $N_h = 8$, $N_p = 10$ for protons. With this choice of window, the minimum energy of SP excitations built from excluded hole states is about 30 MeV. The numbers of various multiple-pair excitations retained in the many-body basis are given in Table VI.5 as a function of $E_{\rm cut}$, together with the total basis size.

Table VI.5 Composition of the HTDA basis for ^{98}Sr with the Daejeon16 interaction and valence window corresponding to $N_h = 16$, $N_p = 14$ for neutrons and $N_h = 8$, $N_p = 10$ for protons.

$E_{\rm cut}$ (MeV)	SP	DP	TP	QP	Total size
10	8	8	0	0	17
20	33	67	17	0	118
30	62	306	192	8	569
40	76	749	1010	161	1997
50	76	1263	3177	1221	5738

The HTDA results for the lowest three eigenstates are presented in Table VI.6.

Table VI.6 Same as Table VI.1 for ^{98}Sr with the Daejeon16 potential for the ground state and first two excited states. The valence window corresponds to $N_h = 16$, $N_p = 14$ for neutrons and $N_h = 8$, $N_p = 10$ for protons.

HTDA ground state $|\Psi_0\rangle$:

E_{cut} (MeV)	E_{corr} (MeV)	$\|\Phi_0\rangle$ (%)	SP (%)	DP (%)	TP (%)	QP (%)
10	−0.760	0.0	97.6	2.3	–	–
20	−0.979	0.1	96.0	3.9	0.0	–
30	−1.177	0.1	94.5	5.4	0.1	0.0
40	−1.226	0.1	94.2	5.6	0.1	0.0
50	−1.231	0.1	93.9	5.9	0.1	0.0

HTDA first excited state $|\Psi_1\rangle$:

E_{cut} (MeV)	E_{corr} (MeV)	$\|\Phi_0\rangle$ (%)	SP (%)	DP (%)	TP (%)	QP (%)
10	−0.400	0.0	2.3	97.7	–	–
20	−0.558	0.0	2.8	96.7	0.5	–
30	−0.762	0.0	3.5	95.1	1.4	0.0
40	−0.811	0.0	3.6	94.9	1.5	0.0
50	−0.825	0.0	3.8	94.6	1.6	0.0

HTDA second excited state $|\Psi_2\rangle$:

E_{cut} (MeV)	E_{corr} (MeV)	$\|\Phi_0\rangle$ (%)	SP (%)	DP (%)	TP (%)	QP (%)
10	−0.034	97.0	3.0	0.0	–	–
20	−0.289	95.2	4.7	0.0	0.0	–
30	−0.464	93.3	6.6	0.1	0.0	0.0
40	−0.510	93.0	6.8	0.1	0.0	0.0
50	−0.515	92.8	7.0	0.2	0.0	0.0

The structure of each of these eigenstates is largely dominated by one configuration:

- the SP configuration of lowest unperturbed excitation energy $2 \times 0.625 = 1.25$ MeV for $|\Psi_0\rangle$;
- the DP configuration of lowest unperturbed excitation energy $2 \times (0.625 + 1.02) = 3.29$ MeV for $|\Psi_1\rangle$;

- the HF solution for $|\Psi_2\rangle$.

A common feature in these eigenstates is that the contributions to their structure of the basis states differing by more than two nucleons from the dominant configuration are rather small (less than about 7% in all three cases). Moreover the structure and correlation energy of these three low-lying HTDA solutions converge with $E_{\rm cut}$.

As a conclusion of these first HTDA calculations we can say that the residual interactions associated with non empirical interactions are expected to be well suited to describe pairing correlations.

Conclusion and outlook

In this thesis, we have developed the Hartree-Fock approximation for the description of deformed nuclei with non-empirical two-nucleon potentials. A detailed study of this approximation with various momentum bases has been performed. The general structure of realistic nucleon-nucleon interactions analyzed in momentum space allowed us to determine the strategy to implement such interactions.

A large part of the present work was devoted to the study of the Hartree-Fock approximation in the momentum space representation. We have shown that the confined plane-wave basis is very efficient in terms of numerical resources compared to the partial-wave basis. In particular, it can be used to construct the symmetry-adapted basis that is necessary to ensure a minimal symmetry at the one-body level. We have chosen a symmetry group generated by the parity, z-signature and time-y-signature operators because it allows one to describe triaxial shapes of nuclei in states that potentially break the time-reversal symmetry at the mean-field level without losing quantum numbers. Indeed its irreducible co-representations are of dimension 1 and are associated with two quantum numbers (brought by the first two, unitary generators). This is in contrast with the group generated by two signature operators in addition to parity and time-reversal operators whose unitary subgroup is non abelian.

The study of the Hartree-Fock convergence with the truncation parameters shows a simple rule to use this basis in which the box size is solely dependent on the nuclear radius. It is worth noting that this dependence is not altered by the presence of the Coulomb force or the two-body kinetic energy correction. On the other hand, the spherical momentum cut-off in the confined plane-wave basis is a variational parameter and one expects to have a solution of lower binding energy as the momentum cut-off increases. Moreover, because of the finiteness (consequence of truncation) and discreteness (resulting from confinement in a box) of the confined plane-wave basis, this cut-off parameter is constrained by the momentum scale of the nuclear interaction and a physical scale generated from the latter and its one-body reduction via the self-consistent process. This means that the momentum truncation in the confined plane-wave basis is essentially governed by the nuclear interaction.

Once the basis parameters have been properly chosen, Hartree-Fock calculations have been performed with several two-nucleon potentials: phenomenological potentials of the Skyrme type without density dependence, chiral potentials developed by Entem and collaborators [13] and by the Bochum group [11], [82], and the Daejeon16 potential [52] originating from a SRG transformed

chiral potential [12] subject to subsequent phase-equivalent transformations, and whose remaining parameters are adjusted to light nuclei. We have found that among these potentials, those of the Bochum group give the least binding in nuclei at the Hartree–Fock level, and that they need a strong renormalization in order to be used in a mean-field calculation. Then we have performed SRG transformations of the chiral potentials using a block-diagonal generator of the transformation. This allows to derive an effective low-momentum potential with a controlled cut-off on relative momenta, hence a natural cut-off parameter for the confined plane-wave basis.

The application of the above effective potentials to Hartree–Fock calculations in doubly open-shell even-even nuclei (^{24}Mg, ^{28}Si, ^{48}Cr and ^{98}Sr) gives similar values of the (axial) quadrupole deformation parameter β_2 for all considered potentials. Moreover these β_2 values are very close to those obtained with phenomenological Skyrme energy-density functionals.

Based on this qualitative success, within the Highly Truncated Diagonalization Approach (HTDA), we have addressed the description of pairing properties with residual interactions constructed from two non-empirical two-nucleon potentials, namely the Daejeon16 potential and the SRG-evolved potential (EM17+SRG(2.0)) starting from the N^{3}LO chiral potential developed by [13], and the phenomenological density-independent force SHZ2. To this aim, we neglect the Coulomb and kinetic corrections and consider only the nuclear force. The valence space used to build excitations of conjugate states in the many-body basis is constructed so that the residual interaction between considered many-body basis states is much weaker than their excitation energy. We study the convergence of HTDA solutions as a function of the excitation energy cut-off ($E_{\rm cut}$) inside the above-defined valence space. In ^{28}Si where weak pairing correlations are expected due to a low level density, EM17+SRG(2.0) yields a comparable HTDA solution with respect to the phenomenological force SHZ2. The convergence for both forces is observed at $E_{\rm cut} \sim 70-100$ MeV. In the second HTDA calculation in ^{98}Sr using the Daejeon16 force, the single-particle spectrum in HF solution exhibits a much larger level density than in ^{28}Si. The convergence is reached at $E_{\rm cut} \sim 50$ MeV with the ground state dominated by excitations of single pairs.

Because the Hartree-Fock approximation often represents the first step in sophisticated many-body methods to solve the nuclear many-body problem (Coupled Cluster [83], Many-Body Perturbation Theory [84], Generator Coordinate method [85], symmetry restoration [71], [85], [86], RPA and its extensions [29]...), the present work could serve as a starting point for these methods. However, to do so one needs to make several extensions. First for the chiral or SRG-based interactions, the three-body interaction has to be added. In such case, owing to its specific properties, the confined plane-wave basis presents an advantage in the center-of-mass motion treatment with respect to the partial-wave basis. Moreover, to treat odd nuclei or finite-seniority states of even-even nuclei, it is possible to extend the current Hartree-Fock implementation by including a blocking procedure of one or more Hartree-Fock orbitals during the iterative process.

Finally within the HTDA framework one can straightforwardly include the residual interaction derived from the Coulomb potential and two-body kinetic energy correction. In particular this would allow to assess the isospin mixing in $N = Z$ nuclei induced by the nuclear interaction, complementing the study initiated in Ref. [78].

Appendix A: Two-nucleon problem

In this appendix, the two-body problem (bound state properties and scattering) is studied in the partial-wave basis. The formalism developed here is used in order to perform a benchmark of two-body matrix elements (as well as the renormalization within the SRG approach, see Chapter II) of the chiral interactions that are employed in this thesis work.

A.1 Two-nucleon bound state: the deuteron

The deuteron ($N = Z = 1$) is the only bound state of two nucleons and has quantum numbers $J^\pi = 1^+$, $T = 0$ (conserved with a very good approximation) and $T_z = 0$. To determine its wave function, let us denote by $\mathbf{k}$ and $\mathbf{K}$ the relative and total momenta of the system, respectively

$$\mathbf{k} = \frac{1}{2}\left(\mathbf{k}_1 - \mathbf{k}_2\right), \tag{A.1}$$

$$\mathbf{K} = \mathbf{k}_1 + \mathbf{k}_2\,, \tag{A.2}$$

and by $\mu = m_n m_p/(m_n + m_p) \approx m_N$ the reduced mass (approximately equal to the nucleon mass $m_N \approx m_n \approx m_p$). The Hamiltonian of the reduced system is

$$\hat{H} = \hat{H}_0 + \hat{V}$$

where $\hat{H}_0 = \frac{\hat{\mathbf{P}}^2}{2\mu}$ is the intrinsic kinetic-energy operator, $\hat{\mathbf{P}}$ is the relative-momentum operator such that $\hat{\mathbf{P}}|\mathbf{k}\rangle = \hbar\mathbf{k}\,|\mathbf{k}\rangle$ and $\hat{V}$ is the nucleon-nucleon interaction, whose matrix elements depend only on $\mathbf{k}$ (and not on $\mathbf{K}$ as seen in chapter I).

A.1.1 Eigenvalue radial equation in momentum space

In momentum-spin-isospin representation $\{|\mathbf{k}SS_zTT_z\rangle, \mathbf{k}\in\mathbb{R}^3, S,T\in\{0,1\}, -S\leq S_z\leq S, -T\leq T_z\leq T\}$, the ground state of the relative motion of the deuteron can be written as

$$\begin{aligned}|\Psi\rangle &= \frac{1}{N_k}\sum_{S,S_z,T,T_z}\int_{\mathbb{R}^3} d^3\mathbf{k}\langle\mathbf{k}SS_zTT_z\,|\,\Psi\rangle\,|\mathbf{k}SS_zTT_z\rangle \\ &= \sum_{\substack{S,T,T_z\\L,J,J_z\\L',J',J'_z}} i^{L-L'}\int dk\,k^2\underbrace{\left[\sum_{S_z}\int_0^{+\infty}d\hat{k}\Big(\mathcal{Y}^{L'S}_{J'J'_z}(\hat{k})\Big)_{S_z}\Big(\mathcal{Y}^{LS}_{JJ_z}(\hat{k})\Big)^*_{S_z}\right]}_{\delta_{LL'}\delta_{JJ'}\delta_{J_zJ'_z}}\langle k(L'S)J'J'_zTT_z\,|\,\Psi\rangle\,|k(LS)JJ_zTT_z\rangle\end{aligned}$$

where we have used a partial-wave expansion to express

$$|\mathbf{k}SS_z\rangle = \sum_{L=0}^{+\infty} i^L\sum_{J=|L-S|}^{L+S}\sum_{J_z=-J}^{J}\Big(\mathcal{Y}^{LS}_{JJ_z}(\hat{k})\Big)^*_{S_z}\,|k(LS)JJ_z\rangle \tag{A.3}$$

with the tensor spherical harmonics of rank-S

$$\mathcal{Y}^{LS}_{JJ_z}(\hat{k}) = \sum_{S_z=-S}^{S}\Big(\sum_{M=-L}^{L}Y_{LM}(\hat{k})\Big)|SS_z\rangle. \tag{A.4}$$

The partial-wave state $|k(LS)JJ_z\rangle$ verifies the orthogonal and closure relations

$$\langle k'(L'S')J'J'_z\,|\,k(LS)JJ_z\rangle = N_k\frac{\delta(k'-k)}{k^2}\delta_{l'l}\delta_{S'S}\delta_{J'J}\delta_{J'_zJ_z}, \tag{A.5}$$

$$\frac{1}{N_k}\sum_{L=0}^{+\infty}\sum_{J=|L-S|}^{L+S}\sum_{J_z=-J}^{J}\int_0^{+\infty}dk\,k^2\,|k(LS)JJ_z\rangle\langle k(LS)JJ_z| = \mathbb{1}. \tag{A.6}$$

Hence, with the notation $\Psi_L^{(SJTT_z)}(k) = \langle k(LS)JJ_zTT_z\,|\,\Psi\rangle$

$$|\Psi\rangle = \frac{1}{N_k}\sum_{L,S,J,J_z,T,T_z}\int_0^{+\infty}dk\,k^2\,\Psi_L^{(SJJ_zTT_z)}(k)\,|k(LS)JJ_zTT_z\rangle\,. \tag{A.7}$$

The eigenvalue equation $\hat{H}|\Psi\rangle = E\,|\Psi\rangle$ thus becomes

$$\begin{aligned}&\frac{(\hbar k)^2}{2\mu}\,\Psi_L^{(SJJ_zTT_z)}(k) + \frac{1}{N_k}\sum_{\substack{L',S'\\J',J'_z\\T',T'_z}}\int_0^{+\infty}dk'\,k'^2\langle k(LS)JJ_zTT_z|\hat{V}|k'(L'S')J'J'_zT'T'_z\rangle\,\Psi_L^{(S'J'J'_zT'T'_z)}(k') \\ &= E\,\Psi_L^{(SJJ_zTT_z)}(k)\,.\end{aligned} \tag{A.8}$$

Because of the symmetries of a nucleon-nucleon interaction of class I, II and III and because we assume that the neutron and proton are identical particles (distinguished by their isospin projection only), the quantum numbers S, J, J_z, T, T_z are conserved and the interaction matrix element does not depend on J_z. Therefore the radial wave function $\Psi(k)$ does not depend on J_z which is

omitted from now on. The isospin quantum number T_z is also omitted in the wave function. We are left with the four quantum numbers L, S, J and T in the notation of the wave function. The latter three are noted as superscripts in parenthis so that the only varying quantum number L labels the various components of the radial wave function. The eigenvalue equation becomes an integral equation

$$\boxed{\frac{(\hbar k)^2}{2\mu}\,\Psi_L^{(SJT)}(k) + \frac{1}{N_k}\sum_{L'}\int_0^{+\infty} dk'\,k'^2\,v_{LL'}^{(SJTT_z)}(k,k')\,\Psi_{L'}^{(SJT)}(k') = E\,\Psi_L^{(SJT)}(k)}\,, \tag{A.9}$$

where we have set $v_{LL'}^{(SJTT_z)}(k,k') = \langle k(LS)JTT_z|\hat{v}|k'(L'S)JTT_z\rangle$.

A.1.2 Numerical resolution by the Lagrange-mesh method

We discretize the momentum variable k according to the upper bound $k_{\max}$ of the integral equation (A.9):

- roots of the Laguerre polynomial if $k_{\max} = \infty$;
- roots of scaled Legendre polynomial if $k_{\max} = \Lambda$ (finite cut-off, as for $V_{\mathrm{low-k}}$ effective interactions).

For definiteness, let us consider the Laguerre polynomial L_n of degree n. The corresponding regularized Lagrange function f_i is given by [87]

$$f_i(\kappa) = \frac{(-1)^i}{\sqrt{\kappa_i}}\,\frac{\kappa}{\kappa-\kappa_i}\,L_n(\kappa)\,e^{-\kappa}\,, \tag{A.10}$$

and satisfies the following property

$$f_j(\kappa_i) = \frac{\delta_{ij}}{\sqrt{\lambda_j}}\,, \tag{A.11}$$

where κ_i is a root of the Laguerre polynomial L_n and λ_i is the associated weight in the Gauss–Laguerre quadrature

$$\int_0^\infty dk\,g(k) \approx \sum_{i=1}^{n}\lambda_i\,g(\kappa_i)\,. \tag{A.12}$$

The functions f_i are not exactly orthogonal but at the Gauss approximation we have

$$\int_0^\infty dk\,f_i(k)\,f_j(k) \approx \delta_{ij}\,. \tag{A.13}$$

The weight λ_i can be calculated using the following relation involving the roots κ_j

$$\ln\lambda_i = \kappa_i - \ln\kappa_i + 2\,\ln n! - \sum_{\substack{j=1\\ j\neq i}}^{n}\ln(\kappa_i-\kappa_j)^2\,. \tag{A.14}$$

The radial wave function $\Psi_L^{(SJT)}(k)$ can be expanded in terms of the regularized Lagrange functions as

$$\Psi_L^{(SJT)}(k) = \sum_{i=1}^{n} C_{L,i}^{(SJT)} \frac{f_i(\kappa)}{\sqrt{h}\,k}\,, \tag{A.15}$$

where $\kappa = k/h$ and h is a scale factor having the dimension of a linear momentum. Inserting expansion (A.15) in Eq. (A.9) and evaluating the integral with a Gauss quadrature, we can write

$$\begin{aligned}
&\frac{\hbar^2}{2\mu}\,(h\kappa)^2 \sum_{i=1}^{n} C_{L,i}^{(SJT)} \frac{f_i(\kappa)}{\sqrt{h}\,h\kappa} + \frac{1}{N_k}\int_0^{+\infty} dk'\,k'^2 \sum_{L'} \langle (h\kappa)(LS)JTT_z|\hat{v}|k'(L'S)JTT_z\rangle \sum_{i=1}^{n} C_{L',i}^{(SJT)} \frac{f_i(\kappa')}{\sqrt{h}\,k'} \\
&\approx \frac{\hbar^2}{2\mu}\,(h\kappa)^2 \sum_{i=1}^{n} C_{L,i}^{(SJT)} \frac{f_i(\kappa)}{\sqrt{h}\,h\kappa} + \frac{1}{N_k}\sum_{j=1}^{n} \lambda_j\, h^2 \kappa_j \sum_{L'} v_{L,L'}^{(SJTT_z)}(h\kappa, h\kappa_j) \sum_{i=1}^{n} C_{L',i}^{(SJT)} \frac{f_i(\kappa_j)}{\sqrt{h}} \\
&= \frac{\hbar^2}{2\mu}\,(h\kappa)^2 \sum_{i=1}^{n} C_{L,i}^{(SJT)} \frac{f_i(\kappa)}{\sqrt{h}\,h\kappa} + \frac{1}{N_k}\sum_{i=1}^{n} \sqrt{\lambda_i}\, h^{3/2}\, \kappa_i \sum_{L'} v_{L,L'}^{(SJTT_z)}(h\kappa, h\kappa_i)\, C_{L',i}^{(SJT)} \\
&= E \sum_{i=1}^{n} C_{L,i}^{(SJT)} \frac{f_i(\kappa)}{\sqrt{h}\,h\kappa}\,.
\end{aligned} \tag{A.16}$$

We can now multiply this equation by $h^{3/2}\,\kappa\, f_j(\kappa)$ and integrate on $[0;+\infty[$ with, again, the Gauss quadrature formula (A.13)

$$\begin{aligned}
&\int_0^{+\infty} d\kappa\,\kappa\, f_j(\kappa) \left[\frac{\hbar^2}{2\mu}\,(h\kappa)^2 \sum_{i=1}^{n} C_{L,i}^{(SJT)} \frac{f_i(\kappa)}{\kappa} + \frac{1}{N_k}\sum_{i=1}^{n} \sqrt{\lambda_i}\, h^3\, \kappa_i \sum_{L'} v_{L,L'}^{(SJTT_z)}(h\kappa, h\kappa_i)\, C_{L',i}^{(SJT)}\right] \\
&\approx \sum_{m=1}^{n} \lambda_m\, \kappa_m\, f_j(\kappa_m) \left[\frac{\hbar^2}{2\mu}\,(h\kappa_m)^2 \sum_{i=1}^{n} C_{L,i}^{(SJT)} \frac{f_i(\kappa_m)}{\kappa_m} + \frac{1}{N_k}\sum_{i=1}^{n} \sqrt{\lambda_i}\, h^3\, \kappa_i \sum_{L'} v_{L,L'}^{(SJTT_z)}(h\kappa_m, h\kappa_i)\, C_{L',i}^{(SJT)}\right] \\
&= \sqrt{\lambda_j}\,\kappa_j \left[\frac{\hbar^2}{2\mu}\,(h\kappa_j)^2 C_{L,j}^{(SJT)} \frac{1}{\sqrt{\lambda_j}\,\kappa_j} + \frac{1}{N_k}\sum_{i=1}^{n} \sqrt{\lambda_i}\, h^3\, \kappa_i \sum_{L'} v_{L,L'}^{(SJTT_z)}(h\kappa_j, h\kappa_i)\, C_{L',i}^{(SJT)}\right] \\
&= E \int_0^{\infty} d\kappa\, f_j(\kappa) \sum_{i=1}^{n} C_{L,i}^{(SJT)}\, f_i(\kappa) \approx E\, C_{L,j}^{(SJT)}\,.
\end{aligned} \tag{A.17}$$

Finally, renaming i and j indices for convenience, we obtain the following discretized radial equation for any $i \in \{1, 2\cdots, n\}$ at the Gauss approximation

$$\boxed{\frac{\hbar^2}{2\mu}\,(h\kappa_i)^2\, C_{L,i}^{(SJT)} + \frac{1}{N_k}\sum_{i'=1}^{n} h^3 \sqrt{\lambda_i \lambda_{i'}}\,\kappa_i\kappa_j \sum_{L'} v_{L,L'}^{(SJTT_z)}(h\kappa_i, h\kappa_{i'})\, C_{L',i'}^{(SJT)} = E\, C_{L,i}^{(SJT)}}\,. \tag{A.18}$$

Let us arrange the components of the one-column matrix $C^{(SJT)}$ as follows

$$C^{(SJT)} = \begin{pmatrix} C^{(SJT)}_{0,1} \\ \vdots \\ C^{(SJT)}_{0,n} \\ \vdots \\ C^{(SJT)}_{L,1} \\ \vdots \\ C^{(SJT)}_{L,n} \\ \vdots \end{pmatrix} \tag{A.19}$$

and let us define a multi-index α representing the orbital momentum L and discretization index i. The eigenvalue equation (A.18) thus takes the more familiar matrix form

$$H^{(SJT)}\, C^{(SJT)} = E\, C^{(SJT)}\,, \tag{A.20}$$

where the hermitian matrix $H^{(SJT)}$ is defined by its elements

$$\boxed{H^{(SJT)}_{\alpha\beta} = H^{(SJT)}_{Li,L'i'} = \delta_{LL'}\delta_{ii'}\,\frac{\hbar^2}{2\mu}\,(h\kappa_i)^2 + h^3\,\sqrt{\lambda_i\lambda_{i'}}\,\kappa_i\kappa_{i'}\,v^{(SJTT_z)}_{L,L'}(h\kappa_i, h\kappa_{i'})}\,. \tag{A.21}$$

A.2 Two-nucleon scattering

Let us consider now the scattering of two nucleons at sufficiently low energies compared to the excitation energy of the lowest nucleon resonance. We thus have to deal with elastic scattering only. Moreover we assume that a non-relativistic description is adequate. We adopt the heuristic stationary-state approach and follow Morrison and Feldt presentation of key definitions and results [88].

A.2.1 S matrix, phase shifts and low-energy scattering parameters

The Møller operators $\hat{\Omega}_\pm$ are defined by

$$\hat{\Omega}_\pm = \lim_{t\to\mp\infty}\, \hat{U}^\dagger(t)\hat{U}_0(t) \tag{A.22}$$

where $\hat{U}(t) = e^{-it\,\hat{H}/\hbar}$ and $\hat{U}_0(t) = e^{-it\,\hat{H}_0/\hbar}$ are the time-evolution operators associated with the Hamiltonian $\hat{H}$ in the center-of-mass frame and the intrinsic kinetic-energy operator $\hat{H}_0$ (free

particle Hamiltonian). They are such that

$$|\Psi(0)\rangle = \hat{\Omega}_+|\Psi_{\text{in}}\rangle = \hat{\Omega}_-|\Psi_{\text{out}}\rangle \,, \tag{A.23}$$

where $|\Psi(0)\rangle$ is the scattering state at $t = 0$ and $|\Psi_{\text{in}}\rangle$, $|\Psi_{\text{out}}\rangle$ are the incoming and outgoing asymptotic scattering states (called in- and out-asymptote). In terms of the evolution operator, these relations are

$$\lim_{t\to\infty} \hat{U}(t)|\Psi(0)\rangle = \lim_{t\to\infty} \hat{U}_0(t)|\Psi_{\text{out}}\rangle \tag{A.24a}$$

$$\lim_{t\to-\infty} \hat{U}(t)|\Psi(0)\rangle = \lim_{t\to-\infty} \hat{U}_0(t)|\Psi_{\text{in}}\rangle \,. \tag{A.24b}$$

The scattering operator $\hat{S}$ is the defined as

$$\hat{S} = \hat{\Omega}_-^\dagger \hat{\Omega}_+ \,, \tag{A.25}$$

and maps a given incoming scattering state into the corresponding outgoing one

$$|\Psi_{\text{out}}\rangle = \hat{S}\,|\Psi_{\text{in}}\rangle \,. \tag{A.26}$$

The probability amplitude for the scattering process $|\mathbf{k}SS_zTT_z\rangle \to |\mathbf{k}'S'S'_zT'T'_z\rangle$ is the matrix element $\langle \mathbf{k}'S'S'_zT'T'_z|\hat{S}|\mathbf{k}SS_zTT_z\rangle$.

Let us introduce the resolvent $\hat{G}(z)$ of the Hamitonian $\hat{H}$ (also called Green's operator) for any complex z which does not belong to the spectrum of $\hat{H}$

$$\hat{G}(z) = (z - \hat{H})^{-1} \tag{A.27}$$

Similarly $\hat{G}_0(z)$ denotes the resolvent of the kinetic-energy operator $\hat{H}_0$ (also called free-particle Green's operator). One can establish the so-called right-side Lippmann–Schwinger equation for the Green's operator

$$\hat{G}(z) = \hat{G}_0(z) + \hat{G}_0(z)\hat{V}\hat{G}(z) \,, \tag{A.28a}$$

and the left-side equation

$$\hat{G}(z) = \hat{G}_0(z) + \hat{G}(z)\hat{V}\hat{G}_0(z) \,. \tag{A.28b}$$

The transition operator $\hat{T}(z)$ is then defined in terms of the Green's operator by

$$\hat{T}(z) = \hat{V} + \hat{V}\hat{G}(z)\hat{V} \tag{A.29}$$

and obeys the right-side Lippmann–Schwinger equation

$$\hat{T}(z) = \hat{V} + \hat{V}\hat{G}_0(z)\hat{T}(z) \,, \tag{A.30a}$$

and the left-side Lippmann–Schwinger equation

$$\hat{T}(z) = \hat{V} + \hat{T}(z)\hat{V}\hat{G}_0(z)\,. \tag{A.30b}$$

From Eqs. (A.28a) to (A.30b) one deduces that

$$\hat{G}_0(z)\,\hat{T}(z) = \hat{G}(z)\,\hat{V} \tag{A.31a}$$
$$\hat{T}(z)\,\hat{G}_0(z) = \hat{V}\,\hat{G}(z)\,. \tag{A.31b}$$

The $\hat{T}$ operator has thus the same symmetry properties as the interaction $\hat{V}$—namely the rotation symmetry and the number of neutrons and protons. In the following we consider interactions which in addition conserve the total spin S of the two-nucleon system, its projection S_z, and the total isospin T of the system.

For real values E the matrix elements $\langle \mathbf{k}'|\hat{T}(E)|\mathbf{k}\rangle$ (omitting spin and isopin degrees of freedom to alleviate the expression) are said to be

(i) on-shell when

$$E = \frac{(\hbar\mathbf{k})^2}{2\mu} = \frac{(\hbar\mathbf{k}')^2}{2\mu}$$

(ii) right-side half-on-shell (or half-on-shell) when

$$E = \frac{(\hbar\mathbf{k})^2}{2\mu} \neq \frac{(\hbar\mathbf{k}')^2}{2\mu}$$

(iii) left-side half-on-shell when

$$E = \frac{(\hbar\mathbf{k}')^2}{2\mu} \neq \frac{(\hbar\mathbf{k})^2}{2\mu}$$

(iv) fully off-shell when

$$E \neq \frac{(\hbar\mathbf{k})^2}{2\mu} \quad \text{and} \quad k \neq k'\,.$$

The right-side half-on-shell T matrix elements are related to the elastic-scattering differential cross section and the on-shell T matrix elements are connected to the scattering matrix elements in momentum representation through

$$\begin{aligned}\langle \mathbf{k}'S'S'_zT'T'_z|\hat{S}|\mathbf{k}SS_zTT_z\rangle = {}& \delta(\mathbf{k}-\mathbf{k}')\delta_{SS'}\delta_{S_zS'_z}\delta_{TT'}\delta_{T_zT'_z} \\ & - 2\pi i\,\delta(E_k - E_{k'}) \lim_{\epsilon\to 0^+} \langle \mathbf{k}'S'S'_zT'T'_z|\hat{T}(E_k + i\epsilon)|\mathbf{k}SS_zTT_z\rangle\,.\end{aligned} \tag{A.32}$$

where $E_k = \frac{(\hbar k)^2}{2\mu}$. The $\hat{S}$ operator thus has the same symmetry properties as the $\hat{T}$ operator. In the LS-coupled partial-wave basis one has

$$\begin{aligned}
&\langle k'(L'S)JJ_zTT_z|\hat{S}|k(LS)JJ_zTT_z\rangle \\
&= \sum_{S_z}\int d^3\mathbf{k}_1 \sum_{S'_z}\int d^3\mathbf{k}_2 \langle k'(L'S)JJ_zTT_z\,|\,\mathbf{k}_1SS_zTT_z\rangle\langle \mathbf{k}_1SS_zTT_z|\hat{S}|\mathbf{k}_2SS'_zTT_z\rangle \times \\
&\langle \mathbf{k}_2SS'_zTT_z\,|\,k(LS)JJ_zTT_z\rangle \\
&= \sum_{S_z}\int d^3\mathbf{k}_1 \sum_{S'_z}\int d^3\mathbf{k}_2 i^{L'-L}\Big(\mathcal{Y}^{L'S}_{JJ_z}(\hat{k}_1)\Big)^*_{S_z}\Big(\mathcal{Y}^{LS}_{JJ_z}(\hat{k}_2)\Big)_{S'_z}\frac{\delta(k_1-k')}{k'k_1}\,\frac{\delta(k_2-k)}{kk_2}\times \\
&\Big(\delta(\mathbf{k}_1-\mathbf{k}_2)\,\delta_{S_zS'_z} - 2\pi i\,\delta(E_{k_1}-E_{k_2})\lim_{\epsilon\to 0^+}\langle \mathbf{k}_1SS_zTT_z|\hat{T}(E_{k_2}+i\epsilon)|\mathbf{k}_2SS'_zTT_z\rangle\Big) \\
&= i^{L'-L}\int dk''\,k''^2\frac{\delta(k''-k')\,\delta(k''-k)}{k''^2kk'}\int d\hat{k}''\sum_{S_z}\Big(\mathcal{Y}^{L'S}_{JJ_z}(\hat{k}'')\Big)^*_{S_z}\Big(\mathcal{Y}^{LS}_{JJ_z}(\hat{k}'')\Big)_{S_z} \\
&\quad - 2\pi i\lim_{\epsilon\to 0^+}\int dk_1\,k_1^2\int dk_2\,k_2^2\,\frac{\delta(k_1-k')}{k'k_1}\,\frac{\delta(k_2-k)}{kk_2}\,\frac{\mu}{\hbar^2}\,\frac{\delta(k_1-k_2)}{k_1}\times \\
&\quad i^{L'-L}\int d\hat{k}_1\int d\hat{k}_2\sum_{S_z}\Big(\mathcal{Y}^{L'S}_{JJ_z}(\hat{k}_1)\Big)^*_{S_z}\Big(\mathcal{Y}^{LS}_{JJ_z}(\hat{k}_2)\Big)_{S_z}\langle \mathbf{k}_1SS_zTT_z|\hat{T}(E_{k_2}+i\epsilon)|\mathbf{k}_2SS'_zTT_z\rangle\,. \qquad \text{(A.33)}
\end{aligned}$$

In the partial-wave basis $\{|k(LS)JJ_zTT_z\rangle\}$, the last line can be identified with the LS-coupled partial-wave matrix element of the $\hat{T}$ operator. One is thus left with

$$\begin{aligned}
\langle k'(L'S)JJ_zTT_z|\hat{S}|k(LS)JJ_zTT_z\rangle = \delta_{LL'}\,\frac{\delta(k-k')}{kk'} - 2\pi i\,\frac{\mu}{\hbar^2}\,\frac{\delta(k-k')}{k}\times \\
\lim_{\epsilon\to 0^+}\langle k'(L'S)JJ_zTT_z|\hat{T}(E_k+i\epsilon)|k(LS)JJ_zTT_z\rangle\,. \qquad \text{(A.34)}
\end{aligned}$$

To define the phase shifts let us first rewrite Eq. (A.34) as

$$\langle k'(L'S)JJ_zTT_z|\hat{S}|k(LS)JJ_zTT_z\rangle = S^{(SJTT_z)}_{L'L}(k)\,\frac{\delta(k-k')}{kk'} \qquad \text{(A.35)}$$

where the S matrix element $S^{(SJTT_z)}_{L'L}(k)$ is defined by

$$\boxed{S^{(SJTT_z)}_{L'L}(k) = \delta_{LL'} - 2\pi i\,\frac{\mu}{\hbar^2}\,k\lim_{\epsilon\to 0^+}T^{(SJTT_z)}_{L'L}(k,k;E_k+i\epsilon)} \qquad \text{(A.36)}$$

with the notation

$$T^{(SJTT_z)}_{L'L}(k',k;z) = \langle k'(L'S)JJ_zTT_z|\hat{T}(z)|k(LS)JJ_zTT_z\rangle\,. \qquad \text{(A.37)}$$

For a fixed value of k and an uncoupled channel ${}^{2S+1}L_J\,(T,T_z)$, the S matrix is diagonal in L and the corresponding element can be parametrized by one real parameter $\delta^{(SJTT_z)}_L(k)$ called a phase shift

$$\boxed{S^{(SJTT_z)}_{LL}(k) \equiv e^{2i\delta^{(SJTT_z)}_L(k)}}\,, \qquad \text{(A.38)}$$

whereas for a coupled channel ${}^3L_J - {}^3(L \pm 2)_J\,(T, T_z)$, in which the total spin is necessarily $S = 1$ and $L = J \mp 1$, the S matrix is two-dimensional and can be parametrized by three real numbers owing to the symmetric and unitary character of the S matrix. In the Stapp parametrization [89], also called "bar-phaseshift" parametrization, we have

$$S_{L'L}(k) \equiv \begin{pmatrix} S_{J-1,J-1} & S_{J-1,J+1} \\ S_{J+1,J-1} & S_{J+1,J+1} \end{pmatrix} \equiv \begin{pmatrix} \cos(2\overline{\epsilon})\, e^{2i\overline{\delta_1}} & i\sin(2\overline{\epsilon})\, e^{2i(\overline{\delta_1}+\overline{\delta_2})} \\ i\sin(2\overline{\epsilon})\, e^{2i(\overline{\delta_1}+\overline{\delta_2})} & \cos(2\overline{\epsilon})\, e^{2i\overline{\delta_2}} \end{pmatrix} \tag{A.39}$$

where the k dependence and the J, $S = 1$, T and T_z quantum numbers have been omitted to alleviate the notation.

The actual calculation of the phase shifts requires to solve the Lippmann–Schwinger equation for the half-on-shell partial-wave T matrix element. This will be done in the next subsection.

At low incident energy, the relative momentum k tends to 0 and the dominant channel of the nucleon-nucleon interaction is a $L = 0$ (uncoupled) channel. In this limit, the corresponding phase shift noted δ_0 can be expanded as

$$\delta_0(k) \approx -a_0 k + o(k^2) \tag{A.40}$$

where a_0 is called the scattering length. One can also expand $k \operatorname{cotan} \delta_0(k)$ as

$$k \operatorname{cotan} \delta_0(k) = -\frac{1}{a_0} + \frac{1}{2}\, r_0\, k^2 + o(k^4) \tag{A.41}$$

where r_0 is called the effective-range parameter.

A.2.2 Lippmann–Schwinger equation for the partial-wave T matrix elements

In the LS-coupled partial-wave basis, the Lippmann–Schwinger for the right-side half-on-shell T matrix elements, with the assumption of a spin conserving interaction, reads

$$T^{(SJTT_z)}_{L'L}(k', k; E_k) = v^{(SJTT_z)}_{L'L}(k', k) + \sum_{L''} \lim_{\epsilon \to 0} \int_0^{+\infty} dk''\, k''^2\, \frac{v^{(SJTT_z)}_{L'L''}(k', k'')\, T^{(SJTT_z)}_{L''L}(k'', k; E_k)}{E_k + i\epsilon - \frac{(\hbar k'')^2}{2\mu}} \tag{A.42}$$

where $E_k = \frac{(\hbar k)^2}{2\mu}$. Owing to the following distribution identity

$$\lim_{\epsilon \to 0^+} \frac{1}{E_k + i\epsilon - E_{k''}} = \mathcal{P}\left(\frac{1}{E_k - E_{k''}}\right) - i\pi\, \delta(E_k - E_{k''})\,, \tag{A.43}$$

where $\mathcal{P}$ denotes the principal value, Eq. (A.42) becomes

$$T^{(SJTT_z)}_{L'L}(k',k;E_k) = v^{(SJTT_z)}_{L'L}(k',k) + \sum_{L''}\left[\mathcal{P}\int_0^{+\infty} dk''\,k''^2\,\frac{v^{(SJTT_z)}_{L'L''}(k',k'')\,T^{(SJTT_z)}_{L''L}(k'',k;E_k)}{E_k - E_{k''}}\right.$$
$$\left. - i\pi\,\frac{\mu}{\hbar^2}\,k\,v^{(SJTT_z)}_{L'L''}(k',k)\,T^{(SJTT_z)}_{L''L}(k,k;E_k)\right]. \tag{A.44}$$

Following Glöckle [90] we introduce the K matrix whose elements in the momentum-spin-isospin partial-wave basis obey the Lippmann–Schwinger equation

$$K^{(SJTT_z)}_{L'L}(k',k;E_k) = v^{(SJTT_z)}_{L'L}(k',k) + \sum_{L''}\mathcal{P}\int_0^{+\infty} dk''\,k''^2\,\frac{v^{(SJTT_z)}_{L'L''}(k',k'')\,K^{(SJTT_z)}_{L''L}(k'',k;E_k)}{E_k - E_{k''}}\,. \tag{A.45}$$

Because the matrix elements of $\hat{V}$ are real, so are those of the K matrix. The T matrix is related to the K matrix through

$$T^{(SJTT_z)}_{L'L}(k',k;E_k) = K^{(SJTT_z)}_{L'L}(k',k;E_k) - i\pi\,\frac{\mu}{\hbar^2}\,k\sum_{L''}K^{(SJTT_z)}_{L'L''}(k',k;E_k)\,T^{(SJTT_z)}_{L''L}(k,k;E_k)\,. \tag{A.46}$$

On energy shell and in matrix form, Eq. (A.46) can be solved as

$$T^{(SJTT_z)}(k,k;E_k) = \left(1 + i\pi\,\frac{\mu}{\hbar^2}\,k\,K^{(SJTT_z)}(k,k;E_k)\right)^{-1} K^{(SJTT_z)}(k,k;E_k) \tag{A.47}$$

and the resulting expression for $T^{(SJTT_z)}_{L''L}(k,k)$ can then be inserted in Eq. (A.46) to yield the half-on-shell T matrix elements. The S matrix can finally be expressed directly in terms of the on-shell K matrix as

$$S^{(SJTT_z)}(k) = \left(1 + i\pi\,\frac{\mu}{\hbar^2}\,k\,K^{(SJTT_z)}(k,k;E_k)\right)^{-1}\left(1 - i\pi\,\frac{\mu}{\hbar^2}\,k\,K^{(SJTT_z)}(k,k;E_k)\right). \tag{A.48}$$

Remark: Phase shifts can be determined directly from on-shell K matrix elements. To derive the expression of δ_L for uncoupled channels, one introduces the notation $x = \pi\frac{\mu}{\hbar^2}\,k\,K^{(SJTT_z)}_L(k,k;E_k)$. The S matrix element then reads

$$S^{(SJTT_z)}_L(k) = \frac{1-ix}{1+ix} = e^{2i\delta_L}$$

hence

$$ix = \frac{1-e^{2i\delta_L}}{1+e^{2i\delta_L}} = -i\,\frac{\sin(2\delta_L)}{1+\cos(2\delta_L)} = -i\,\tan\delta_L\,.$$

Therefore one obtains the relation

$$\boxed{\tan\delta^{(SJTT_z)}_L(k) = -\pi\frac{\mu}{\hbar^2}\,k\,K^{(SJTT_z)}_L(k,k;E_k)}\,, -\frac{\pi}{2} \leqslant \delta_L \leqslant \frac{\pi}{2}. \tag{A.49}$$

A.2.3 Numerical method

Let us address the numerical aspects in the general case of the fully off-shell K matrix, the third argument being denoted by the energy E or a momentum square q^2 such that $E = (\hbar q)^2/(2\mu)$. The Lippmann–Schwinger equation is

$$K^{(SJTT_z)}_{L'L}(k',k;q^2) = v^{(SJTT_z)}_{L'L}(k',k) + \frac{2\mu}{\hbar^2}\sum_{L''}\mathcal{P}\int_0^{+\infty} dk''\, k''^2\, \frac{v^{(SJTT_z)}_{L'L''}(k',k'')\, K^{(SJTT_z)}_{L''L}(k'',k;q^2)}{q^2-k''^2}\,. \tag{A.50}$$

To deal with the principal value one can use the following property

$$\mathcal{P}\int_0^{+\infty}\frac{dk''}{q^2-k''^2} = 0 \tag{A.51}$$

to rewrite Eq. (A.50) in the following form

$$\begin{aligned} K^{(SJTT_z)}_{L'L}(k',k;q^2) =& v^{(SJTT_z)}_{L'L}(k',k) + \frac{2\mu}{\hbar^2}\sum_{L''}\int_0^{+\infty}\frac{dk''}{q^2-k''^2}\times \\ & \left[k''^2 v^{(SJTT_z)}_{L'L''}(k',k'')K^{(SJTT_z)}_{L''L}(k'',k;q^2) - q^2 v^{(SJTT_z)}_{L'L''}(k',q)K^{(SJTT_z)}_{L''L}(q,k;q^2)\right]. \end{aligned} \tag{A.52}$$

Let us denote by $f(k'')$ the following function

$$f(k'') \equiv v^{(SJTT_z)}_{L'L''}(k',k'')K^{(SJTT_z)}_{L''L}(k'',k;q^2)\,. \tag{A.53}$$

Equation (A.52) can then be written as

$$K^{(SJTT_z)}_{L'L}(k',k;q^2) = v^{(SJTT_z)}_{L'L}(k',k) - \frac{2\mu}{\hbar^2}\sum_{L''}\int_0^{+\infty} dk''\,\frac{k''^2 f(k'') - q^2 f(q)}{k''^2-q^2}\,. \tag{A.54}$$

The integrated function in Eq. (A.54) has a continuous extension in $k''=q$

$$\lim_{k''\to q}\frac{k''^2 f(k'') - q^2 f(q)}{k''^2-q^2} = f(q) + \frac{1}{2}\,q\,f'(q)\,, \tag{A.55}$$

where f' denotes the derivative of f with respect to its variable. Therefore Eq. (A.54) is nonsingular.

For low-momentum interactions with a sharp cutoff Λ, one can split the integral into two parts, the one over $[\Lambda;+\infty[$ being easily calculated:

$$\begin{aligned} K^{(SJTT_z)}_{L'L}(k',k;q^2) =& v^{(SJTT_z)}_{L'L}(k',k) + \frac{2\mu}{\hbar^2}\sum_{L''}\Bigg\{\int_0^{\Lambda}\frac{dk''}{q^2-k''^2}\times \\ & \left[k''^2 v^{(SJTT_z)}_{L'L''}(k',k'')K^{(SJTT_z)}_{L''L}(k'',k;q^2) - q^2 v^{(SJTT_z)}_{L'L''}(k',q)K^{(SJTT_z)}_{L''L}(q,k;q^2)\right] \\ & + q^2 v^{(SJTT_z)}_{L'L''}(k',q)K^{(SJTT_z)}_{L''L}(q,k;q^2)\int_{\Lambda}^{+\infty}\frac{dk''}{k''^2-q^2}\Bigg\}, \end{aligned} \tag{A.56}$$

where

$$\forall q < \Lambda \, , \int_{\Lambda}^{+\infty} \frac{dk''}{k''^2 - q^2} = \frac{1}{2q} \, \ln\left(\frac{\Lambda + q}{\Lambda - q}\right) \, . \tag{A.57}$$

Therefore one obtains

$$\begin{aligned} K_{L'L}^{(SJTT_z)}(k', k; q^2) =& v_{L'L}^{(SJTT_z)}(k', k) + \frac{2\mu}{\hbar^2} \sum_{L''} \Bigg\{ \int_0^{\Lambda} \frac{dk''}{q^2 - k''^2} \times \\ & \left[k''^2 v_{L'L''}^{(SJTT_z)}(k', k'') K_{L''L}^{(SJTT_z)}(k'', k; q^2) - q^2 v_{L'L''}^{(SJTT_z)}(k', q) K_{L''L}^{(SJTT_z)}(q, k; q^2) \right] \\ & + \frac{1}{2} \, q \, \ln\left(\frac{\Lambda + q}{\Lambda - q}\right) \, v_{L'L''}^{(SJTT_z)}(k', q) K_{L''L}^{(SJTT_z)}(q, k; q^2) \Bigg\} \, , \end{aligned} \tag{A.58}$$

When q is different from k (fully off-shell case), one has to rely on an iterative method, which converges if the Born series converges

$$\hat{T}(E) = \hat{V} + \hat{V}\hat{G}_0(E)\hat{V} + \hat{V}\hat{G}_0(E)\hat{V}\hat{G}_0(E)\hat{V} + ... = \hat{V} \sum_{n=0}^{\infty} \left(\hat{G}_0(E)\hat{V}\right)^n \, . \tag{A.59}$$

The Weinberg eigenvalues, which are the eigenvalues $\eta(E)$ of $\hat{G}_0(E)\hat{V}$, provide a criterion for the convergence of the Born series. If one considers complex values of E and a given partial-wave channel, then the Born series in that channel converges if all the corresponding eigenvalues are inside the unit circle of the complex plane. When a channel has a bound state, there is at least one eigenvalue $\eta(E)$ with $E < 0$ outside the unit circle on the real axis.

On the contrary when q is equal to k (right half-on-shell case), one can discretize the integral by a Gauss-like quadrature rule [91]. As the interaction v has a cut-off Λ, the Gauss–Legendre quadrature is adequate. Choosing k' among the mesh points $\mathcal{K} = \{k_1, \cdots, k_n\}$ and considering $k \notin \mathcal{K}$ as a parameter, one can write

$$\begin{aligned} K_{L'L}^{(SJTT_z)}(k_i, k; k^2) = v_{L'L}^{(SJTT_z)}(k_i, k) + \frac{2\mu}{\hbar^2} \sum_{L''} \Bigg\{ \sum_{j=1}^{n} \frac{w_j}{k^2 - k_j^2} \times \\ \left[k_j^2 v_{L'L''}^{(SJTT_z)}(k_i, k_j) K_{L''L}^{(SJTT_z)}(k_j, k; k^2) - k^2 v_{L'L''}^{(SJTT_z)}(k_i, k) K_{L''L}^{(SJTT_z)}(k, k; k^2) \right] \\ + \frac{1}{2} \, k \, \ln\left(\frac{\Lambda + k}{\Lambda - k}\right) \, v_{L'L''}^{(SJTT_z)}(k_i, k) K_{L''L}^{(SJTT_z)}(k, k; k^2) \Bigg\} \quad 1 \leqslant i \leqslant n \end{aligned} \tag{A.60}$$

and

$$\begin{aligned} K_{L'L}^{(SJTT_z)}(k, k; k^2) = v_{L'L}^{(SJTT_z)}(k, k) + \frac{2\mu}{\hbar^2} \sum_{L''} \Bigg\{ \sum_{j=1}^{n} \frac{w_j}{k^2 - k_j^2} \times \\ \left[k_j^2 v_{L'L''}^{(SJTT_z)}(k, k_j) K_{L''L}^{(SJTT_z)}(k_j, k; k^2) - k^2 v_{L'L''}^{(SJTT_z)}(k, k) K_{L''L}^{(SJTT_z)}(k, k; k^2) \right] \\ + \frac{1}{2} \, k \, \ln\left(\frac{\Lambda + k}{\Lambda - k}\right) \, v_{L'L''}^{(SJTT_z)}(k, k) K_{L''L}^{(SJTT_z)}(k, k; k^2) \Bigg\} \, . \end{aligned} \tag{A.61}$$

Let us transfer all the unknowns to the left side

$$
\begin{aligned}
&K_{L'L}^{(SJTT_z)}(k_i,k;k^2) - \frac{2\mu}{\hbar^2}\sum_{L''}\Bigg\{\sum_{j=1}^{n}\frac{w_j}{k^2-k_j^2}\times \\
&\Big[k_j^2 v_{L'L''}^{(SJTT_z)}(k_i,k_j)K_{L''L}^{(SJTT_z)}(k_j,k;k^2) - k^2 v_{L'L''}^{(SJTT_z)}(k_i,k)K_{L''L}^{(SJTT_z)}(k,k;k^2)\Big] \\
&+\frac{1}{2}\,k\,\ln\left(\frac{\Lambda+k}{\Lambda-k}\right) v_{L'L''}^{(SJTT_z)}(k_i,k)K_{L''L}^{(SJTT_z)}(k,k;k^2)\Bigg\} \\
&= v_{L'L}^{(SJTT_z)}(k_i,k) \quad 1\leqslant i\leqslant n
\end{aligned}
\tag{A.62}
$$

and

$$
\begin{aligned}
&K_{L'L}^{(SJTT_z)}(k,k;k^2) - \frac{2\mu}{\hbar^2}\sum_{L''}\Bigg\{\sum_{j=1}^{n}\frac{w_j}{k^2-k_j^2}\times \\
&\Big[k_j^2 v_{L'L''}^{(SJTT_z)}(k,k_j)K_{L''L}^{(SJTT_z)}(k_j,k;k^2) - k^2 v_{L'L''}^{(SJTT_z)}(k,k)K_{L''L}^{(SJTT_z)}(k,k;k^2)\Big] \\
&+\frac{1}{2}\,k\,\ln\left(\frac{\Lambda+k}{\Lambda-k}\right) v_{L'L''}^{(SJTT_z)}(k,k)K_{L''L}^{(SJTT_z)}(k,k;k^2)\Bigg\} \\
&= v_{L'L}^{(SJTT_z)}(k,k)\,,
\end{aligned}
\tag{A.63}
$$

that is, using the notation $k_{n+1}=k$

$$
\begin{aligned}
&\sum_{L''}\Bigg(\sum_{j=1}^{n}\Big[\delta_{L'L''}\delta_{ij} - \frac{2\mu}{\hbar^2}\frac{w_j k_j^2}{k^2-k_j^2}\,v_{L'L''}^{(SJTT_z)}(k_i,k_j)\Big]K_{L''L}^{(SJTT_z)}(k_j,k;k^2) \\
&+\Big\{\delta_{L'L''}\delta_{i\,n+1} + \frac{2\mu}{\hbar^2}\left[\sum_{m=1}^{n}\frac{w_m k^2}{k^2-k_m^2} - \frac{1}{2}\,k\,\ln\left(\frac{\Lambda+k}{\Lambda-k}\right)\right] v_{L'L''}^{(SJTT_z)}(k_i,k)\Big\}K_{L''L}^{(SJTT_z)}(k_{n+1},k;k^2)\Bigg) \\
&= v_{L'L}^{(SJTT_z)}(k_i,k) \quad 1\leqslant i\leqslant n+1\,.
\end{aligned}
\tag{A.64}
$$

For given values of L and k, one has to solve an inhomogeneous linear system whose unknowns are $K_{L''L}^{(SJTT_z)}(k_i,k;k^2)=K_\alpha$, where the conserved quantum numbers S, J, T, and T_z as well as L and k values are omitted to alleviate the notation, and $\alpha=(L'',i)$ is a double index.

References

[1] D. Vautherin and D. M. Brink, *Hartree-Fock calculations with Skyrme's interaction.* Phys. Rev. C **5**, 626 (1972).

[2] D. Vautherin, *Hartree-Fock calculations with Skyrme's interaction.* Phys. Rev. C **7**, 296 (1973).

[3] D. R. Hartree. Proc. Camb. Phil. Soc. **24**, 89 (1928).

[4] V. A. Fock. Z. Phys. **61**, 126 (1930).

[5] M. Bender and P. H. Heenen, *Self-consistent mean-field models for nuclear structure.* Rev. Mod. Phys. **75** (2003).

[6] J. R. Stone and P.-G. Reinhard, *The Skyrme interaction in finite and nuclear matter.* Prog. Part. Nucl. Phys. **57**, 587-657 (2007).

[7] L. M. Robledo, T. R. Rodríguez, and R. R. Rodríguez-Guzmán, *Mean field and beyond description of nuclear structure with the Gogny force.* J. Phys. G: Nucl. Part. Phys. **46**, 013001 (2019).

[8] D. J. Gross and F. Wilczek, *Asymptotically Free Gauge Theories I.* Phys. Rev. D **8**, 3633 (1973).

[9] R. Machleidt and D. R. Entem, *Chiral effective field theory and nuclear forces.* Phys. Rep. **503**, 1-75 (2011).

[10] S. Weinberg, *Nuclear forces from chiral lagrangians.* Phys. Lett. B **251**, 2 (1990).

[11] P. Reinert, H. Krebs, and E. Epelbaum, *Semilocal momentum-space regularized chiral two-nucleon potentials up to fifth order.* Eur. Phys. J. A **54**: 86 (2018).

[12] D. R. Entem and R. Machleidt, *Accurate charge-dependent nucleon-nucleon potential at fourth order of chiral perturbation theory.* Phys. Rev. C **68**, 041001 (2003).

[13] D. R. Entem, R. Machleidt, and Y. Nosyk, *High-quality two-nucleon potentials up to fifth order of the chiral expansion.* Phys. Rev. C **96**, 024004 (2017).

[14] R. Machleidt, *Advances in Nuclear Physics, Volume 19, Chapter 2.* Eds. Springer-Verlag (1989).

[15] R. B. Wiringa, V. G. Stoks, and R. Schiavilla, *Accurate nucleon-nucleon potential with charge-independence breaking.* Phys. Rev. C **51**, 38 (1995).

[16] R. Machleidt, *High-precision, charge-dependent Bonn nucleon-nucleon potential*. Phys. Rev. C **63**, 024001 (2001).

[17] S. Bogner, R. J. Furnstahl, and A. Schwenk, *From low-momentum interactions to nuclear structure*. Prog. Part. Nucl. Phys. **65**, 94-147 (2010).

[18] R. J. Furnstahl and K. Hebeler, *New applications of renormalization group method in nuclear physics*. Rep. Prog. Phys. **76**, 126301 (2013).

[19] B. R. Barrett, P. Navrátil, and J. P. Vary, *Ab-initio No-Core Shell Model*. Prog. Part. Nucl. Phys. **69**, 1 (2013).

[20] A. Tichai, E. Gebrerufael, K. Vobig, and R. Roth, *Open-shell nuclei from No-Core Shell Model with perturbative improvement*. Phys. Lett. B **786**, 448-452 (2018).

[21] J. P. Vary, R. Basili, W. Du, M. Lockner, P. Maris, D. Oryspayev, S. Pal, S. Sarker, H. M. Aktulga, E. Ng, M. Shao, and C. Yang, *Ab initio No-Core Shell Model with Leadership Class Supercomputers*. ArXiv:1803.04101v1 [nucl-th] (2018).

[22] K. Tsukiyama, S. K. Bogner, and A. Schwenk, *In-Medium Similarity Renormalization Group for Nuclei*. Phys. Rev. Lett. **106**, 222502 (2011).

[23] J. Simonis, S. R. Stroberg, K. Hebeler, J. D. Holt, and A. Schwenk, *Saturation with chiral interactions and consequences for finite nuclei*. Phys. Rev. C **96**, 014303 (2017).

[24] E. Bebrerufael, K. Vobig, H. Hergert, and R. Roth, *Ab-initio description of open-shell nuclei*. Phys. Rev. Lett. 118, 152503 (2017).

[25] G. Hagen, T. Papenbrock, M. H. Jensen, and D. J. Dean, *Coupled-cluster computations of atomic nuclei*. Rep. Prog. Phys. **77**, 9 (2014).

[26] Z. H. Sun, T. D. Morris, G. Hagen, G. R. Jansen, and T. Papenbrock, *Shell model coupled cluster method for open shell nuclei*. Phys. Rev. C **98**, 054320 (2018).

[27] W. H. Dickhoff and C. Barbieri, *Self-consistent Green's function method for nuclei and nuclear matter*. Prog. Part. Nucl. Phys. **52**, 2 (2004).

[28] V. Somà, C. Barbieri, and T. Duguet. Phys. Rev. C **87**, 011303 (2013); Phys. Rev. C **89**, 024323 (2014).

[29] M. Grasso, *Effective density functionals beyond mean field*. Prog. Part. Nucl. Phys. **106**, 256-311 (2019).

[30] D. Lacroix, T. Duguet, and M. Bender, *Configuration mixing with the energy density functional formalism: Removing spurious contributions from nondiagonal energy kernels*. Phys. Rev. C **79**, 044318 (2009).

[31] M. Bender, T. Duguet, and D. Lacroix, *Particle-number restoration within the energy density functional formalism*. Phys. Rev. C **79**, 044319 (2009).

[32] T. Duguet, M. Bender, K. Bennaceur, D. Lacroix, and T. Lesinski, *Particle-number restoration within the energy density functional formalism: Nonviability of terms depending on noninteger powers of the density matrices*. Phys. Rev. C **79**, 044320 (2009).

[33] P. Ring and P. Schuck, *The Nuclear Many-Body Problem*. Ed. Springer-Verlag (1980).

[34] E. N. E. van Dalen and H. Müther, *Triaxial deformation in nuclei with realistic NN interactions*. Phys. Rev. C **90**, 034312 (2014).

[35] M. V. Stoitsov, W. Nazarewicz, and S. Pittel, *New discrete basis for nuclear structure studies*. Phys. Rev. C **58**, 2092 (1998).

[36] J. L. Bloas, *PhD Thesis*. CENBG, University of Bordeaux (2011).

[37] E. M. Henley and G. A. Miller, *Mesons in nuclei*. p. 405, editors M. Rho and D. H. Wilkinson, North-Holland, Amsterdam (1979).

[38] J. Schwinger, *Quantum Mechanics: Symbolism of Atomic Measurement*. p. 183-190, Chap. 4, Ed. Springer-Verlag (2001).

[39] A. Messiah, *Mécanique Quantique*. Tome II, Ed. Dunod, Paris (1960).

[40] D. A. Varshalovich, A. N. Moskalev, and V. K. Kherkonskii, *Quantum Theory of Angular Momentum*. World Scientific, Singapore (1988).

[41] K. A. Bruecker, C. A. Levinson, and H. M. Mahmoud, *Nuclear Saturation and two-body forces. I. Central forces*. Phys. Rev. **95**, 217 (1954).

[42] K. A. Bruecker, *Nuclear Saturation and two-body forces. II. Tensor forces*. Phys. Rev. **96**, 508 (1954).

[43] K. A. Brueckner, *Two-body forces and nuclear saturation. III. Details of the structure of the nucleus*. Phys. Rev. **97**, 1353 (1955).

[44] S. Shen, H. Liang, J. Meng, P. Ring, and S. Zhang, *Fully self-consistent relativistic Brueckner-Hartree-Fock theory for finite nuclei*. Phys. Rev. C **96**, 014316 (2017).

[45] H. Tong, X. L. Ren, P. Ring, S. Shen, S. Wang, and J. Meng, *Relativistic Brueckner-Hartree-Fock theory in nuclear matter without the average momentum approximation*. Phys. Rev. C **98**, 054302 (2018).

[46] S. Okubo, *Diagonalization of Hamiltonian and Tamm-Dancoff equation*. Prog. Theor. Phys. **12**, 5, 603-622 (1954).

[47] K. Suzuki and S. Y. Lee, *Convergent theory for effective interaction in nuclei*. Prog. Theor. Phys. **64**, 6, 2091-2106 (1980).

[48] K. Suzuki, *Construction of hermitian effective interaction in nuclei: general relation between hermitian and non-hermitian forms*. Prog. Theor. Phys. **68**, 1, 246-260 (1982).

[49] A. Calci, *PhD Thesis: Evolved chiral hamiltonians at the three-body level and beyond*. Darmstadt University (2014).

[50] H. Hergert, S. K. Bogner, S. Binder, A. Calci, J. Langhammer, R. Roth, and A. Schwenk, *In-medium similarity renormalization group with chiral two- plus three-nucleon interactions*. Phys. Rev. C **87**, 034307 (2013).

[51] A. Ekström, G. Jansen, K. Wendt, G. Hagen, T. Papenbrock, B. Carlsson, C. Forssén, M. Hjorth-Jensen, P. Navrátil, and W. Nazarewicz, *Accurate nuclear radii and binding energies from a chiral interaction*. Phys. Rev. C **91**, 051301 (2015).

[52] A. Shirokov, I. Shin, Y. Kim, M. Sosonkina, P. Maris, and J. Vary, *N^3LO NN interaction adjusted to light nuclei in ab exitu approach*. Phys. Lett. B **761**, 87-91 (2016).

[53] E. Epelbaum, A. Nogga, W. Glöckle, H. Kamada, U. Meissner, and H. Witala, *Three-nucleon forces from chiral effective field theory*. Phys. Rev. C **66**, 064001 (2002).

[54] R. J. Furnstahl, *The Renormalization Group in Nuclear Physics*. Nucl. Phys. B Proc. Suppl. 00, 1-37 (2012).

[55] B. Bally, *PhD Thesis*. CENBG, University of Bordeaux (2014).

[56] J. Dobaczewski, J. Dudek, S. G. Rohozinski, and T. R. Werner, *Point symmetries in the Hartree-Fock approach*. Phys. Rev. C **62**, 014310, 014311 (2000).

[57] M. Moshinsky, *Transformation brackets for harmonic oscillator functions*. Nucl. Phys. **13**, 104 (1959).

[58] R. Balian and E. Brézin, *Angular Momentum Reduction of the Fadeev Equations*. Il Nuovo Cimento, Vol. **LXIIB**, N.2 (1969).

[59] C. W. Wong and D. M. Clement, *Vector bracket and transformed wave function of a few-body state*. Nucl. Phys. A **183**, p. 210-224 (1972).

[60] D. Baye and P.-H. Heenen, *Generalised meshes for quantum mechanical problems*. J. Phys. A: Math. Gen. **19**, 2041 (1986).

[61] D. Baye, *The Lagrange-mesh method*. Phys. Reps **565**, p. 1-108 (2015).

[62] W. Ryssens, P.-. Heenen, and M. Bender, *Numerical accuracy of mean-field calculations in coordinate space*. Phys. Rev. C **92**, 064318 (2015).

[63] H. Bethe, *Splitting of terms in crystals*. Ann. Physik **3**, 133-206 (1929).

[64] J. O. Dimmock, *Representation theory for non-unitary groups*. J. Math. Phys. **4**, 10 (1963).

[65] M. Hamermesh, *Group theory and its application to physical problems*. Ed. Addison-Wesley (1962).

[66] A. Bulgac and M. M. Forbes, *Use of the discrete variable representation basis in nuclear physics*. Phys. Rev. C **87**, 051301 (2013).

[67] M. Beiner, H. Flocard, Nguyen Van Giai, and P. Quentin, *Nuclear ground-state properties and self-consistent calculations with the Skyrme interaction*. Nucl. Phys. A **238**, 29-69 (1975).

[68] L. Bonneau and P. Quentin, *Fission barriers and fission paths of the ^{70}Se nucleus within a microscopic approach*. Phys. Rev. C **72**, 014311 (2005).

[69] N. Pillet, P. Quentin, and J. Libert, *Pairing Correlations in an Explicitly Particle-Number Conserving Approach*. Nucl. Phys. A **697**, 141 (2002).

[70] K. Sieja, *PhD Thesis*. CENBG, University of Bordeaux (2007).

[71] C. Robin, N. Pillet, D. P. Arteaga, and J.-F. Berger, *Description of nuclear systems with a self-consistent configuration-mixing approach: Theory, algorithm and application to the ^{12}C test nucleus*. Phys. Rev. C **93**, 024302 (2016).

[72] Meng-Hock Koh, Dao Duy Duc, T. V. Nhan Hao, Ha Thuy Long, P. Quentin, and L. Bonneau, *Band-head spectra of odd-mass heavy nuclei within a microscopic approach*. Eur. Phys. J. A **52**, 3 (2016).

[73] C. Bloch and A. Messiah, *The canonical form of an antisymmetric tensor and its application to the theory of superconductivity*. Nucl. Phys. **39**, 95 (1962).

[74] B. Zumino, *Normal forms of complex matrices*. J. Math. Phys. **3**, 1055 (1962).

[75] F. Herbut and M. Vujičič, *Antilinear Operators in Hatree-Bogolyubov Theory. I*. Phys. Rev. **172**, 1031 (1968).

[76] J.-F. Berger, M. Girod, and D. Gogny, *Time-dependent quantum collective dynamics applied to nuclear fission*. Comp. Phys. Comm. **63**, 365 (1991).

[77] J. Dobaczewski, H. Flocard, and J. Treiner, *Hartree–Fock–Bogolyubov description of nuclei near the neutron drip line*. Nucl. Phys. A **422**, 103 (1984).

[78] J. L. Bloas, L. Bonneau, P. Quentin, J. Bartel, and D. D. Strottman, *Effect of pairing correlations on the isospin-mixing parameter in deformed N=Z even-even nuclei*. Phys. Rev. **86**, 034332 (2012).

[79] J. Le Bloas, L. Bonneau, P. Quentin, J. Bartel, and D. D. Strottman, *Erratum: Effect of pairing correlations on the isospin-mixing parameter in deformed N=Z even-even nuclei*. Phys. Rev. **91**, 049901(E) (2015).

[80] W. Satula, J. Dobaczewski, W. Nazarewicz, and T. R. Werner, *Isospin-breaking corrections to superallowed Fermi β decay in isospin- and angular-momentum-projected nuclear density functional theory*. Phys. Rev. C **86**, 054316 (2012).

[81] J.-P. Delaroche, M. Girod, J. Libert, H. Goutte, S. Hilaire, S. Péru, N. Pillet, and G. F. Bertsch, *Structure of even-even nuclei using a mapped collective Hamiltonian and the D1S Gogny interaction*. Phys. Rev. C **81**, 014303 (2010).

[82] E. Epelbaum, H. Krebs, and U.-G. Meissner, *Precision Nucleon-Nucleon Potential at Fifth Order in the Chiral Expansion*. Phys. Rev. Lett. **115**, 122301 (2015).

[83] G. Hagen, T. Papenbrock, D. J. Dean, and M. Hjorth-Jensen, *Ab initio coupled-cluster approach to nuclear structure with modern nucleon-nucleon interactions*. Phys. Rev. C **82**, 034330 (2010).

[84] A. Tichai, J. Langhammer, S. Binder, and R. Roth, *Hartree–Fock many-body perturbation theory for nuclear ground-states*. Phys. Lett. B **756**, 283 (2016).

[85] B. Bally, B. Avez, M. Bender, and P.-H. Heenen, *Beyond Mean-Field Calculations for Odd-Mass Nuclei*. Phys. Rev. Lett. **113**, 162501 (2014).

[86] J. A. Sheikh, J. Dobaczewski, P. Ring, and L. M. Robledo, *Symmetry restoration in mean-field approaches*. ArXiv:1901.06992v1 [nucl-th] (2019).

[87] G. Lacroix, C. Semay, and F. Buisseret, *Lagrange-mesh calculations in momentum space*. Phys. Rev. E **86**, 026705 (2012).

[88] M. A. Morrison and A. N. Feldt, *Through scattering theory with gun and camera: Coping with conventions in collision theory*. Am. J. Phys. **75**, 67 (2006).

[89] H. Stapp, *Phase-shift analysis of 310 MeV proton-proton scattering experiments*. Phys. Rev. **105**, 302 (1957).

[90] W. Glöckle, *The quantum mechanical few-body system*. p. 84-86, Springer-Verlag (1983).

[91] A. Heidari, S. Vedad, A. A. Bég, and M. Ghorbani, *A numerical method for solving the Lippmann-Schwinger integral equation with the radial interaction potentials*. Fundamental J. Modern Physics **2**, 119 (2011).

Titre : Approximation de Hartree-Fock pour les noyaux déformés avec un potentiel général à 2-corps et corrélations d'appariement avec une interaction résiduelle cohérente.

Résumé : Dans ce travail, nous étudions l'approche Hartree-Fock (HF) dans l'espace impulsion pour les noyaux déformés avec un potentiel nucléon-nucléon (NN) général. La structure d'un tel potentiel est analysée à partir de ses symétries et sa construction est réalisée dans une représentation tensorielle séparable des opérateurs d'impulsion-spin-isospin. En plus, pour traiter des interactions à basses impulsions, nous mettons en oeuvre l'approche du groupe de renormalisation par transformation de similarité du potentiel. Plusieurs bases en impulsion sont étudiées : l'onde plane, l'onde partielle et l'onde plane confinée. L'implémentation de l'approche HF est validée en comparaison avec un code HF-Skyrme en base d'oscillateur harmonique. Nous trouvons que la base d'onde plane confinée offre le plus d'avantages : flexibilité du choix du groupe de symétrie auto-cohérente, facilité du calcul des éléments de matrice de l'interaction (nucléaire, Coulomb et la correction cinétique du centre de masse), optimisation des ressources (temps et mémoire). Elle fait intervenir deux paramètres : la taille de boîte de confinement (cube) et la coupure sur l'impulsion individuelle. Nous montrons que cette coupure a un lien direct avec la coupure d'impulsion de l'interaction et que la taille de boîte est essentiellement liée à celle du noyau. Des calculs de propriétés globales du noyau sont effectués dans des noyaux magiques et pair-pairs déformés dans la région de masse A $<$ 100 avec divers potentiels récemment dévéloppés. A partir de la solution HF obtenue, les corrélations d'appariement sont étudiées avec l'interaction résiduelle dans le cadre du formalisme HTDA (*Highly Truncated Diagonalization Approach*). En particulier, la convergence en fonction de l'espace du modèle a été abordée.

Mots-clés : champ moyen déformé, Hartree-Fock, corrélations d'appariement, interaction résiduelle, formalisme HTDA.

Title: Hartree-Fock approximation for deformed nuclei with a general two-nucleon potential and pairing correlations with a consistent residual interaction.

Abstract: In this work, we develop the Hartree-Fock (HF) approach for deformed nuclei in momentum space with a general two-nucleon potential. The structure of such a two-nucleon potential is investigated in the momentum space starting from its symmetries. Its construction is realized in a tensorial separable momentum-spin-isospin representation. Moreover, to treat low-momentum interactions, we also implement the *Similarity Renormalization Group* approach. Three momentum bases are studied: the plane-wave, the partial-wave and the confined plane-wave. The numerical implementation is validated against an existing HF-Skyrme code in the harmonics oscillator basis. We find that the confined plane-wave basis provides many advantages over the two others, namely: flexible construction of symmetry-adapted bases, efficient calculation of matrix elements (nuclear, Coulomb and center of mass kinetic correction) and optimization in ressources (time and memory). This basis is characterized by two parameters: the confinement box size (cube) which can be essentially related to the nuclear radius and a single-particle momentum cut-off which is directly linked to the cut-off in relative momentum of the interaction. Bulk properties of some spherical and deformed even-even nuclei with mass A $<$ 100 are calculated with recently developed NN potentials. The resulting residual interaction is derived to study pairing correlations within the *Highly Truncated Diagonalization Approach*. In particular, we address the convergence with the model space.

Keywords: deformed mean field, Hartree-Fock, pairing correlations, residual interaction, HTDA formalism.

Centre d'Étude Nucléaires de Bordeaux-Gradignan, UMR 5797 du CNRS/IN2P3 et de l'Université de Bordeaux.
CENBG, Chemin du Solarium, Le Haut Vigneau, CS 10120, F-33175 Gradignan Cedex.